University of Kerbala
College of Education for pure Science
Department of Chemistry

Synthesis and Characterization of Zinc Sulfide Nanoparticles and its Application in Removal of Methylene blue Dye from its Aqueous Solutions

A Thesis
Submitted to the Council of College of Education for pure Science
University of Kerbala/ In Partial Fulfillment of the Requirements for the
Degree of Master in Chemistry Sciences
Written by

Ameer Qasim Abed

Supervised by

Asst. Prof. Dr.

Aula Mahdi Al Hindawi

2022 A.D .

Asst. Prof. Dr.

Hasan F. Alesary

1444 A.H.

بِسْمِ اللهِ الرَّحْمنِ الرَّحِيمِ

((وَجَعَلْنَا مِنَ الْمَاءِ كُلَّ شَيْءٍ حَيٍّ))

صَدَقَ الله اَلعلَي الَعظِيْم

سورة الأنبياء

الاية

﴿٣٠﴾

Committee Certification

We are the examination committee, certify that we have read the thesis entitled **(Synthesis and Characterization of Zinc Sulfide Nanoparticles and its Application in Removal of MB Dye from its Aqueous Solutions)** and examined the student **(Ameer Qasim Abed)** in its content and that in our opinion it is adequate as a thesis for the degree of Master of Science in chemistry.

Chairman Signature:
Name: Prof. Dr. Hamida Idan Salman
Address: University of Kerbala
Date: / /2022

Member
Signature:
Name: Asst.Prof.Dr. Asmaa Kadim Ayal
Address : University of Baghdad
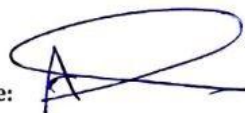**Date:** / / 2022
Supervisor and Member
Asst.Prof. Dr. Aula Mahdi Abd Ali
Address: University of Kerbala
Date: 7 /11 / 2022

Member
Signature:
Name: Asst.Prof.Dr. Ahmed Saadoon Abbas
Address: University of Babylon
Date: / / 2022
Supervisor and Member
Asst. Prof.Dr. Hasan Fisal Namaa
Address: University of Kerbala
Date: / / 2022

Approved for the college council....

Name: Prof. Dr. Hamida Idan Salman

Dean of the college of Education for Pure Sciences
Date: / / 2022

Supervisor Certification

We certify that this **thesis (Synthesis and Characterization of Zinc Sulfide Nanoparticles and its Application in Removal of MB Dye from its Aqueous Solutions)** was placed under supervision in chemistry department of College of Education for Pure Sciences, University of Kerbala Partially fulfilling the requirements for a master's degree in chemistry sciences for the student **(Ameer Qasim Abed)**

Signature:

Asst. Prof .Dr. *Aula Mahdi Al Hindawi*
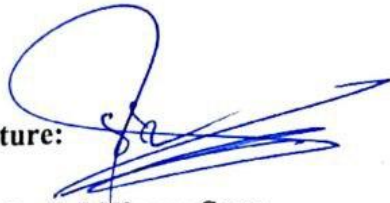
Supervisor

Date: 13 / 11 / 2022

Signature:

Asst. Prof .Dr. Hasan F. Alesary

Supervisor

Date: /   / 2022

In view of the available recommendations I forward this thesis for debate by the examining committee.
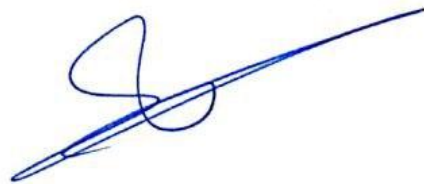
Signature:

Name: Dr. Sajid Hassan Guzar

Date: / /2022

Head of Chemistry Department

Amendment Report

This is to certify that the thesis entitled (**Synthesis and Characterization of Zinc Sulfide Nanoparticles and its Application in Removal of MB Dye from its Aqueous Solutions**) and corrected the grammatical mistakes I found. The thesis is therefore qualified for debate.

Signature:

Name: Dr. Tafeey Majeed

Address: Kerbala university /college of Educ for Human Sciences

Date: 13/11/ 2022

Dedication

To my mother …

To my family who make my dreams possible

To my wife, who supported me along the way

To my friends…

Who helped me all the time

Ameer

Acknowledgements

First of all, I want to thank the Almighty Allah who enabled me with power during this work in particular. I would like to extend my deep thanks, gratitude, and appreciation to my supervisors *Asst. Prof. Dr. Aula Mahdi Al Hindawi* and *Asst. Prof. Dr. Hasan F. Alesary* for their continuous support and invaluable suggestions and great contributions.

Also, I want to thank all members in department of chemistry in College of Education for Pure Sciences, University of kerbala, for their worthless support during this work.

Finally, I want to thank my family and friend for their continual support throughout this journey. They were my source of encouragement along the way.

Summary

This work focused mainly on the synthesis and characterization of zinc sulfide nanocrystals using chemical precipitation approach. Zinc sulfide nanoparticles with quasi-spherical shape have been fabricated by controlling the concentration of the starting materials, reaction time and pH of the solution. The formation of zinc sulfide nanocrystals was confirmed through TEM, FE-SEM, XRD and EDX techniques. The band gap energy was measured from the UV-Vis spectrum and was found to be 3.8 eV, the observation of blue shift with respect to the bulk ZnS is attributed to the effect of quantum confinement. The adsorption behavior of ZnS nanoparticles was demonstrated and it was found that ZnS particles have the ability to adsorb methylene blue dye (MB) from aqueous solution. It was found that with increasing amount of ZnS in the dye solution, the removing for MB increased.

In the second part of this project, zinc sulfide nanoparticles were prepared using green methods. In this method, parts of plants are used as reducing agents and protecting agents rather than using chemical materials. Parameters such as the concentration of the extract and pH of the solution were modified to control the growth process of ZnS nanoparticles. The band gap energy was determined from the absorption spectrum and found to be 3.93 eV, which is in blue shift compared to bulk ZnS. FTIR spectrum identifies the functional groups that could be attached to the prepared ZnS particles. ZnS nanoparticles' adsorption behavior was demonstrated, and it was found that a small amount of ZnS particles (0.1 g) are able to adsorb methylene blue dye (MB) from wastewater.

	Contents	
	Acknowledgements	
	Summary	
	Contents	I - I V
	List of tables	V
	List of figures and schemes	VI -VII
	List of abbreviations and symbols	IV

Table list of abbreviations	
List of abbreviations and symbols	The Meaning of symbol
E_g	band gap energy
θ	Bragg angle.
B:ZnS	Broccoli with Zinc sulphide
C_t	Concentration of substrate at time t of irradiation.
CB	Conduction Band
eV	electron Volt
FE-SEM	Field Emission-Scanning Electron Microscopy
FTIR	Fourier Transfer Infra-Red Spectrometer
FWHM	Full width half –maximum
C_o	Initial Concentration
n	Integer called the order of reflection (n=1, 2, 3)
MB	Methylene blue dye
NPs	Nanoparticles
D	The average crystallite size
K	The constant crystal lattice
β	The full width at half maximum in radians
%DR	The percentage of dye removal
λ	The wavelength of x-ray.
TEM	Transmission Electron Microscopy
TNF	Tumor necrosis factor
UV-Vis	Ultraviolet-visible spectrophotometer
VB	Valance Band
XRD	X-Ray Diffraction
ZB	Zinc blend
ZnS	Zinc sulphide

1.1 Nanotechnology

Nanotechnology, in recent years, has been considered to be one of the most interesting research areas. It deals with the formation and manipulation of objects on the nanoscale (1-100 nm), at which nearly all materials show different properties, and indeed new features appear, that differ significantly, from those of bulk counterparts.[1]

For example, it is well known that bulk gold does not show catalytic activity (inert chemically), however, as the gold cluster sizes shrink to the nanoscale level, it becomes an excellent catalyst.[2] Bulk copper can be easily bent but when its dimensions are reduced to less than 40 nm, it exhibits a very hard structure.[3] Classification of nano materials according to their dimensions :(0 D, 1D, 2D, 3D) NPs.

and according to the composition: (organic, Inorganic,hybride)NPs.

1.2 Applications of nanotechnology

Nanomaterials have a larger number of atoms on their surface compared to the interior atoms, leading to an increase in the surface to area ratio and the surface energy.

These dramatic increments in the ratios of the surface-to-area are believed to make great changes in their physical and chemical properties.[4,5] These properties pave the way to use the nanostructures in many potential applications (see Figure 1.1). In industrial and electronic sectors, the use of nanomaterials is expected to improve the products' features such as increasing the efficiency of solar cells and light bulbs. In the medical fields[6], many metals and semiconductors nano-materials exhibit antimicrobial, antiviruses, and antibacterial activities.[7,8]

The development of nanotechnology opens a new world for early diagnosis and treatment of diseases such as cancers and inflammation.[9] Moreover, nanostructures are being used to improve the environment, they used for removal contaminations and treating water.[10] Nanotechnology play a role in making the industrial materials digestible or to changing them to another biodegradable forms.

Nanomembrane technology depends on using carbon-nanotube as a member to filter or separate the unwanted gases (CO_2 gas) and to prevent their penetrating to our environment. Carbon nanotube membranes exhibit an ability to capture gases with efficiency more than 100 times other conventional membranes.

Figure 1.1 Scheme shows applications of nanotechnology.[11]

1.3. Formation of Nanostructures

Top-bottom and bottom-up approaches have been developed and used for the formation of nanomaterials.[12] Figure 1.2 shows the two techniques that are used for synthesis of nanostructures.
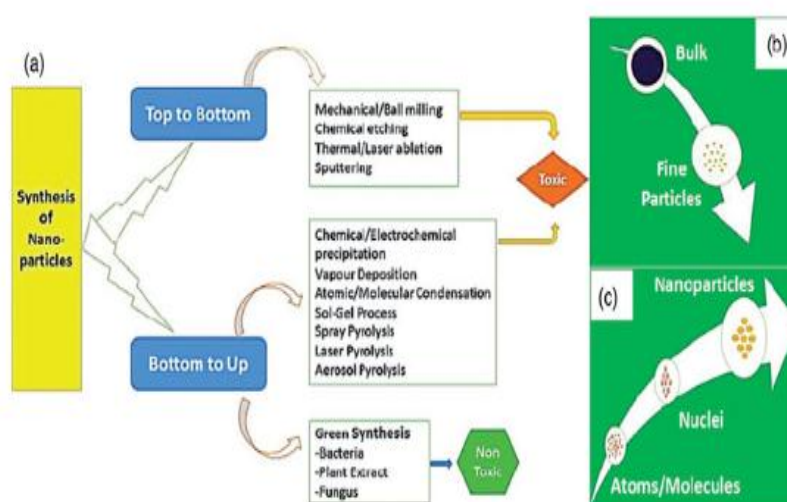
Figure 1.2 Illustration showing the top-to-bottom and bottom-to-up approaches.

1.3.1 Top-bottom approaches

The idea behind the top-bottom approaches is to transition the large-scale materials (bulk materials) to small nanoparticles using methods such as milling or attrition, lithography and repeated quenching.[13]

Mechanical milling can produce particles with diameters ranging from a couple of tens to several hundred nanometers. On the other hand, milling technique has certain limitations such as broad size distributions of the resultant milled

particles and a varied particle morphology. Also, the particles produced may have picked up impurities from the milling medium and defects on their surfaces that can result from attrition.[14]

Repeated quenching (repeated thermal cycling) is a technique used to produce nanoparticles which involved breaking down bulk materials into fine particles.[11] In this method only materials with very low thermal conductivities can be used. In other words, it cannot be used with very poor thermal conductivity materials. As well as, it is difficult to design and control the shape and size of the desired nanostructure.

Lithography is another example of a top-down method which sees widespread use in the manufacture of printed circuits and computer boards. However, it is expensive because it requires venture sources, i.e., electrons beams with high energies and support equipment. [15]

1.3.2 Bottom-up approaches

Bottom-up approaches are the most common methods used in the synthesis of nano-objects. The concept of the bottom-up approach is the self-assemble the atoms and/or molecules into nuclei and then form nanoscale particles.[16] There are many different methods used in bottom-up approaches, such as chemical vapor deposition, sol-gel, electro deposition, and the solvothermal method.[17,18]

Chemical vapor deposition is a process in which the substrate is exposed to one or more volatile precursors, which react and/or decompose on the substrate surface to produce the desired nanomaterials. For instance, carbon nanotubes can be formed by this method by passing any source of carbon (methane or acetylene) over catalyst (Ni, Fe or Co)[19,20] when the formal decomposed into carbon atoms, carbon nanotubes can be produced via the catalyst. Therefore,

chemical vapor deposition is considered an economical technique to synthesizing carbon nanotubes.

A Sol-gel method is a chemical method used for the synthesis of various nanostructures, especially metal oxide nanoparticles. In this technique, the molecular precursor (usually metal alkoxide) is dissolved in water or alcohol and converted to gel by heating and stirring by hydrolysis/alcoholysis. Sol-gel approach has several advantages; it is used to produce metastable materials with high purities and compositional homogeneities at reasonable temperatures. In addition, this technique allows for the control of shape, porosity and composition to obtain materials with high surface-to-area ratios.

The Chemical precipitation method is considered a broad chemical method for preparing nanomaterials. This method involves essential processes such as chemical reaction, nucleation and growth, and secondary processes such as agglomeration, attrition, and breakage. Due to the difficulties with avoiding nucleation during the subsequent growth of nuclei, the particles obtained with a conventional precipitation process are relatively large with broad size distributions.[21]

Although precipitation is the most widely used method, it is difficult to control the associated size, shape, and dispersion.[22,23] the nanoparticles produced by this method tend to be polydisperse and have a uniform shape. However, by controlling parameters such as pH, starting material concentrations, ionic strength of the precipitation medium, and reaction temperature, one is able to control the crystal or\and particle sizes, shapes, and the crystal structures. In addition, the number of stabilizing ions, the presence of other ions, chelation, and adsorption of additives on the nuclei and growing crystals are all factors that could affect the size and morphology of the resultant nanoparticles.

1.3.2.1 Biological methods (green chemistry)

Various chemical techniques can be chosen for the synthesis of nanoparticles because of their rapid reaction times and their ability to produce monodisperse nanoparticles. Techniques such as chemical reduction, electrochemical reduction, photochemical reduction, and heat evaporation have all been employed to control nanoparticle composition. Although all these techniques can produce NPs, they have some disadvantages such as the high price of the process and not being environment friendly, since they result in considerable amounts of pollution because of the toxic solvents and reducing agents that are used.

To avoid these drawbacks, green chemistry approaches have been proposed and used for the production of nanoparticles that are simple, convenient, less energy-conception, kinder to the environment, minimize the usage of unsafe materials and maximize the efficiency of the process as shown in Figure 1.3.
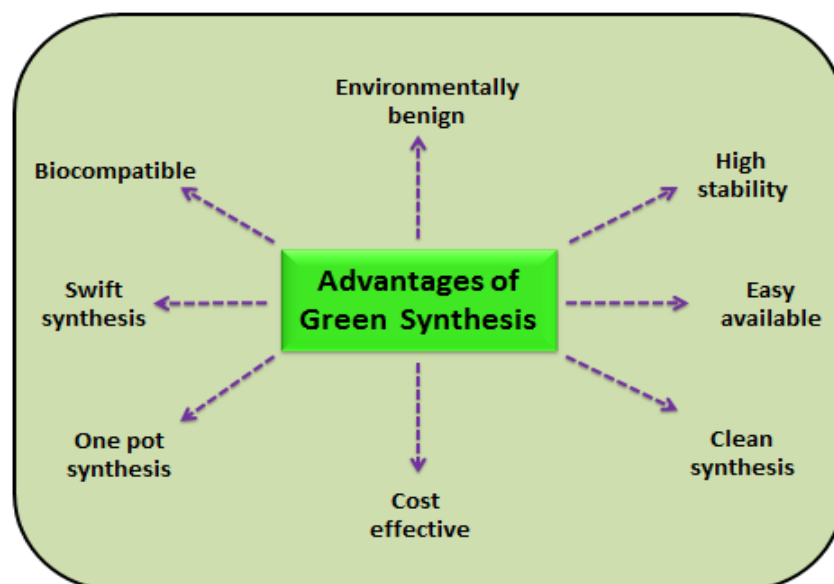
Figure 1.3 Diagram showing some advantages of green synthesis

1.3.2.1.1 Using bacteria for fabricating nanomaterials

Under mild cultivation conditions, bacteria represent one of the fastest growing microorganisms. They can detoxify the chemical, thereby; they can survive and grow in areas where the concentration of toxic metals is quite intense. They have been employed, recently, to synthesize different types of nanostructures. These nanomaterials can be used in safety applications such as cosmetics and clothes without causing any risk to humans since these materials are not toxic.[24]

The exact process for the synthesis of nanoparticles is yet to be invented. This is because different biological agents have different mechanisms for synthesis. The most reliable mechanism for the synthesis of nanoparticles is that enzymes and proteins are secreted either intracellularly or extracellularly during the metabolic activities of bacteria which serve as bio-reduction and bio-stabilization.[25] The underlying mechanism of ZnS nanostructure formation using bacterial microorganisms requires further complex steps including; biosorption and bioreduction as shown in Figure 1.4. The first step is initiated by trapping ions (Zn^{+2}) on the surface of the bacterial cell through physical and chemical interactions.[26]
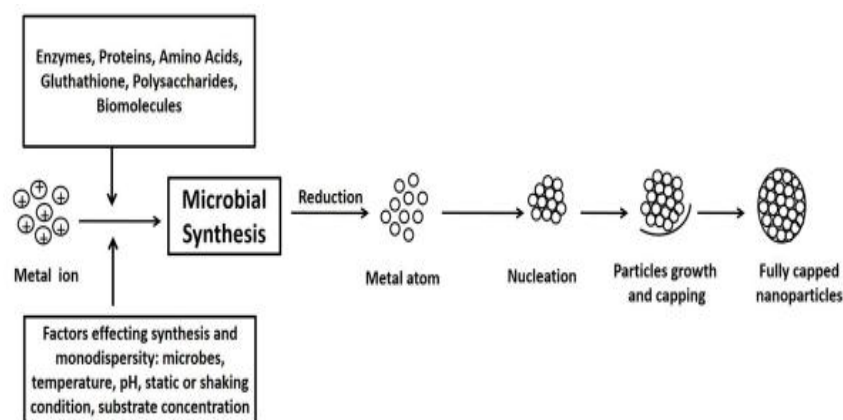
Figure 1.4 Diagram showing the mechanism of nanoparticle synthesis by microbes, this photo reproduced from ref. **[27]**

Interestingly, Suriyaraj et al. (2019)[28] have described the synthesis of ZrO_2 nanoparticles using extremophilic Acinetobacter sp. bacterial. The finding showed that ZrO_2 particles are not toxic to the fibroblast cells of the mouse. Gong et al. have reported the bio-faibrication of zinc sulfide nanoparticles using environmentally friendly bacteria Desulfovibrio desulfuricans. The resulted ZnS NPs have an average diameter of 5-8 nm. UV-Vis spectroscopy recorded the maximum absorption of biosynthesized ZnS particles .It was shifted towards shorter wavelengths compared to the bulk ZnS. According to the authors, ZnS NPs were formed in the cell and then delivered to the solution. They also reported that the majority of ZnS particles were concentrated in the cell membrane, then cell wall and cytoplasm.[29]

1.3.2.1.2 Using fungi in preparing process of nanoparticles

Fungus is a eukaryote micro-organism that digests food externally and absorbs nutrients through the cell wall by decomposing organic matter. They belong to the autotropic organisms.[30] Fungi are known to reproduce by spores, they obtain their carbon and energy from other organisms. Due to special features such as their ability to secrete digestive enzymes into their food to obtain the nutrients required for their growth. They are considered ideal bio templates for the synthesis of nanoparticles.

This process is similar to the synthesis of nanoparticles from bacterial species, however, it is more advantageous due to the fungus's potential to endure severe synthesis conditions. Also one of their important advantages is their accelerated growth in controllable ways, which is why fungal species are preferable for the biosynthesis of nanoparticles.

Verticillium fungal species are utilized to prepare silver nanoparticles. When the fungal biomass is exposed to a solution containing Ag ions, the metal ions are reduced and silver nanoparticles are formed with a diameter of 25 ± 12 nm. Microscopic studies for the fungal cells showed that Ag nanoparticles were produced under the cell wall. Their interpretation is enzymes that are present in the cell wall membrane are responsible for the reduction of metal ions. The latter were not toxic to the fungal cells and they found that after the bio-fabrication of Ag particles, cells continued to proliferate.[31]

1.3.2.1.3 Fabrication of nanomaterials using Algae

Another way to synthesize nanoparticles is from Algae, Algae consists of a large heterogeneous collection of plants that differ in size, habitat, physiology, reproduction, and biochemistry. Algae are considered both eukaryotic and prokaryotic, acquiring their nutrients through the photosynthetic process. Sometimes they are considered terrestrial plants because they use chlorophyll for photosynthesis. Some algae expel fucoidans from their cell walls such as seaweeds, these fucoidans contain several sulfated esters and fucose, displaying numerous bioactivities including antioxidant and anticoagulant properties. These biomolecules (fucose and sulfated esters) are then used for the green synthesis of nanomaterials.[32]

Algae have many bio-active components such as polyphenols, polyunsaturated fatty acids, proteins, etc.[33] These components can act as capping and reducing agents to produce nanostructures. Two mechanisms for the biosynthesis of nanoparticles using algae were suggested, extracellular and intracellular. Extracellular includes the reduction of metal ions to its nanoparticles on the surface of algae, whilst the latter also involves the reduction of metal ions but through enzymatic activity, this occurs in the wall and membrane of the cell (see Figure 1.5).[34]

Chlamydomonas reinhardtii (an alga that lived in freshwater) was used to synthesize zinc sulfide nanoparticles.. FTIR spectrum showed the presence of protein on the ZnS nanoparticles' surface. UV-Vis spectroscopy recorded the maximum absorption of biosynthesized ZnS particles at 310 nm which is shifted towards the higher energies.[35]
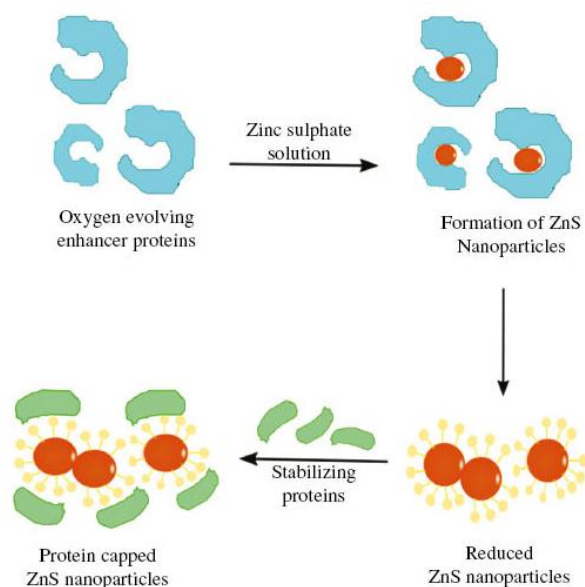
Figure 1.5 Mechanism explaining the formation process of ZnS NPs using Chlamydomonas alga. This photo reproduced from [35].

1.3.2.1.4 Preparation of nanomaterials using plant extract

Plants are the most widespread, cost-efficient, and locally available material for the synthesis of nanomaterials. Compared to other green materials plants have remarkable benefits. Various plant parts can be used to synthesize nanomaterials, for instance, leaves, fruit, roots, flowers, and in some cases tubers. The plant materials can be collected from different sources, washed, and then either dried or ground to form a powder. The plant parts may also be boiled to acquire the plant extract. These plant extracts contain biomolecules like

amino acids, enzymes, tannins, sugar, flavonoids, and many more, all of which are used to stabilize the desired nanoparticles.[36]

One of the advantages of using plants to synthesize nanoparticles is its faster in contrast with microbial routes, the synthesis process occurs within a few minutes to several hours while other microbial communities take days.[37] Another thing is that the whole synthesis process can be controlled and manipulated however wanted. Finally, the use of plants has less health risk. [38]

The importance of green synthesis over chemical and physical synthesis is due to it being environmentally friendly, rapid, and simple and there is no requirement for the use of high temperature, pressure, toxic material and pressure.[39]

The basic principle of the plant extract method is that biomolecules such as phenols, polyphenolics, and flavonoids which exist in the extract could cap and reduce the metal ions and form metallic nanoparticles. There are two mechanisms to explain the formation process of nanoparticles using plant extract: intracellular and extracellular. A metal-rich medium (soil and hydroponic solution) is required to form metallic nanoparticles in the intracellular mechanism, which means further efforts are needed such as culture, monitoring, and collecting nanoparticles. On the other hand, the extracellular mechanism, which is shown in Figure 1.6, includes preparing the extract solution from the plant parts, then mixing it with a solution containing the metal salt solution. Nanoparticles formed through these biological techniques are used in agriculture, drug delivery, environmental, medical, and cosmetics fields as they are non-toxic particles.
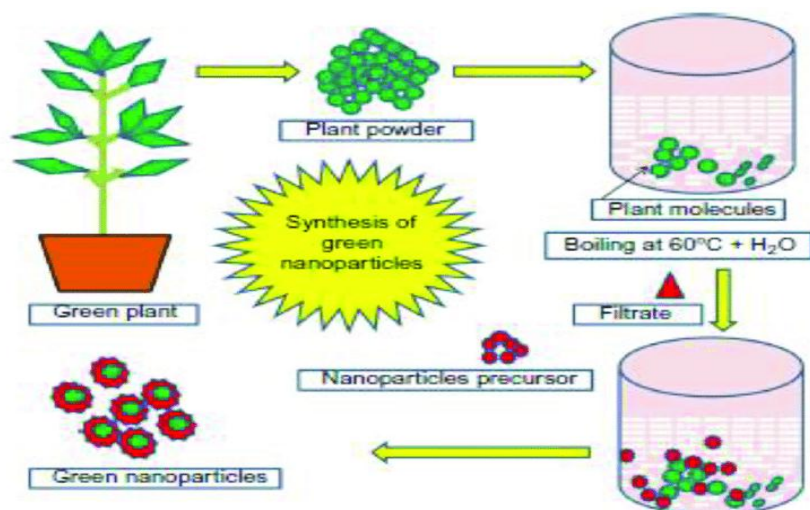
Figure 1.6 Scheme showing the synthesis process of Nanoparticles using plant extract as a reducing and capping agents. This scheme was taken from.[40]

In literature, various studies have been performed about the formation of semiconductor particles from plant extract. Nonetheless, few works were done about using the plant extract method for preparing ZnS nanoparticles. Thereby, here we report, for the first time, the fabrication of zinc sulfide nanoparticles from broccoli extract. This extract acts as a capping agent which expects to prevent or reduce the aggregation process of ZnS nanoparticles and control their stability, size and shape.

1.4 Semiconductors

Semiconductors are solid materials in which the electric current travels with difficulty, the electrical conductivity of which is controlled by the addition of other elements in trace amounts. Semiconductors have conductivity lies in the range between conductivity of conductors and insulators (see Figure 1.7). Semiconductors can be found either as free element such as selenium and silicon or compound form such as tin sulfide, gallium arsenide and zinc sulfide.
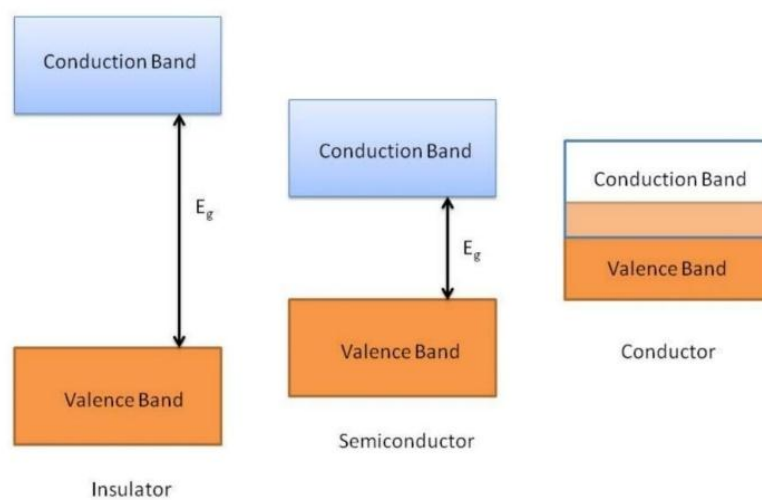
Figure 1.7 Diagram of the band structure of insulators, semiconductors and conductors, where E_g represents the band gap. This image was taken from ref.[41].

1.4.1 Development of semiconductors

Many works have been performed to improve and study the properties of semiconductor materials and their applications. In 1886, diode rectifiers were produced, for the first time, from Germanium semiconductors.[42] In 1906, the American inventor of the electric motor invented the first solid-state electronic component: a radio wave detector, which used metals in contact with semiconductor material such as silicon or lead sulfide.[43]

The invention of solar cells in the forties is considered the most achievement in the semiconductor technology.[44] The year 1962 witnessed the innovation of the first semiconductor laser.[45] It is characterized by very small size, high efficiency of generated light and power consumption (compared to other types), and thereby sees widespread use in many applications. It is found in CDs, DVDs, laser printers, optical discs, pens, and laser games. It has many colors, including red, green and blue. [46]

Semiconductors are applied in low temperature printing process that aims to manufacture low-cost solar cells. It is even used in manufacturing the nano-transistors that are more powerful, faster, and highly energy efficient.

Nowadays, devices and equipment that include semiconductor materials are the basis of modern electronics, which include radio, digital cameras, laptops, quantum computers, and many other devices.[47]

1.5 Nanometer-sized semiconductors

At the nano scale level, semiconductors possess remarkable properties which differ completely from their bulk counterparts and discrete molecules as shown in Figure 1.8. Semiconductor nanoparticles which are commonly called quantum dots have a diameter of less than 10 nm, at that size the quantum confinement effect is observed.[48]
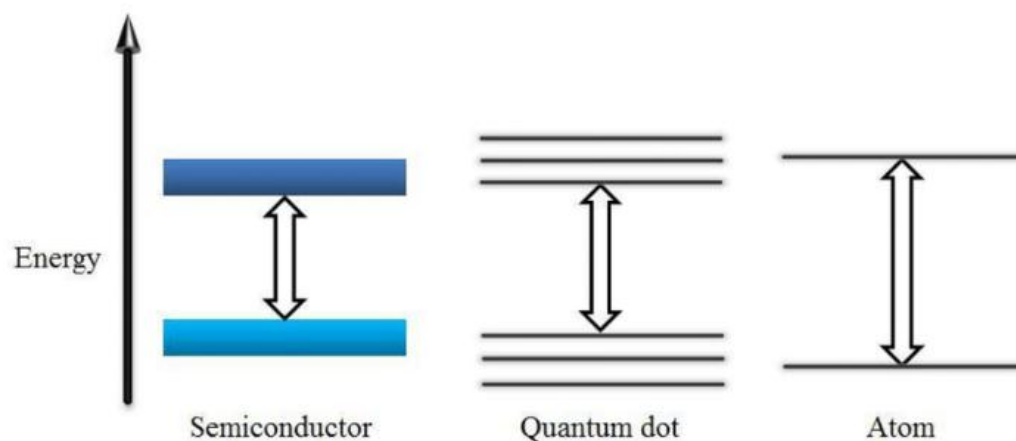
Figure 1.8 Comparison of band gap energy in bulk, nano and atomic scale, showing the dependent of the band gap on the size.

In semiconductor nanoparticles, atoms get closer and begin to form bonds.[49] The energy levels of the atoms starts to divided into groups of closely spaced energy levels. When the atoms reach the lowest energy band consists of valence orbitals, the equilibrium between atoms occur. The first band is called the valence band. It contains permissible energy levels of low energy and is completely or partially filled with electrons, and indeed cannot be free of them. These electrons are called valence electrons. The second band is called the conduction band which contains permissible energy levels with high energies, higher than permissible energy levels in the valence band and it is empty band.

The electronic properties, optical properties and conductivity of semiconductors can be monitored via the band gap energy. Band gap energy is the difference in energy between valence and conduction bands. Electrons could move from the valence band to the conduction band through the band gap if they gain sufficient energy from an external source (such as heat energy, light energy, or the effect of an electric field),[50] which is equal or higher than the band gap energy. As a result, the electron in the valance band will excite leaving a hole in the conduction band. The hole and electron have the same magnitude but opposite polarity and they form together exciton, which collapses quickly. Thereby, as

the particle size reaches the nanoscale and becomes less than the exciton size (1 nm to 100 nm)[51] the electrons cannot move about as freely at that scale and become restricted. The confinement of the electrons causes them to react differently to light and this phenomenon called quantum size effect.[52]

As shown in Figure 1.9 two kinds of band gaps can be found in semiconductors: direct band gap and indirect band gap. The direct band gap occurs when the conduction band's minimum is located directly above the valence band's maximum in momentum space. As a result, no momentum transfer is needed to move the electron from the valence band to the conduction band. However, indirect band-gap semiconductors do not have the lowest part of the conduction band energy at such a point. Thereby, the fast electron has to transfer momentum to an electron in the valence band in order to excite it into the conduction band.[53]
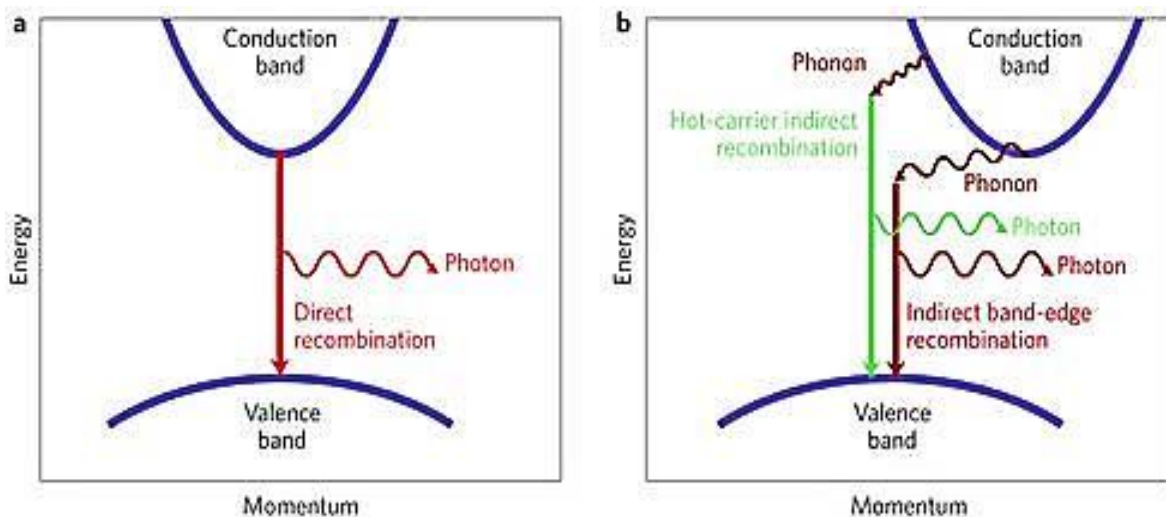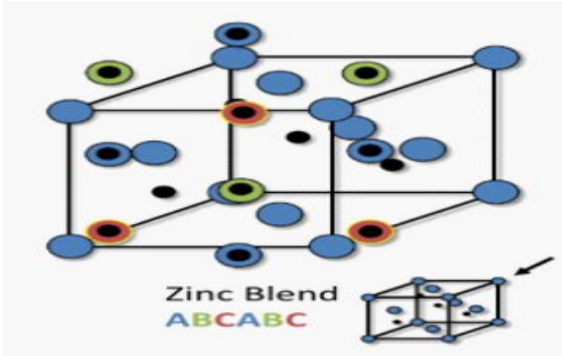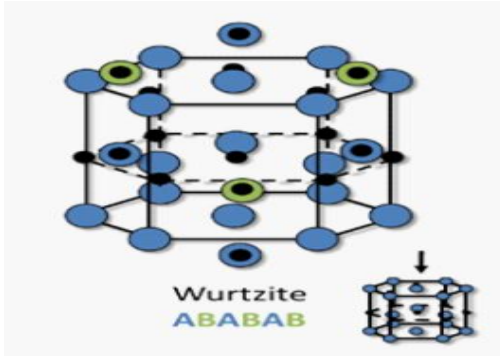
Figure 1.9 Simplified optical transition of a semiconductor. (a) Direct band gap, and (b) indirect band gap.[51]

1.6 Bulk zinc sulfide

Zinc sulfide (class of II-VI semiconductors) is the main source of zinc. It has wide band gaps of about 3.54-3.91 eV in the bulk form[54], and so are deemed ideal for short wavelength optoelectronic applications.[55,56] ZnS is a non-toxic, abundant, and environmentally friendly substance with high chemical stability in contrast to oxidation and hydrolysis. Furthermore, it is very stable across a large pH range and can be prepared from earth-abundant materials, in addition, it is widely utilized in various applications, for example, solar cells, electronics, catalysts, light emitting diodes (including lasers), active sensors, and wastewater treatment.[57,58]

In general, ZnS compound is a polymorphous material because they exist in nature in two crystalline structures: Zinc Blende and Wurtzite. In these two forms, the coordination geometry at zinc and sulfur is tetrahedral. The two forms have the same closest-neighbor connections; however, there is a slight difference in the distances and angles to the neighbor's. Table (1.1) reports the differences among the crystal structures of these zinc sulfide forms.**[54,59]**

Table (1-1) Differences in crystal structure of two ZnS phases

Zinc Blende (ZB)	Wurtzite Zinc (WZ)
1. Cubic	1. Hexagonal
2. It is more stable than Wurtzite	2. Lest stable than Zinc Blende
3. Band gap of ZB is approximately 3.54 eV	3. Band gap is 3.91 eV

1.7 ZnS nanostructures

Compared to bulk ZnS, nanocrystal zinc sulfide has interesting properties due to the size confinement effect.[60,61] The quantum size effect becomes obvious when the particle radius reaches the Bohr radius of the exciton (electron-hole pair). [62] As the particle size decreases the number of atoms in the particles decreases too, this leads to reduction the overlap of atoms orbitals, and consequently, the width of the valance and conduction bands narrows and the energy gap between them increases. Therefore, the absorption edge will be shifted towards higher energies (blue shift).[63] It is well known that zinc sulfide (ZnS) has a wide direct band gap (E_g = 3.6 eV at 27 ^{o}C), which emits light in the UV region of the electromagnetic spectrum .[64] This property increases the lifetime of excitation resulting in reduced recombination. Moreover, using a plant extract as a capping agent leads to minimization of the agglomeration and the formation of nanoparticles with small sizes and large surface-to-area ratios which properly have an affinity to adsorb contaminants.

1.7.1 Applications of zinc sulfide nanocrystals

Zinc sulfide nanostructures have remarkable optical properties and tunable photoluminescence when compared to their bulk counterparts because of the size quantum confinement effects.[61] The distinctive features of ZnS nanoparticles pave the way for using ZnS particles in our life. ZnS particles have tunable band gaps which make them important in many potential applications such as in the electronics and biological applications. [65] [66]   Zinc sulfide is well-known as phosphor material, therefore, it can be used in a variety of luminescence applications including electroluminescence and photoluminescence. This property opens the door to their use in the manufacturing of solar cells, infrared windows, laser, displays and sensors**.**[67]

The photoluminescence intensity of nanoparticles is about 25 times brighter than that of bulk particles; making them a good candidate to use in many

devices compared the bulk semiconductors.[68] Regarding photocatalytic activity, ZnS nanoparticles are capable of splitting water to generate hydrogen with the help of solar energy.[69] The generated hydrogen is employed in clean energy systems.[65] This remarkable property opens the door to their use in reducing pollutants from water. Nanoparticles also play a role in the cosmetic industry; they can be dispersed in a wide range of cosmetics like foundations, lipsticks, and many more. Because they provide high UV protection, they can be used in sunscreens. In terms of medical application, ZnS particles are used successfully for wound healing and repair due to their biological activities in inhibiting the fetal bovine serum and reducing the production of collagen.[70] According to the Labiadh group research, ZnS nanoparticles exhibit antibacterial and antiviral properties, in addition to, the higher antioxidant property.[71] Very recent study (2022)[72] shows that ZnS nanoparticles can be used in treating cancer cells in vitro, in particular leukemia cells, through generating reactive oxygen species followed by killing cancer cells by TNF-α factor. Finally, due to the high activity of semiconductor materials (they act as fluorescent materials), they have been used in the identification of DNA.[73] Figure 1.10 summarizes the most important application of ZnS nanoparticles.
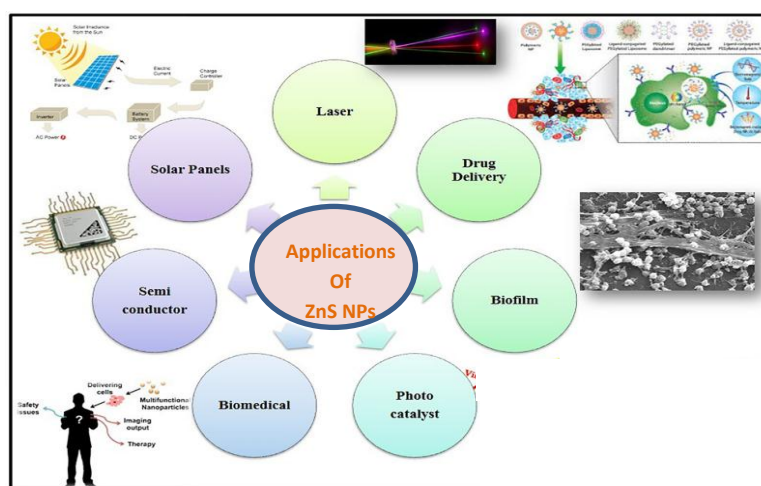
Figure 1.10: Potential applications of ZnS nanoparticles.

1.7.2 Literature review about preparing zinc sulfide nanostructures

Many efforts have been performed to developing methods for producing metal and semiconductor nanoparticles with various sizes and shapes such as sol-gel, chemical precipitation, biosynthetic methods and laser deposition.[74-77] Zinc sulfide nanoparticles can be prepared by, for example, sol-gel,[78] microwave assisted,[79] chemical precipitation,[80] and sonochemical method.[81]

Figure 1.11 summarized the most commonly used methods for producing zinc sulfide nanostructures. In this section we will mention few of the previous studies about the formation of ZnS nanoparticles.
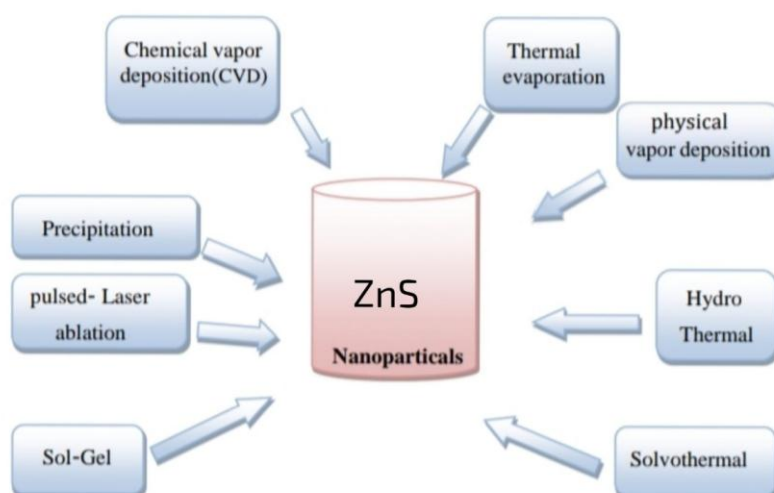
Figure 1.11 Various approaches for synthesis ZnS nanoparticals.

Different plant species have been used to fabricate nanoparticles using water or methanol as solvents. For example, zinc sulfide nanoparticles were synthesized successfully using Tridax procumbens extract as a protecting agent. The authors found that zinc sulfide nanoparticles have potential antimicrobial activity against different bacteria and fungus cultures.[82] Chandran et al. used a

hydrothermal approach to generate bare ZnS nanoparticles and then used Scherrer equation to compute the average crystallite size of the sample, which was found to be 20-36 nm. [83]

Pathak teams used[84] a mechanochemical method to make zinc sulfide nanoparticles, and the crystallite size of the as-prepared nanoparticles was determined to be in the range of 4–7 nm. Goharshadi et al. performed experiments to produce ZnS nanoparticles with an average particle size of 2 nm using ultrasonics with irradiation, without the use of a surfactant, at high temperatures. They discovered that by employing 0.2 g ZnS NPs at a neutral pH, the photocatalytic activity of zinc sulfide quantum dots for the breakdown of reactive black 5 (type of Azo dye) could be examined in short time (10 minutes).[85]

Shanmugam groups noted that the cerium-doped zinc sulfide nanorods had a flower-shaped morphology, indicating that they were successfully synthesized in air environment using a simple chemical precipitation process.[86]

Parvaneh and coworkers utilized the precipitation approach to make ZnS nanoparticles with EDTA as a stabilizer and capping agent, [87] whereas Ayodhya and coworkers[40] used the same method with different capping agents such as PVP (polyvinyl pyrrolidone) and PVA (polyvinyl acetate).

ZnS particles were prepared using Stevia rebaudiana leave extract as a nontoxic and bio-reductant agent. It was concluded that the ZnS crystals have size of 8.35 nm based on XRD calculations[88].

The bio fabrication of ZnS particles using various microorganisms was demonstrated. In 2018, Ohara et al. prepared zinc sulfide nanoparticles using bacteria (Shewanella oneidensis MR-1) as a bio-reducing agent. Their resulted particles have an average size of 5-6 nm and spherical shape. They also concluded that the protein molecules from bacteria absorbed on the surface of ZnS nanoparticles.[89]

Bera and colleagues found that doping increased the size of the crystals produced for bare ZnS and Mn-doped ZnS nanoparticles.[90]

The authors also studied the cytotoxic effects of their prepared ZnS particles against cancer cell MCF-7. [91]

Acalypha indica and Tridax procumbens plant extracts were used as capping agents. The microscopic techniques revealed that ZnS nanoparticles have a diameter of 20 -50 nm and they have a spherical and hexagonal shape. The UV-Visible spectrum showed a significant decrease in the band gap energy 2.69 eV when compared to the bulk ZnS 3.36 eV which indicated the formation of ZnS is at the nanoscale level.

The XRD pattern showed the as-prepared ZnS nanoparticles had a hexagonal crystal structure (wurtzite). According to the authors, the resulted ZnS nanoparticles have antibacterial properties, and these properties increase as the concentration of the extract increase. As well as, the antibacterial activity of ZnS NPs formed in the presence of plant extract is high concerning pure ZnS.[92]

Zhang et al. (2022) described a simple and fast method for the preconcentration and determination of trace amounts of methylene blue (MB) from water samples, using zinc sulfide nanoparticles. Their finding showed that ZnS nanoparticles with a size range from 60 to 200 nm are able to depredate the dye under Xe illumination (the degradation rate was 99.76 % after two hours and a half of illumination.[93]

1.8 Broccoli

A winter vegetable, broccoli belongs to the Brassicaceae family, which is an annual herbaceous plant similar in morphology to cauliflower. It is ranked 31st in the world in terms of production. It is grown for its inflorescences that are eaten in the flower bud stage. As shown in Figure 1.12, the vegetable, with its

thick, soft pods, are one of the richest crops in this family in terms of nutritional value and the most widely used in terms of nutritional therapeutic value. It contains many vitamins and minerals, and is rich in beta-carotene, its leaves are a source of polyphenols, fats, and fibers.[94]

It also contains antioxidants that prevent the risk of cancer because they contain glucoraphanin, which enhances the body's immunity against stomach cancer, and the compound carbinol-3-indole, which prevents breast and colonic cancer, and enhances liver function. [95]

The plant-mediated composition of nanoparticles could be intra-cellular or extra-cellular. The intra-cellular method entails the composition of nanoparticles by growing the plant in metal-rich organic media, while the extra-cellular method involves employing plant extract obtained from heating and pulverizing the plant in question in a solvent or aqueous medium.[96]
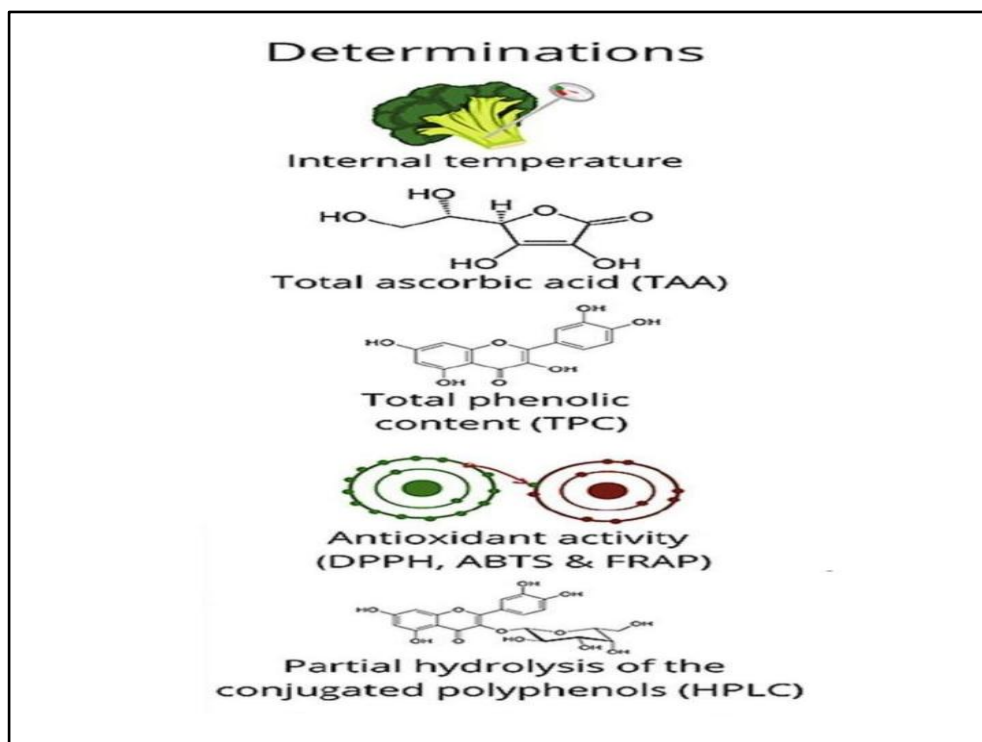
Figure 1.12 Chemical composition of broccoli

1.9 Water Pollution

Large amounts of wastewater are generated by industrial activities that rely on commercial colorants, which are then discharged into rivers, landfills, and nearby water sources if not properly managed.[97,98] Highly reactive and toxic dyes are concentrated in wastewater from these industrial processes, which subsequently act as major pollutants.[99]

The discharge of dye-containing effluents into the water environment is undesirable due to their low biodegradability. Therefore, considerable studies have been devoted to developing efficient water remediation methods.[100] To remove organic and inorganic contaminants from wastewater, various methods have been used such as chemical oxidation (chlorination and ozonization), adsorption, and air stripping methods.[101] All these methods are used intensively to treat water pollution, however, they have some disadvantages.

Chemical oxidation (chlorination and ozonation) as a decontamination method is unable to break down all organic substances and it is only cost-effective for removing pollutants in high concentrations. Chlorination produces disinfecting byproducts(DBPs) like trihalomethanes, which have been identified as potential carcinogens and also cause secondary pollution[102].

The presence of nitrite and suspended solid particles reduces the efficiency of this process, necessitating large investments in filter systems.   In   terms of ozonation, it is extremely irritating and possibly toxic, so off-gases from the contactor must be destroyed to prevent worker exposure. [103]

Activated carbon has been reported to be used in adsorption techniques, which has shown considerable promise in usefully removing organic pollutants, but the regeneration procedure is also costly. Since carbon is a non-selective adsorbent that adsorbs almost all natural organic matter present in water, the method's effectiveness is significantly reduced, resulting in the inability to accumulate pollutants. Other techniques, such as the air stripping method, which are used

for decontaminating water by extracting volatile organics. It has a high capacity for wastewater treatment. However, instead of being destroyed, the pollutants will transfer from water into the air, which is a disadvantage. This creates a new environmental problem: air pollution, which necessitates the use of air-cleaning techniques.

Advanced oxidation processes (AOPs), which have been shown to be effective in the destruction of refractory pollutants, have emerged as leading alternatives to conventional water purification in the last decade (e.g. microorganisms, industrial toxins).[104] A total of AOPs makes up a promising group. The ability to exploit the high reactivity of hydroxyl (OH) radicals in driving the oxidation process makes this wastewater treatment technology, particularly noteworthy.

1.10 dyes

They are colored materials that can be linked in some way to the material to be dyed or painted to give it bright colors. This could protect from light rays, oxygen, and certain acids and bases, as well as during washing. It contains molecules that have groups that give it color, called chromophores. By fixation, they are called auxochromes, where these groups are classified according to the intensity of the color.[105] The dyes are also characterized by their ability to absorb light radiation in the visible spectrum from 380 to 750 nm.

Dyes have been used in many fields such as textile industry, manufacture of plastic materials and building paints, cosmetics industry, food industry (food coloring) and printing (ink and paper).[106]

1.10.1 Methylene blue dye

Methylene blue dye is also called tetramethylthionine chloride; aromatic chemicals are amongst the cationic dyes. As seen in Figure 1.13 that methylene blue has the chemical formula $C_{16}H_{18}N_3SCl$, and it is a solid in the form of a dark green odorless powder,[107,108] which gives a blue solution when dissolved in water.

Figure 1.13 Structural formula of methylene blue

1.10.1.1 Physical and chemical properties of methylene blue

Methylene blue has the physical and chemical properties reported in Table 1.2 [109]

Table 1.2 The physical and chemical properties

Methylene blue	Chemical name
$C_{16}H_{18}N_3SCl$	Chemical formula
Dimethylaminophenazathioniumchloride (3.7-bis tetramethylthionine chloride)	Nomenclature according to (IUPAC)
M = 319.85 g/mol	molar mass
100 -110°C	melting point

1.10.1.2 Toxicity of methylene blue dye

Continuous exposure to methylene dye causes various health problems, such as nausea, vomiting, and eye burns. In the case of inhalation, breathing becomes rapid or difficult, as well leading to an increase in heart rate. Ingestion will cause gastrointestinal irritation, profuse sweating, mental confusion, burning sensations, anemia and high blood pressure.[110,111]

In nature, dyes release nitrates and phosphates which may become toxic in the lifecycles of fish in the water. Its consumption by aquatic plants accelerates its spread and leads to depletion of oxygen through the process of photosynthesis in the deepest layers of rivers and stagnant water, and the accumulation of matter also leads to the organic matter in waterways that gives rise to bad taste, the spread of bacteria, unpleasant odors, and unnatural colors.

It is well known that industrial waste from textile and dyeing factories, among others, contains a large amount of dyes and active substances, as well as dissolved salts, which cause significant environmental damage in many countries. By conducting studies with a view to treating them and in order to remove dyes from these wastes before they drain into rivers, research has shown many biological treatment methods (aerobic and anaerobic treatments), as well as chemical methods (ion exchange, oxidation by oxygen and ozone), and physicochemical methods (membrane separation, coagulation, agglomeration and adsorption) can be used. [112]

1.10.1.3 Adsorption of methylene blue dye

Methylene blue dye (tetra methylthionine chloride) is considered to be one of the most common dyes used in textile, rubbers, pesticides, varnishes and pharmaceuticals.[113]

However, this dye causes serious problems to the environment and living organisms.[114] It is well known that about 10-15% of these dyes (from the various industries) are lost as waste in the water, causing major problems for living organisms.[115] The interest in removing them increased after realizing that many of the raw materials used in the preparation of these dyes are carcinogenic.[116] [117] Therefore, it is preferable to remove these substances from the water before pushing them into the environment, not only for aesthetic reasons but also due to their toxicity and effects that many scientists in various disciplines are increasingly interested in identifying and removing such pollutants from the environment.

Many adsorbents have been used for adsorbing methylene blue dye (MB) from water sources such as graphene activated Charcoal, and magnetic composite (which is formed from graphene oxide and magnetic chitosan).[118]

Activated carbon is an adsorbent that is used to remove different kinds of inorganic pollutants such as heavy and organic elements, various dyes, and phenols because of its high adsorption capacity. However, activated carbon has some limitation such as its high cost and reuse problems, as well as the difficulty of separating it from wastewater.[119]

An alternative and low-cost semiconductor nanomaterials have been used for water purification.[120]   Due to their small-sized and optical properties, they are used either as photocatalysis or adsorbents. To the best of our knowledge, this new modification of the prepared zinc sulfide nanoparticles has never been utilized for the adsorption of dyes.   In this work, as-prepared zinc sulfide nanoparticles have been used to remove MB dye from aqueous solutions.

1.11 Adsorption

Adsorption is defined as the process of collecting particles dissolved in solution, which is called the adsorbate substance, on the surface of a solid or liquid substance, which is called the adsorbent surface. It is natural that the states of

matter that have specific surfaces in space are the liquid and solid states. Therefore, the areas of surface contact or interfaces that can lead to adsorption are solid-liquid, liquid-liquid, solid-gas, solid-solid, and liquid-gas.

1.11.1 Types of adsorption

1.11.1.1 Physical Adsorption

This type occurs when the adsorbate layer is bound to the adsorbent surface with certain forces. These forces are called physical forces or van der Waals forces. The attraction is not fixed to a specific site and the adsorbate is comparatively free to move on the surface. Physical adsorption is a relatively weak, reversible, form of adsorption that can allow for multilayer adsorption.

1.11.1.2 Chemical Adsorption

Some degree of chemical bonding between adsorbate and adsorbent[121] can be describe by strong attraction. Adsorbed molecules are not free to move on the surface. There is a high degree of specificity and typically only a monolayer is formed. The process is seldom reversible. Figure 1.14 shows the differences between the two kinds of adsorption.
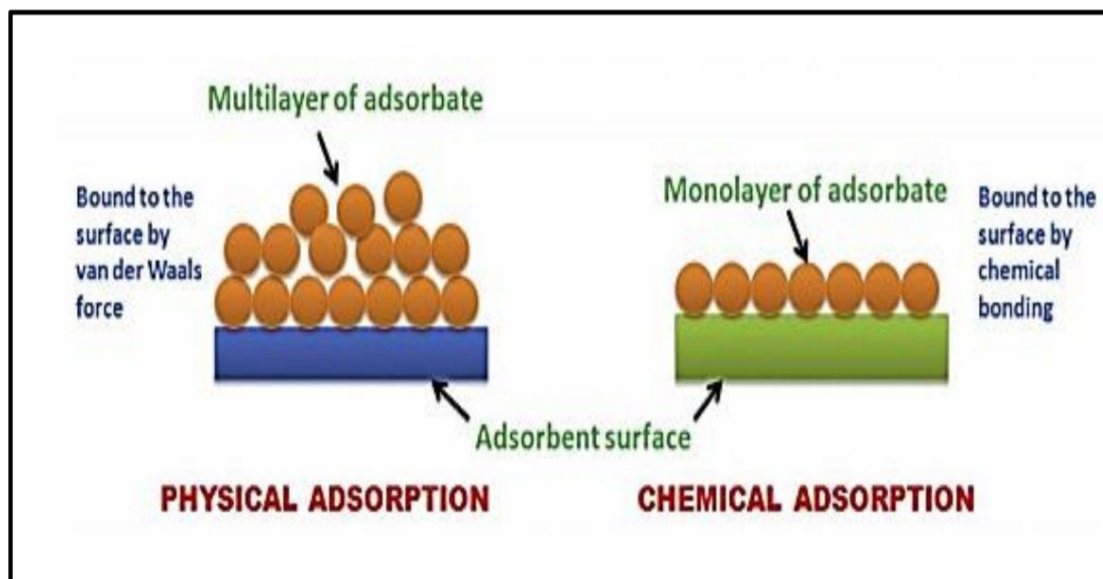
Figure 1.14 Differences between physical adsorption and chemical adsorption. [122]

1.11.2 Adsorption Mechanism

The adsorption mechanism can be summarized according to the following steps.[123]

1- Solute molecules approach the adsorbent surface.

2- Solute molecules are bound to the adsorbent surface.

3- Solute molecules leave the adsorbent surface sites and enter the pores on the adsorbent surface.

4- The overlap of the solute molecules and their available sites on the internal surfaces are linked to the pores and capillary microchannels of the adsorbent's solid surface.

1.11.3 Factors that affect the adsorption

1-Initial concentration of adsorbate

The adsorption process is affected by the initial concentration of the adsorbate, which is due to the exposure of a larger amount of molecules or the adsorbable ions to the active sites in the adsorbent surface at high concentrations, leading to increased adsorption speed.

2-Nature of the Adsorbent

Adsorption is affected by the nature of the adsorbent surface and the presence of polar groups on the surface, as well as by the surface area and the size of the pores and the increase in the number of effective sites on the surface. As the adsorption on the surface of the material increases The solid with a decrease in its particle size (increased surface area), and the adsorbent material that has narrow- open pores has greater strength and ability to adsorption, taking into account the size of the molecule adsorbate. The adsorbent material with narrow pores cannot adsorb particles of a size larger than the size of pores. Therefore, the increase in the surface area leads to an increase in the amount of adsorption to the absorbent surface due to the increase in the number of active sites on the surfaces that increase the adsorption capacity.[94]

3-Effect of Solubility

It is well known that as the solubility of solute increases, the extent of adsorption decreases. Factors that affect solubility include ionization (solubility is lower when compounds are uncharged), polarity (as polarity increases, one observes higher solubility because water is a polar solvent), and molecular size (higher molecular weight suggests lower solubility). [95]

4- **Effect of pH**

pH often affects the surface charge on the adsorbent as well as the charge on the solute. Generally, for organic materials, as pH decreases adsorption increases.[123, 124]

5- Effect of Temperature

Adsorption reactions are typically exothermic. Therefore, as the temperature increases the extent of adsorption decreases.[124,125]

6- Effect of Ionic strength

The ionic strength of electrolyte salts greatly affects the adsorption process through its effect on the solubility of the adsorbate material, and on the physical properties of the adsorbent surface. The solubility of the electrolyte salts used was higher than the solubility of the adsorbate in the solvent leads to an increase in the adsorption capacity. However, if the adsorbate is in an ionic form, the increase in the ionic strength leads to an increase in the solubility of the adsorbate[126]. Therefore, it can be expected that the adsorption capacity will decrease and, in some adsorption states, a competition occurs between the adsorbate and ionic salts for the active sites of the adsorbent surface; if the rate of adsorption of these salts is faster than the adsorbate, this leads to a reduction in adsorption capacity. [124]

7- Effect of Equilibrium Time

The time during which equilibrium occurs between the adsorbate and the adsorbent, or it is the time during which there is no decrease in the concentration of the solution. This time may range from hours to days, or even to weeks. [125]

Aims of Study

1. This study aims to synthesize semiconductor nanoparticles (ZnS) using the chemical precipitation method and green method. In the chemical precipitation methods, the nanostructures are produced through three stages chemical reaction followed by nucleation and growth of particles. The resulted particles may agglomerate during the formation process, which possibly leads to producing broad size distribution.

2. One of the key objectives of this project is to demonstrate a green synthesis technique to see whether this allows access to smaller and uniformed ZnS particles than observed previously with the chemical precipitation technique. This study thereby involves the addition of a suitable amount of broccoli flower extract to the precursor's solution, which, will hopefully reduce the agglomeration of atoms and form small ZnS nanoparticles.

3. Another target is to exploit these ZnS particles to remove the methylene blue dye from the wastewater.

4. Related to this, we to investigat the influence of the as-prepared particles on the dye adsorption. This can be achieve by comparing the adsorption rate of methylene blue dye using ZnS particles formed in the presence of broccoli extract with that recorded in the absence of broccoli extract.

CHAPTER TWO

EXPERIMENTAL PART

2.1 Introduction

This chapter will focus on the materials and will describe the key items of equipment that were employed in this project for fabrication and characterizing zinc sulfide nano-sized structures. We will also explain the preparation method of ZnS nanoparticles using chemical precipitation method and green synthesis.

2.2 Chemical Materials

In this work, deionized water was used as a reaction medium. Broccoli plants were purchased from local market in Kerbala. Other chemical materials that were used in this work are represented in Table 2.1.

Table 2.1 Chemical materials and their formula

NO.	Chemical materials	purity %	Company supplied
1	Methylene blue	90	Sigma Aldrich
2	Hydrochloric acid (HCl).	(36.5-38.0)	J. K. Baker, Netherlands
3	Sodium sulfide ($Na_2S.x\ H_2O$)	99	Thomas Baker
4	Sodium hydroxide (NaOH).	99	Panareac, Spain
5	Zinc sulfate hepta-hydrate ($ZnSO_4.7H_2O$).	99	Thomas Baker

2.3 Instruments used

A variety of instruments were used to form zinc sulfide nanoparticles, which are shown in Table 2.2.

Table 2.2 Instrumentation and manufacturers

No.	Instrument	Company	Work Place
1	Oven Memort. L OD- 080+ N	Labtech , Korrea	University of Kerbala
2	Themo stated Shaker	GFL (D-3006)-Germany.	University of Kerbala
3	Centrifuge-Hettich	Universall, Germany.	University of Kerbala
4	Hot plate Stirrer	Heido-MrHei-Standard, Germany	University of Kerbala
5	Transmission electron microscopy (TEM)	Zeiss Model SIGMA VP	Iran
6	X-Ray Diffraction Spectrophotometer(XRD)	X pert pro-PANalytical	Iran
7	PH meter	Korrea.PHOENIK	University of Kerbala
8	Field Emission-Scanning Electron Microscopy (FE-SEM)	SIGMA VP	Iran
9	UV-Vis spectrophotometer Double Beam-1800	Shimadzu-Japan	University of Kerbala
11	Electric Sensitive, Balance.TP-214	Germany Denver	University of Kerbala
12	Fourier transform infrared(FT-IR)	IRAffinity-1S instrument Shimadzu, Jaban	University of Kerbala
13	Blender	Chine	University of Kerbala

2.4 Samples preparation

2.4.1 Preparation of sodium sulfide solution

0.01M of Na_2S solution was prepared by dissolving 0.07804 g of in 100 mL of deionized water as shown in Figure 2.1. The prepared solution was stirred for half an hour before storing it in a dry place for further use.

Figure 2.1 Images for Na_2S flakes (a) and the colorless Na_2S solution (b).

2.4.2 Preparation of ZnSO$_4$ solution

0.01M of ZnSO$_4$ solution was prepared by dissolving 0.2875 g of zinc sulfate hepta-hydrate (ZnSO$_4$.7H$_2$O) in 100 mL of deionized water as shown in Figure 2.2. The prepared solution was stirred for 30 min before stirring in a dry place.

Figure 2.2 Images showing ZnSO$_4$ powder (a) and the colorless ZnSO$_4$ solution (b).

2.4.3 Preparing broccoli extract

The fresh broccoli flowers were collected and washed with tap water and then with deionized water to get rid of the dust. The flowers were dried in the shade for five days. The broccoli flowers were ground into a fine powder using a mill (see Figure 2.3).

To prepare the broccoli extract, 10 g of the broccoli powder was dissolved in 100 mL of deionized water. The solution was then heated for 10 min at 50 °C with stirring. Thereafter, filtration was achieved using filter paper No. 1, and the filtride was kept in fridge before using to synthesis ZnS nanoparticles.
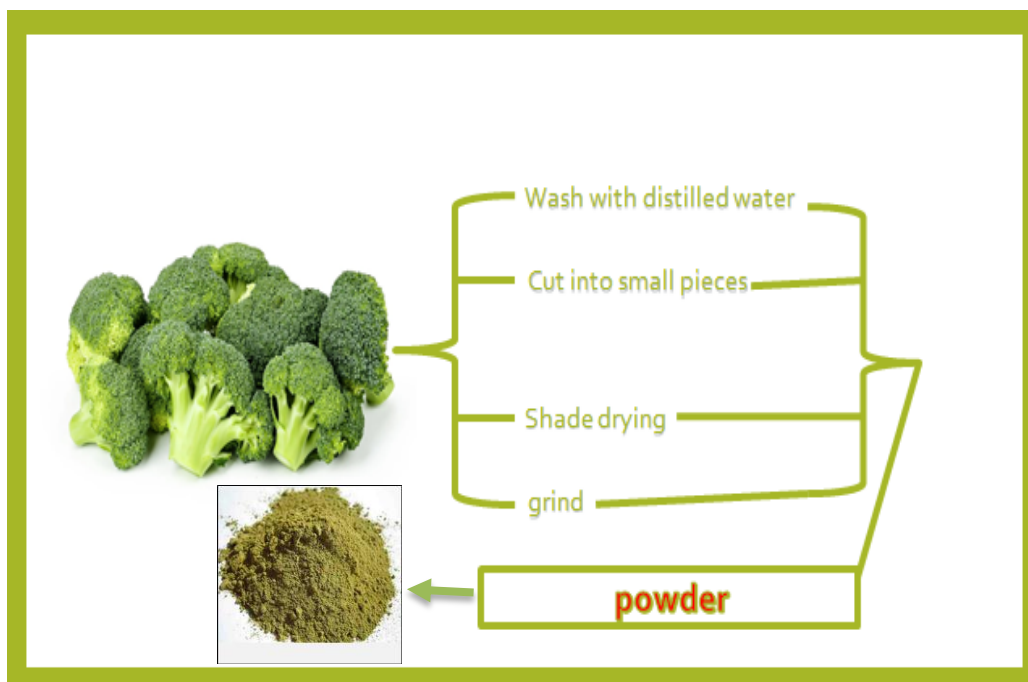
Figure 2.3 Illustration showing the method for preparing broccoli extract.

2.4.4 Preparation of methylene blue (MB) dye

Standard solution of methylene blue dye (10 ppm) was prepared by dissolving (0.005 g) of the dye in 500 mL de-ionized water.

2.4.5 Preparation 0.1 M of NaOH

To prepare sodium hydroxide solution, 0.4 g of NaOH flakes was dissolved in 100 mL of deionized water with a continuous stirring for approximately 15 min at 25 ^{o}C.

2.4.6 Preparation 0.1 M of HCl

0.85 mL of hydrochloric acid was added into a cleaned and dried 100 mL volumetric flask and the size was completed to 100 mL deionized water.

2.5 Chemical Precipitation Method

2.5.1 Synthesis of ZnS nanoparticles

An appropriate amount of zinc sulfate heptahydrate ($ZnSO_4.7H_2O$) (0.01 M) was dissolved in 100 ml of deionized water with a continuous stirring for approximately half an hour. To this solution, 0.01 M of sodium sulfide was added slowly and the solution was then left on a magnetic stirrer for a while at 25 ^{o}C. A cloudy white solution was obtained after 1 hour, which indicated the formation of zinc sulfide nanoparticles[127]. This solution will be a subject for studying the optical properties of ZnS NPs. Figure 2.4 shows a summary for the formation process of ZnS NPs.

In order to obtain ZnS NPs powder, the solution was centrifuged for 25 min at 4000 rpm, and the precipitate was then washed twice with deionized water to get rid of any unwanted materials. Finally, the precipitate was dried at 100 ^{o}C and kept in clean container for further uses.

Synthesis of ZnS Nanoparticles

Na$_2$S

½ h

Na$_2$S solution

Magnetic Stirrer

ZnSO$_4$

½ h

ZnSO$_4$ solution

A cloudy white Solution (ZnS NPs)

After 1h

Centrifuge

Oven

ZnS nanoparticles (white powder)
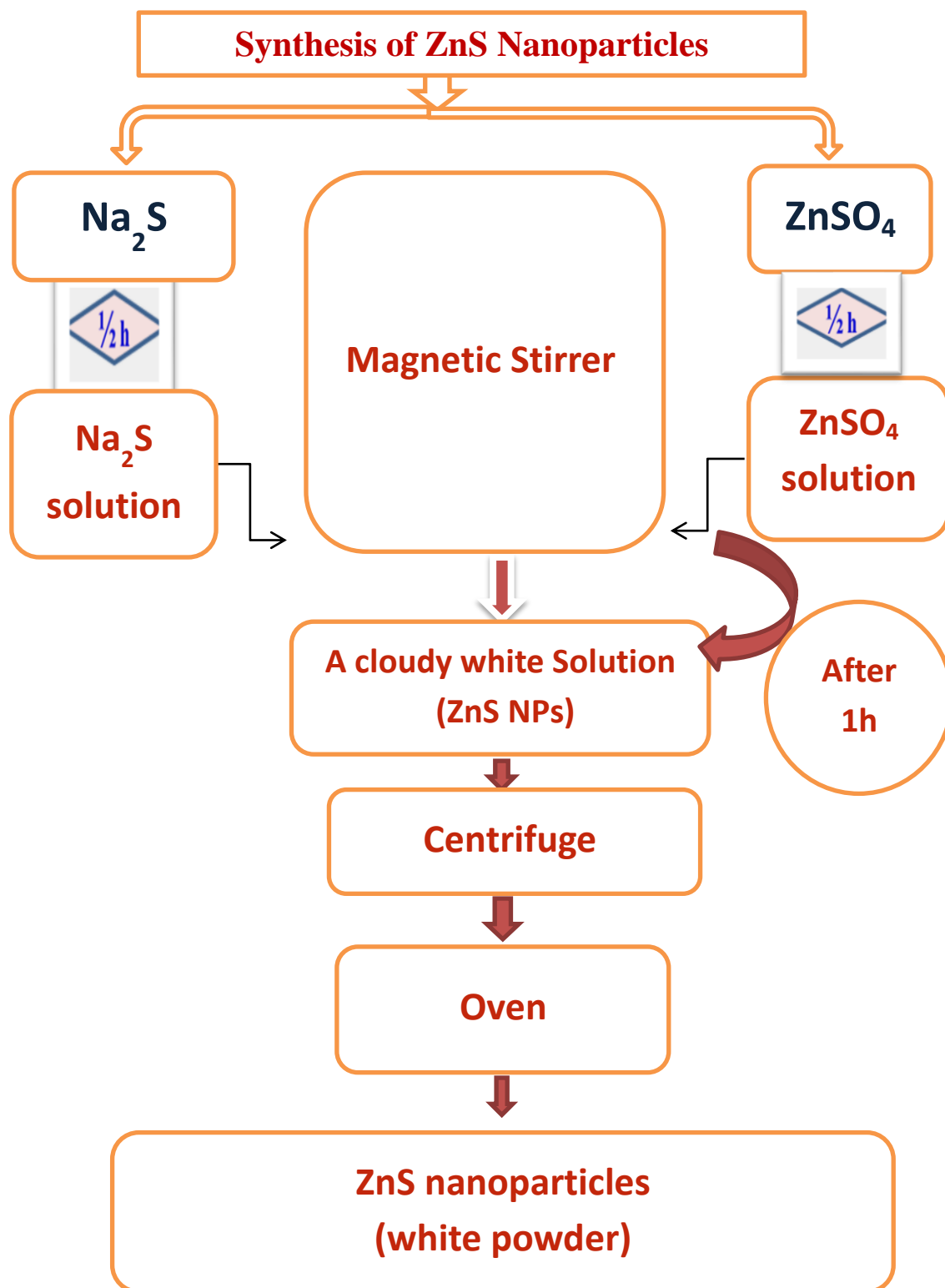
Figure 2.4 Diagram showing the formation process of ZnS nanoparticle.

2.5.2 The influence of pH on the formation process of ZnS NPs

The effect of pH on the formation process of zinc sulfide nanoparticles was studied to determine the best conditions to form ZnS NPs. After mixing $ZnSO_4$ and Na_2S solutions, the pH of the solution was adjusted by adding suitable amounts of either (0.1 M) HCl or (0.1 M) NaOH to make the solution pH in the range of 3–11.

2.5.3 The effect of temperature on the ZnS NPS

In this work, the effect of temperature on the growth process of ZnS nanoparticles was investigated too. After mixing $ZnSO_4$ (0.01 M) solution and Na_2S (0.01 M) solution, 25 mL of which was put into three different conical flasks. These flasks were then stirred for 60 min. One of the flasks was heated to 25 ^{o}C, another to 50 ^{o}C, the third one was heated to 70 ^{o}C.

2.5.4 Adsorption process for methylene blue dye

2.5.4.1 The effect of contact time on the adsorption

The adsorption behavior of zinc sulfide nanoparticles for methylene blue dye was investigated. 0.3 g of as-prepared ZnS particles was added into 20 mL of methylene blue solution (the initial concentration C_o was 5 ppm) under continuous stirring for different times at 25 ^{o}C.

2.5.4.2 The effect of zinc sulfide nanoparticles weight on the adsorption

Several solutions were synthesized by adding different amounts of zinc sulfide (0. 1, 0.2, 0.3, 0.4 and 0. 5 g) to 20 mL of methylene blue dye (5ppm), UV-Visible spectra were then recorded after filtration.

2.5.4.3 The effect of temperature on the adsorption process

To determine the temperature required for adsorption, different samples were prepared by mixing 20 mL of MB solution (5ppm) with 0.3 g of the prepared zinc sulfide particles at (25, 30, 40, and 50 ^{o}C). These samples were stirred for 15 min at a speed of 1 40 tr/min then filtered. The absorbance of the supernatants was then recorded by UV-Vis spectrophotometer.

2.5.4.4 pH influences on the adsorption

Several samples were prepared by mixing 20 mL of MB solution (5ppm) with 0.3 g of zinc sulfide particles at different pH values (4, 7, and 10). These samples were shaking for 15 min at 140 tr/min then filtered. The absorbance of the supernatants was then recorded by UV-Vis spectrophotometer.

2.6 Green synthesis approach

2.6.1 The bio-fabrication of zinc sulfide (B:ZnS) nanoparticles

To prepare ZnS particles using green synthesis, different amount of broccoli extract (6,10,20,40) ml was added to the zinc sulfate heptahydrate and stirred for a few minutes as seen in Figure 2.5. Sodium sulfide solution was then added slowly to the mixture and stirred for one hour. A cloudy white solution was obtained which indicated the formation of ZnS nanoparticles. Finally, the precipitate (zinc sulfide particles) was washed several times with deionized water and dried to 100 ^{o}C**.**

Figure 2.5 Broccoli extract with zinc sulfate heptahydrate solution.

2.6.2 The influence of the concentration of broccoli extract on the ZnS nanoparticles absorption

The effect of broccoli flower extract concentration on the ZnS nanoparticles formation was studied by changing the amount of the extract (6 mL, 10 mL, 20 mL and 40 mL). The reaction was carried out at room tempter for 60 min stirring.

2.6.3 The influence of pH on the formation of B:ZnS nanoparticles

PH of the solution was adjusted by adding either 0.1 M of NaOH or 0.1 M of HCl, to make the solutions pH: 3, 5, 7, 9, 11, and 12. Thereafter, the absorbance of these solutions was measured at room temperature ^{o}C after 60 min of mixing using a UV- Vis spectrophotometer.

2.6.4 Preparation of B:ZnS:MB solutions

The absorption behavior of zinc sulfide nanoparticles for methylene blue dye was investigated. 0.3 g of B:ZnS particles were added into 20 mL of methylene blue solution (the initial concentration C_o was 5 ppm) under continuous stirring for different times at room temperature.

2.6.4.1 Effect of contact time on the adsorption

To study the ability of B:ZnS nanoparticles, which were formed in the presence of broccoli extract, as an adsorbent, 20 mL of MB solution (5 ppm) was mixed with different time of bio-fabrication zinc sulfide particles at 30 ^{o}C. This sample was shaken for different periods (5-60 minutes) at a speed of 140 tr/min before being filtered. The absorbance of the supernatants was then measured using an UV-Vis spectrophotometer.

2.6.4.2 Effect of Adsorbent dosage on the Adsorption

The effect of zinc sulfide nanoparticles weight on the adsorption process was studied. Different quantities of B:ZnS particles (0.1, 0.2, 0.3, 0.4, and 0.5 g) were mixed with 20 mL of MB dye solution (5 ppm) and then the spectra of the supernatants were recorded after centrifuging.

2.6.4.3 The effect of pH on the removal of MB dye

The effect of pH on dye removal was studied. pH was varied from (4,7,10) by adding either 0.1 M of HCL or 0.1 M NaOH to the solution contains 0.3 g of B:ZnS and 20 mL MB.

2.7 Calibration curve for of MB dye solutions

Six solutions of methylene blue dye were prepared with different concentrations (1, 2, 3, 5, and 10 ppm) as shown in Figure 2.6. To determine the best concentration of the dye, calibration curve was plotted (see Figure 2.7).
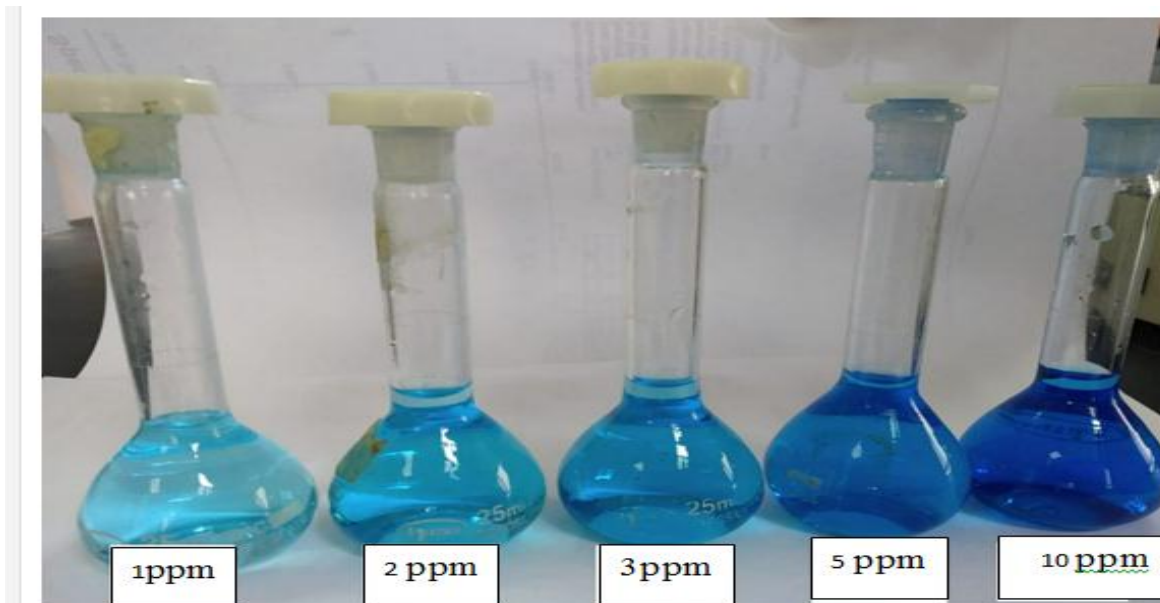
Figure 2.6 A series of different colored methylene blue solutions at different concentrations.
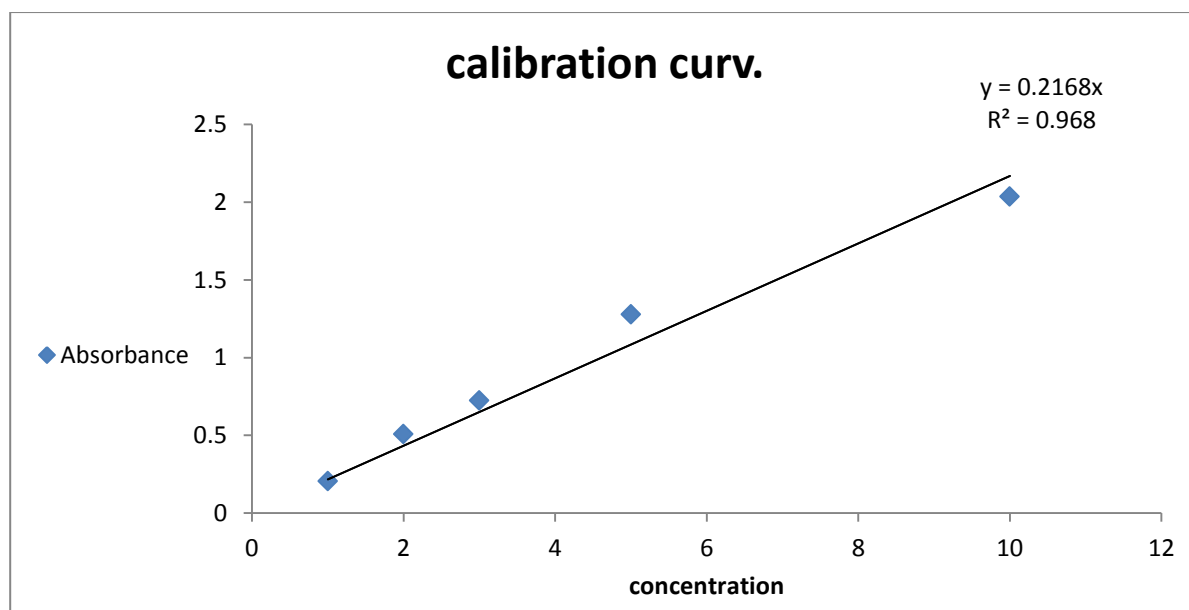
Figure 2.7 The calibration curve of methylene blue dye.

Table 2.3 Showing the absorbance corresponding concentration.

Absorbance	concentration
0.205	1
0.509	2
0.725	3
1.278	5
2.035	10

2.8 Characterization of ZnS nanoparticles

In this work, the formation of zinc sulfide was confirmed through different techniques. UV-Vis spectrometer was utilized to study the optical properties of as-prepared ZnS nanoparticles. FT-IR spectrophotometer was used to confirm the formation of ZnS particles and to identify the functional groups that are possibly present on the ZnS particle surface. The particles shape and size were characterized by FE-SEM and Transmission Electron Microscopy TEM. ImageJ software program was used to calculate the particles size.[128]

The presence of zinc and sulfur elements in ZnS particles was confirmed using Energy Dispersive X-ray spectroscopy. The crystalline structure and the crystallite size were determined from XRD technique.

2.8.1 UV-Visible spectrophotometry

To ascertain that ZnS nanoparticles have formed successfully and to study their adsorption effect, UV-Visible spectrometry was used. All spectra measurements were recorded using a scanning UV-1800 spectrophotometer (Shimadzu, Japan), This is shown in Figure 2.8. Quartz cuvettes with a path length of 1 cm were used. UV-visible spectroscopy depends on the transmission of visible light or ultraviolet rays through the sample to determine the presence of the light-absorbing substance inside the sample. The process of photon absorption within

the wavelength range (200 nm to 800 nm) usually leads to the occurrence of transition electrons within the absorbing molecule.

Figure 2.8 Image shows UV-Visible spectrophotometry

2.8.2 Fourier Transform Infrared Analysis (FTIR)

Fourier transform infrared spectroscopy (FTIR) was used to identifying the chemical composition of materials and the most important functional groups that are possibly exist on the ZnS particles. The FT-IR spectra were recorded in the range 400 to 4000 cm^{-1} using IRAffinity-1S instrument (Shimadzu, Jaban), see Figure 2.9. Voltage of 220 to 240 V was applied. The most interesting point about this type of FTIR spectroscopy is a very small solid sample that is required; and the sample will be placed on zinc selaned lens instead of mixing with KBr in conventional FTIR spectroscopy.

Figure 2.9 Image shows Fourier Transform Infrared (FTIR) spectrophotometer.

2.8.3 Field Emission Scanning Electron Microscopes (FE-SEM)

To study the structural properties of zinc sulfide nanoparticles, microscopic techniques were employed. FE-SEM (see Figure 2.10) is an advanced microscope that gives information about the surface morphology and has the ability to observe very fine features. It has a wide range of magnification (10 - 500,000 times) compared to the magnification of the better optical microscope.[129]

FE-SEM produces high resolution images and less electrostatic distortion. It can be used to image different samples, for example, inorganic samples such as ceramics, metals, and composite materials, and organic samples such as cells, membranes, enzymes, and polymers.[130]

In FE-SEM, images are produced by scanning the sample surface with a focused electronic beam. The interaction of electrons with the sample atoms leads to producing signals that carry information about the surface topography.
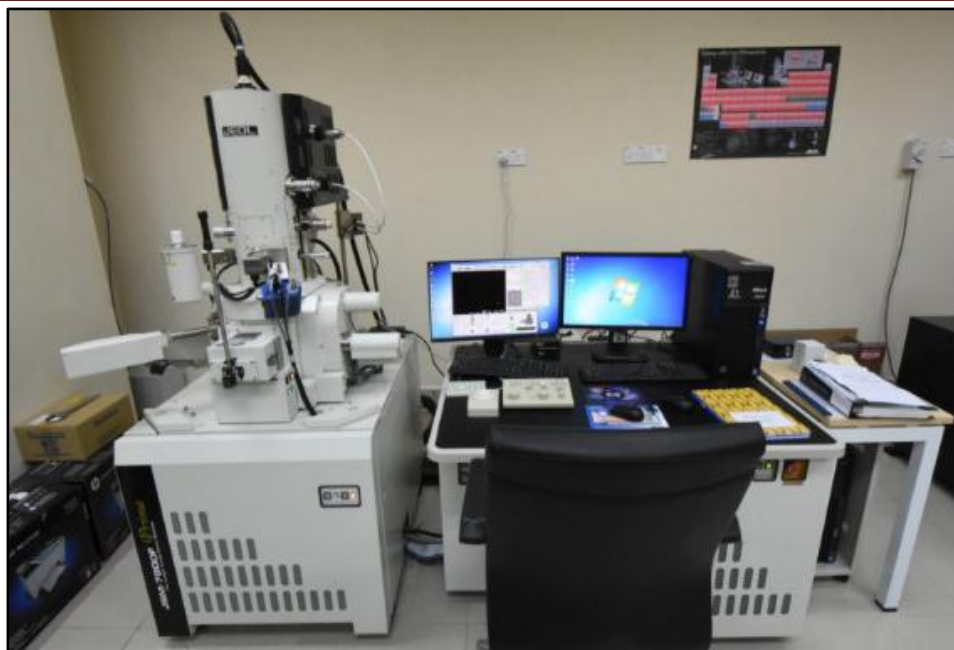
Figure 2.10 Image shows Field-Emission Scanning Electron Microscopy.

2.8.4 Transmission Electron Microscopy (TEM)

Transmission electron microscopy (TEM) is an invaluable tool for investigation of nano-sized materials (see Figure 2.11). It offers useful information about their shape, size and crystal structure. The best resolution can be achieved by TEM is ~ 1Å which is higher than that of other types of electronic microscopes. TEM can be used with wide range of materials even with the biological-samples.[131]

 TEM is considered as an expensive tool as it works under high vacuum to prevent or reduce the scattering of elections by background gasses which are possibly present inside it. Furthermore, the preparation of sample is complicated because the sample must be very thin to allow the electron beam to pass through it. The sample should also be conductive to avoid charging, meaning the non-conductive sample must be covered with a metallic layer such as layer of gold.

In the TEM technique, a beam of electrons, which is usually formed by the thermionic emission, pass through a very thin sample and interacts with it. Images produce as a result of the interaction of electrons with the sample.[132]

Figure 2.11 Image showing the (TEM) Microscopy

2.8.5 Energy Dispersive X-rays spectroscopy (EDX)

Electron microscopies (TEM and SEM) are sometimes X-rays equipped with small device called energy dispersive X-rays spectroscopy (see Figure 2.12). EDX is an analytical technique used to analyze elements to know the chemical properties of samples, and it is one of the types of X-rays spectroscopy. This method is based on the interaction of a sample with an X-rays excitation source. The principle behind this method is that each element has an atomic structure that allows for a different set of peaks in the X-rays emission spectrum. In the EDX analysis method, the electron beam hits the sample, excites an electron, and the electron explodes creating an electron hole in the electronic structure of element.
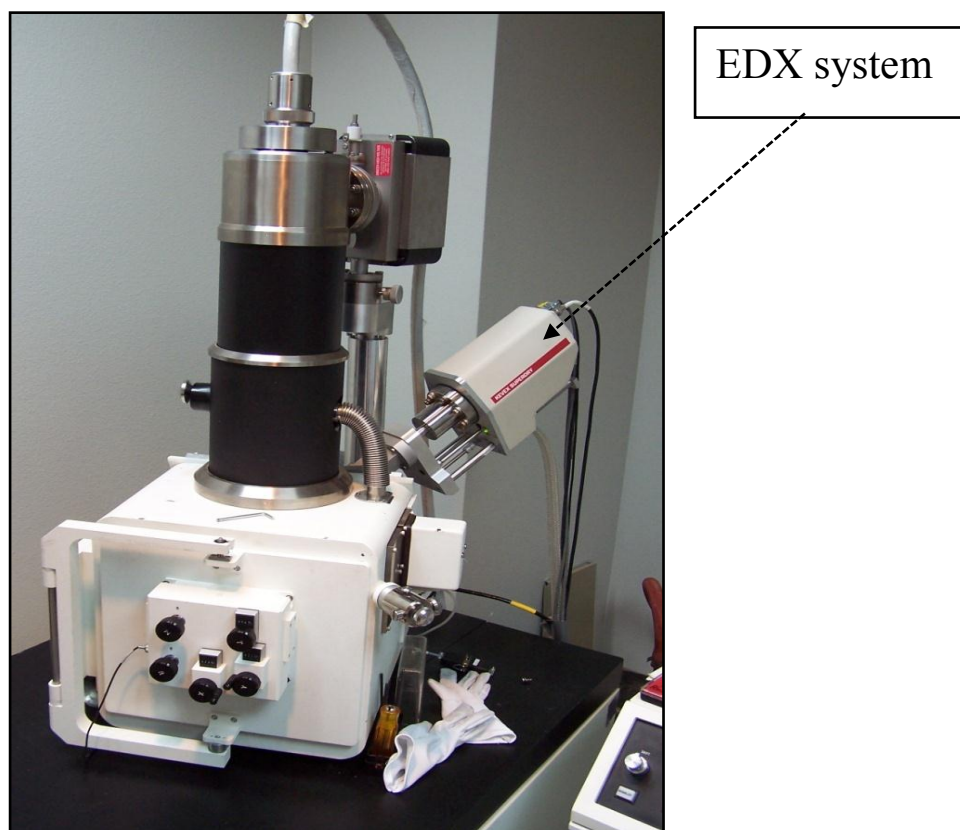
Figure 2.12 Image shows Energy dispersive X-rays device.

2.8.6 X-rays Diffraction (XRD)

XRD is a non-destructive analytical technique that provides information about the crystal structure, chemical composition, and physical properties of materials and thin layers of crystalline materials. These techniques rely on observing the scattering of X-rays (when they are falling on the sample) as a function of the angle of the incidence beam. The crystalline structure of our particles was determined using the XRD instrument (X pert pro-PANalytical company).
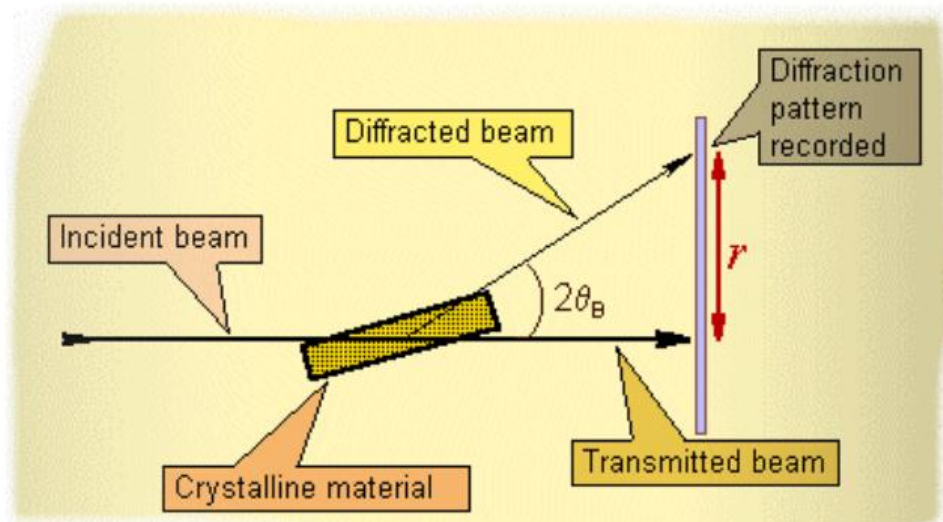
Figure 2.13 Scheme showing the basic principle for(XRD) technique.

Figure 2.13 shows the basic principle of XRD device. When high-speed electrons hit a target surface, an x-ray will produce. This ray will interact with the electrons of the atoms which are present in the crystal. The atomic planes allow a part of the ray to pass while the other part will reflect. The incident angle (θ) is similar to the reflected angle which is known Bragg angle as shown in Figure 2.14.[133] Bragg's law based on the fact that the difference in the path between two rays is equal to multiples of the wavelength.

$n\lambda = 2 \, d \sin \theta$…….. (2.1)

Whereas:

θ: Bragg angle in degree.

λ: the wavelength of X-ray (CuKα1) (λ=0.154)

n: an integer called the order of reflection (n=1, 2, 3)

d: the distance between the set of levels.

The X-ray diffraction pattern is considered as a thumbprint to diagnose the substance by comparing the chart of the sample with the standard global information bases such as the Center International Data Diffraction (ICDD).
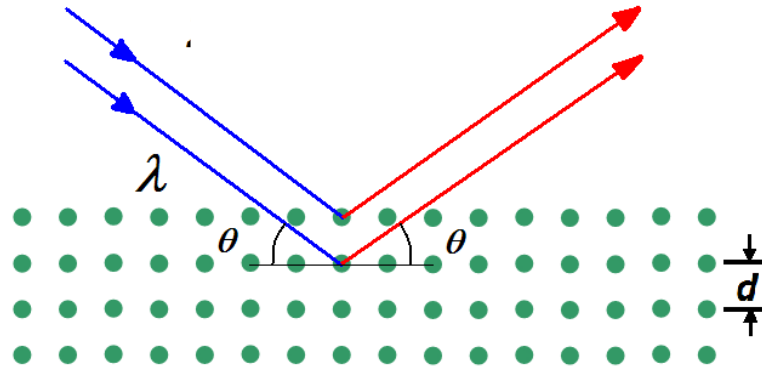
Figure 2.14 Illustration showing Bragg's law

CHAPTER THREE

RESULTS AND DISCUSSION

3.1 Introduction

In this chapter, the optical and structural properties of ZnS NPs before and after the addition of broccoli extract will be explained, the findings will be then compared to see whether the extract has an influence on the ZnS particles properties. The adsorption effect of ZnS nanoparticles for methylene blue dye will study too.

3.2 properties of ZnS NPs result from chemical precipitation method

3.2.1 Optical properties of ZnS nanoparticles

3.2.1.1 The effect of precursor's concentration on the absorption process of ZnS nanoparticles.

In order to establish the best condition to prepare ZnS nanoparticles, different concentrations of precursors were selected (0.1 M, 0.01M and 0.001 M). Figure 3.1 shows that by mixing 0.001 M of sodium sulfide with 0.001 M of zinc sulfate, a weak absorption peak at 298 nm was observed and the peak intensity is low. At higher concentration of 0.1 M of starting materials, abroad peak at 420 nm was observed. The best peak was noticed when the concentration was 0.01M, at this concentration the absorption peak was found to be ~ 296 nm. This blue shift (compared to the bulk ZnS 340 nm) could be attributed to the quantum confinement.[134]
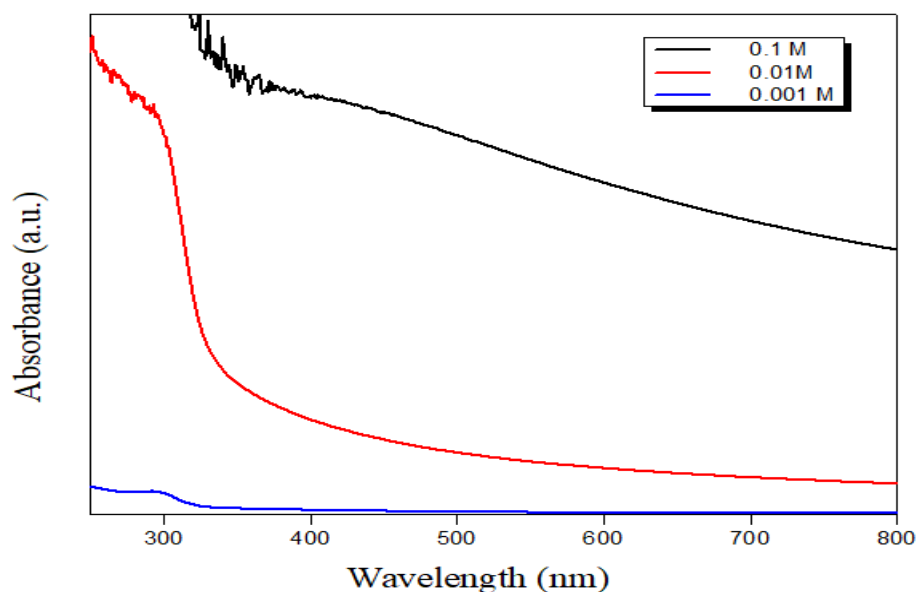
Figure 3.1 UV-Vis spectra of zinc sulfide nanoparticles as a function of the concentration of the starting materials sodium sulfide and zinc sulfate. The reaction time was 1 hour.

3.2.1.2 The effect of reaction time on the absorption of zinc sulfide nanoparticles

The effect of the reaction time on the absorption band of ZnS nanostructures was investigated. After the addition of 0.01 M of sodium sulfide to 0.01 M of zinc sulfate, the solution was stirred for different times (0, 1, 2 and 3 hours) at room temperature. It is clear from Figure 3.2 that after stirring for 3 hours, absorption band becomes broad and shift towards longer wavelengths compared with bulk ZnS. This could be due to the agglomeration process of ZnS nanoparticles. An intense absorption peak at 295 nm was observed when the solution mixed for one hour at room temperature at pH =5.
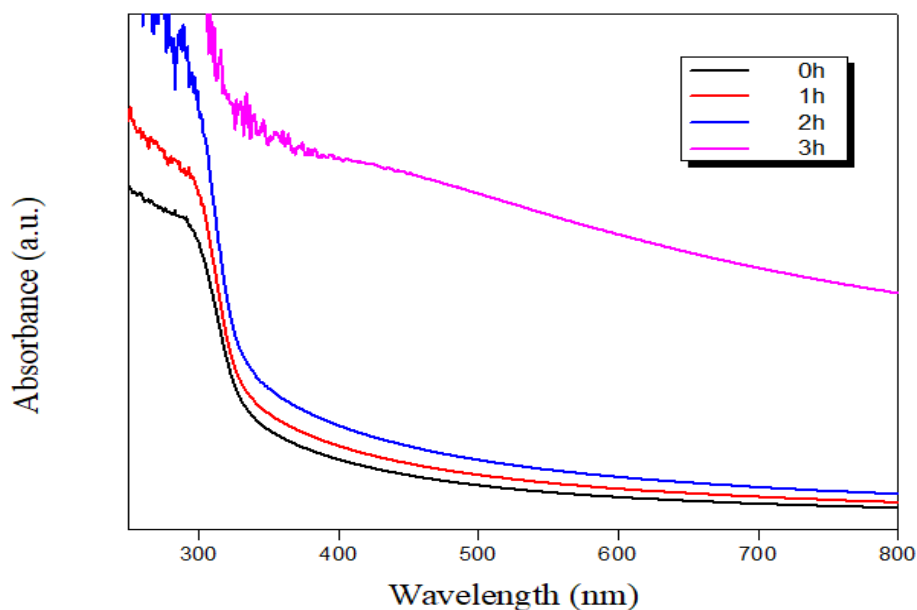
Figure 3.2 The optical absorption spectrum of ZnS nanoparticles at different reaction time, the concentration of the precursors was (0.01 M) at pH =5.

3.2.1.3 The effect of pH on the ZnS formation

The effect of pH on the formation process of ZnS particles was studied. Different pH values were chosen (3, 5, 7, 9 and 11) by adding 0.1 M of HCl and 0.1 M of NaOH. It seems from Figure 3.3 that the intensity of the peaks increases at higher pH values. However, at a pH of 11, the intensity of the ZnS peak starts to decrease and becomes lesser at pH= 9. This could be because of the formation of zinc hydroxide due to increasing hydroxide ions in the solution, which leads to reduced Zn^{2+} ions.[135] One of the key aims of this project is to explore the adsorption of methylene blue dye on the ZnS particle's surface, therefore, producing small ZnS nanoparticles is our goal. In this work, from here onwards the pH solution was adjusted on 5.
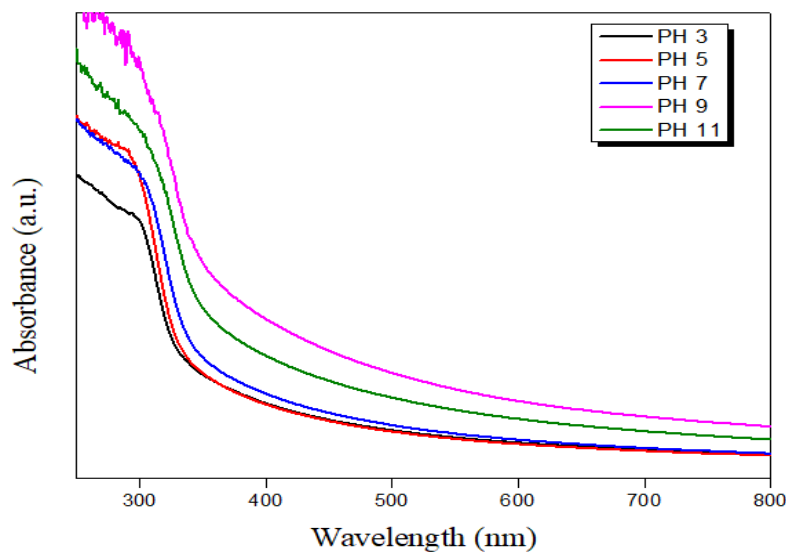
Figure 3.3 The effect of pH on the absorption spectra of as-prepared ZnS nanoparticles, the concentration of the precursors was 0.01 M and the reaction time was 1 hour.

3.2.1.4 The effect of temperature on the ZnS formation

It is clear from Figure 3.4 that the absorption band of ZnS NPs depends strongly on the reaction temperature. At room temperature (25 ^{o}C), the absorption peak was measured to be ~ 295 nm, which is in a blue shift from that of bulk ZnS (340 nm), [127] and the peak intensity is high compared with that of 50 ^{o}C. Therefore, the best temperature to prepare ZnS nanoparticles is 25 ^{o}C.
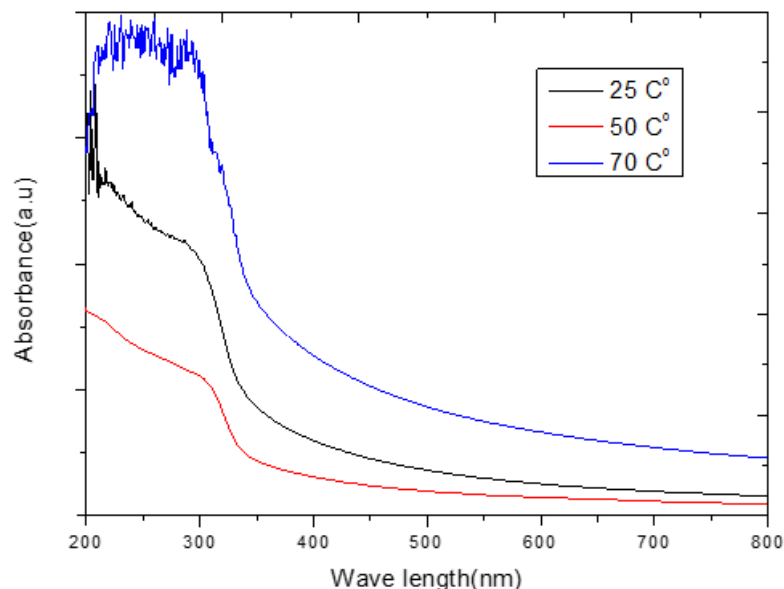
Figure 3.4 The effect of temperature on the absorption spectra of as-prepared ZnS nanoparticles, the concentration of the precursors was 0.01 M and the reaction time was 1 hour.

3.2.1.5 Absorption spectrum and band gap for ZnS nanoparticles

After establishing the favorable conditions to study the optical properties of ZnS particles, the band gap was estimated from the absorption edge of as-prepared ZnS nanoparticles. UV-Vis absorption spectrum, which is recorded in the range of 250 – 800 nm, shows an absorption peak of ZnS at lower wavelengths ~296 nm compared to the absorption peak of bulk ZnS at 340 nm.[136]

The Band gap energy of ZnS nanoparticles can be calculated using tauc relationship.[137] The extrapolation of the liner portion of the UV-Vis spectrum against the photon energy (*hv*) gives a band gap energy value of 3.8 eV for the ZnS nanoparticles (see Figure 3.5), which is higher than that of bulk ZnS (*Eg* = 3.6 eV). [138,139]

$$\alpha h v = C \ (h v - E_g)^n \quad \ldots\ldots\ldots\ldots\ldots\ldots\ldots.(3.1)$$

Where (n) is the direct electronic transition which is equal to 0.5.[140] (α) is the absorption coefficient, h is the Plank's constant and v is the frequency of light. (E_g) is the band gap energy and C is the constant.
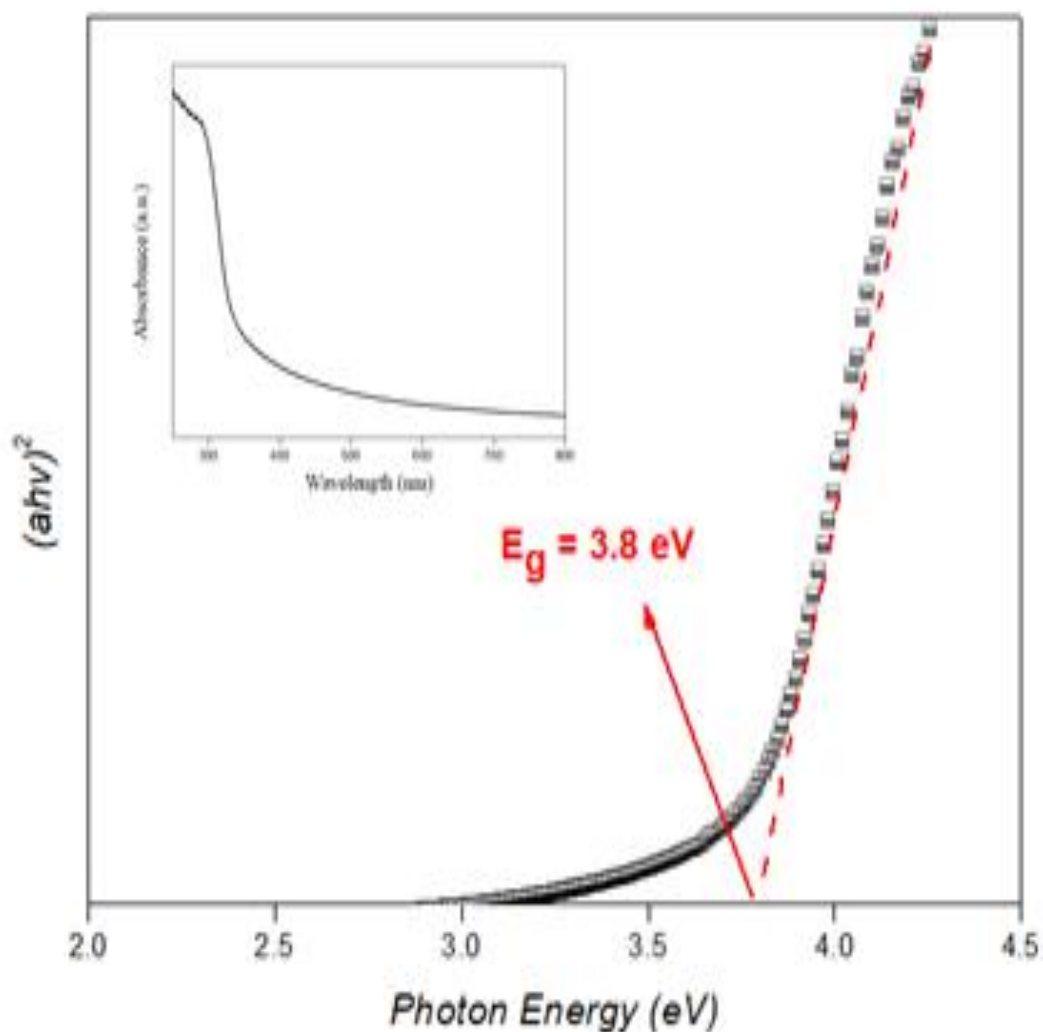
Figure 3.5 Band gap energy of ZnS particles calculated from the Tuac equation. The extrapolation gives E_g of 3.8 eV. The inset shows the absorption spectrum of ZnS nanoparticles at 25 $^{\circ}$C and after one hour starring.

3.2.2 Structural properties

3.2. 2.1 Field Emission Scanning Electron Microscopy

The surface morphology of the prepared ZnS nanoparticles was examined using Field Emission Scanning Electron Microscopy. It is clear from FE-SEM image (Figure 3.6(a)) that the particles have a spherical shape and the size of these spherical nanoparticles is identified to be ~ 8 nm to 10 nm.
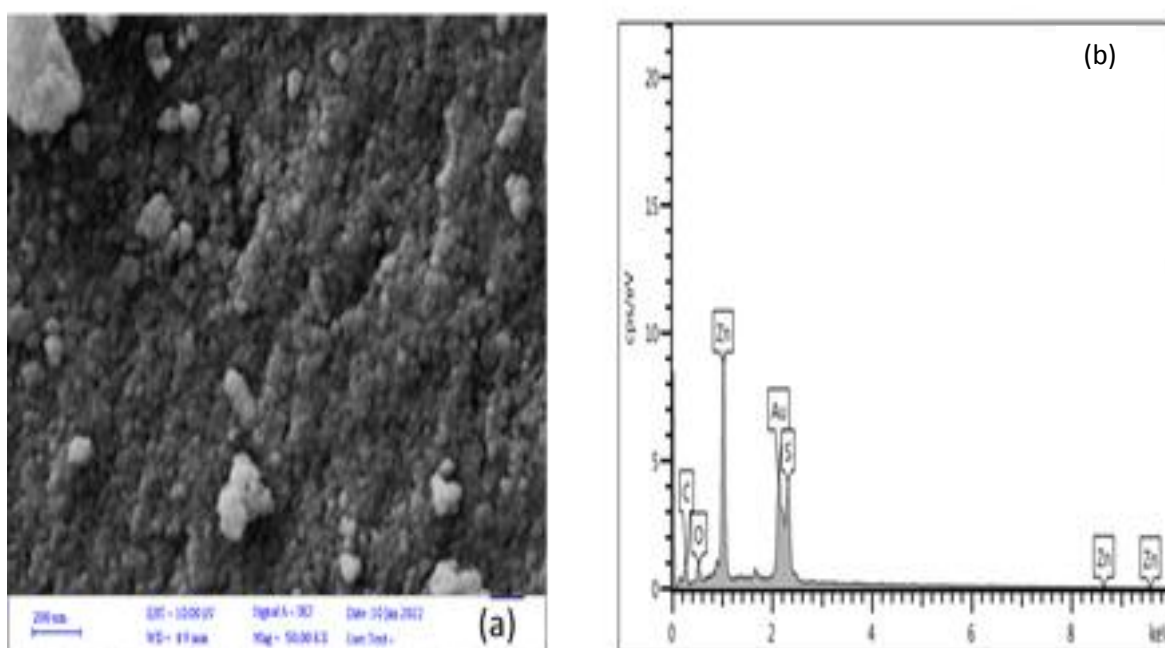
Figure 3.6 FE-SEM images of ZnS nanoparticles, the scale bar of image (a) is 200 nm. EDX graph of ZnS nanoparticles formed from chemical precipitation method (b).

The elemental analysis of our sample was identified using Energy Dispersive X-rays spectroscopy. As it seen from Figure 3.6(b) that the most abundant elements are Zn and S, this result confirms the formation of pure ZnS particles. The presence of gold element peak in the graph is attributed to the coverage process of ZnS particles with gold metal (to produce conducting sample) before measuring the FE-SEM. Finally, the appearance of carbon element is referred to the latex of the sample holder of FE-SEM as a result of incomplete coating of the sample.[141]

3.2.2.2 Transmission Electron Microscopy

To study the shape and size of ZnS nanoparticles transmission electron microscopy was used. It is clear from TEM images in Figure 3.7 that the majority of ZnS nanoparticles have spherical shape and some of them clustered together. The size of these particles was analyzed using imageJ software[141] and it was found to be around 10 nm in average.
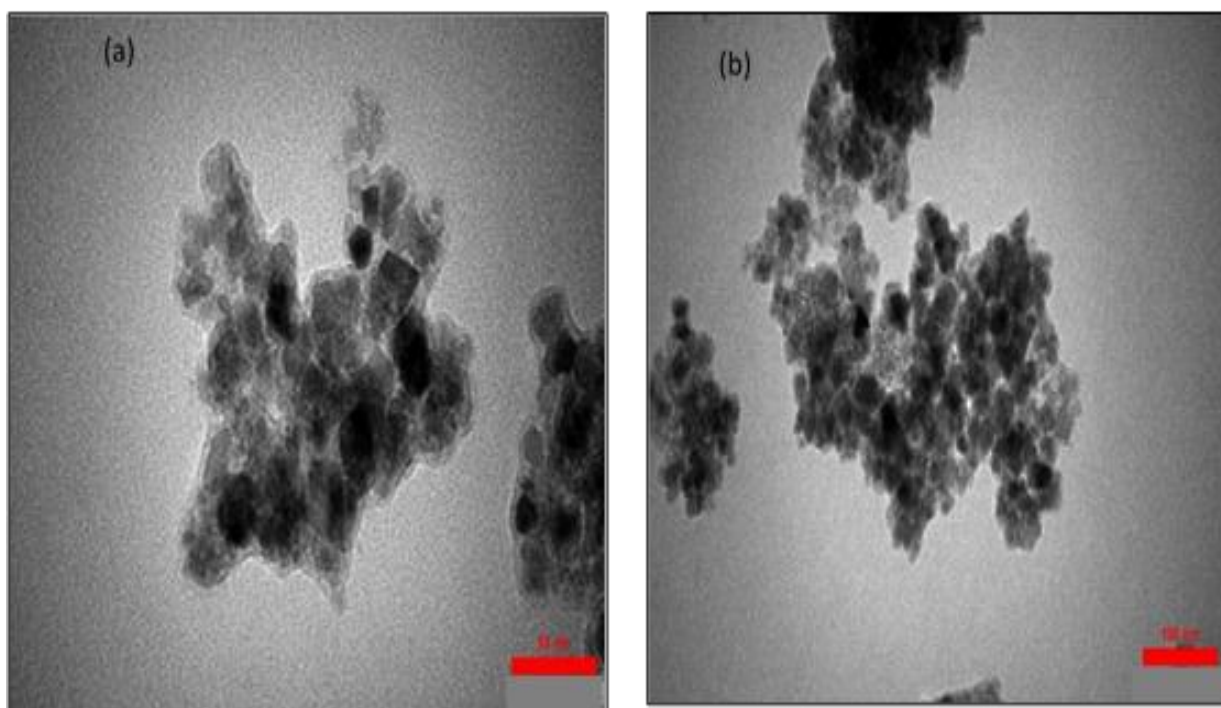
Figure 3.7 TEM images of ZnS nanoparticles formed using chemical deposition method. The scale bar of image (a) is 50 nm and image (b) is 100 nm.

3.2.2.3 Crystalline structure of ZnS nanoparticles

It is obvious from Figure 3.8 that our prepared ZnS particles have a crystalline structure. XRD pattern revels three diffraction peaks at 29.2^o, 49° and 56° which related to 111, 220 and 311 planes, respectively, suggesting the formation of cubic structure. This finding is in good agreement with the results obtained in recent experiments.[127] The peaks indicating a cubic structure for the synthesized nanocrystals because of the low-temperature process, the hexagonal ZnS is

relatively difficult to prepare. The cubic ZnS is stable at room temperature, while the hexagonal ZnS is formed at high temperatures. No other peaks were noticed in Figure 3.8 confirming the purity of our ZnS nanocrystals. The crystallite size of ZnS was calculated from Scherre equation[142] and it was found to be ~ 1.5 nm.

$$D = \frac{K\lambda}{\beta \cos\theta} \quad \ldots\ldots\ldots\ldots\ldots(3.2)$$

Where D is the average crystallite size, k is the constant crystal lattice (0.94), λ = 0.154 nm which is the wavelength the incident X-rays beam, β is the full width at half maximum in radians and θ is the Bragg's angle in radians.
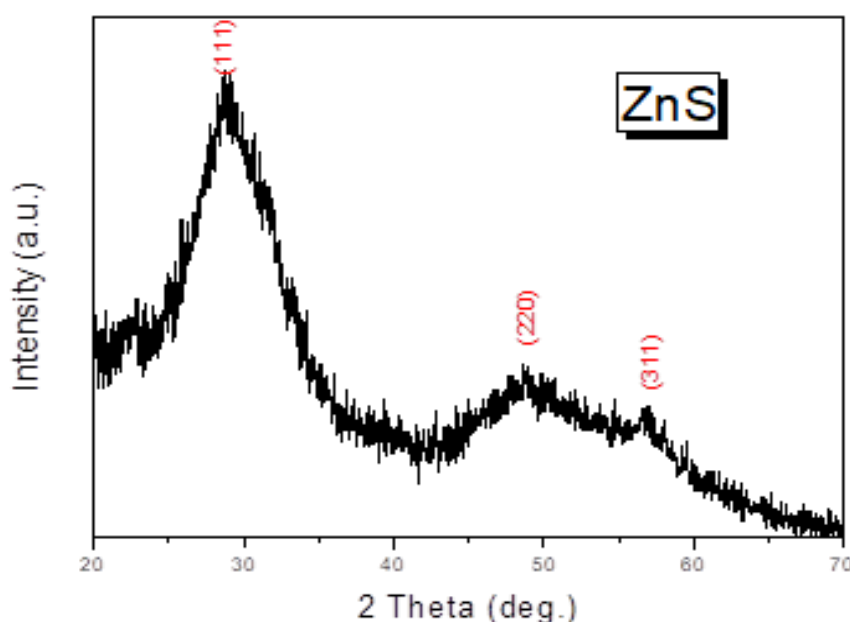
Figure 3.8 XRD pattern of ZnS nanoparticles.

Table 3.1 shows the crystallite size and the distance between lattice planes. Direct evidence for the formation of ZnS at the nano-scale level has been presented by studying the crystalline structures of ZnS due to the appearance of wide peaks which indicates the formation of small size ZnS crystallites.[143]

Table 3.1 Crystallite size and theta position for ZnS particles.

2θ deg.	FWHM	Crystallite size D(nm)	Average D(nm)	d-spacing [Å]
29.2	4.9	1.675382978	1.471931622	3.05986
49	6	1.455059914		1.85667
56	7	1.285351973		1.63008

3.2.2.4 Fourier transformation infrared spectrum (FTIR) for ZnS particles

Figure 3.9 shows a broad absorption band centered at 3450 cm^{-1} can be attributed to O-H stretching mode of H_2O which could be adsorbed on the surface of zinc sulfide particles. Peaks that appear at region 612 and 657 are assigned to the Zn-S bond confirming the formation of ZnS particles. [144] The sharp peaks centered at 1058 cm^{-1} may be attributed to S-O stretching. The peak 1629.55 cm^{-1} could be assigned to H-O-H bending.
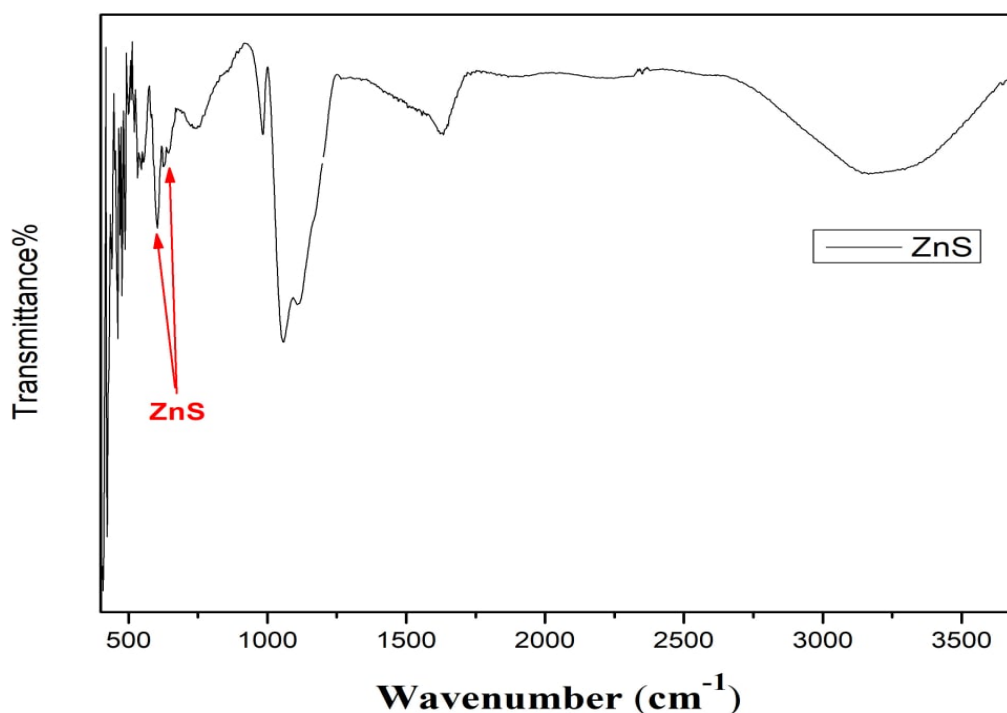
Figure 3.9 FTIR spectrum of ZnS nanoparticles.

3. 3 Adsorption behavior of ZnS nanoparticles resulted from chemical precipitating method

3.3.1 Effect of the contact time on the adsorption

To determine the time required for the dye to be adsorbed, different samples were prepared by mixing 20 ml of MB solution (5ppm) with 0.3 g of our prepared zinc sulfide particles at 25 ^{o}C. These samples were shaking for different periods of time (5-60 minutes) at a speed of 140 tr/min then filtered. The absorbance of the supernatants was then recorded by UV-Visible spectrophotometer. It is clear from Figure 3.10 that the peaks intensity of MB dye decreases as the contact time increase, which confirms the adsorption of the dye on the surface of ZnS nanoparticles.
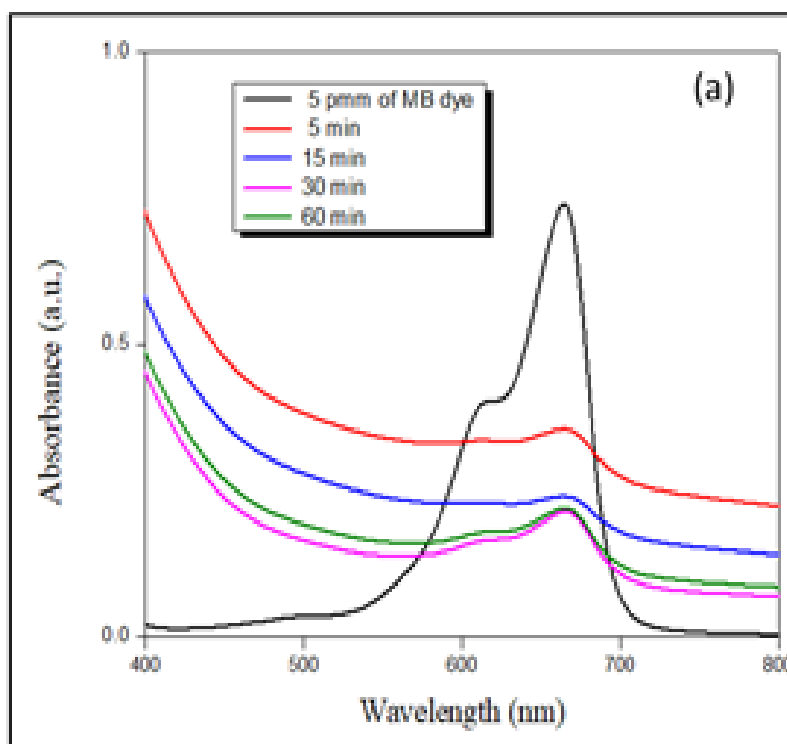
Figure 3.10 UV-Vis spectra of zinc sulfide nanoparticles with MB dye as a function of the contact time.

3.3.2 Effect of adsorbent weight on adsorption process

The effect of ZnS nanoparticles weight on the adsorption process of MB dye was investigated. Figure 3.11 show that when the amount of ZnS particles increases the adsorption of the dye on their surfaces increases too.   Percentage of dye removal (*%DR*) was obtained using the following equation 3.3:

$$\text{Dye removal \%} = \frac{(C_i - C_e)}{C_i} \times 100 \qquad \text{... ... ...} \quad (3.3)$$

Where C_i is the initial concentration of MB dye (mg/ L), and C_e is the equilibrium concentration of MB dye after adsorption (mg/L). [145, 146] The best removal ratio was found to be 80% at pH = 4.
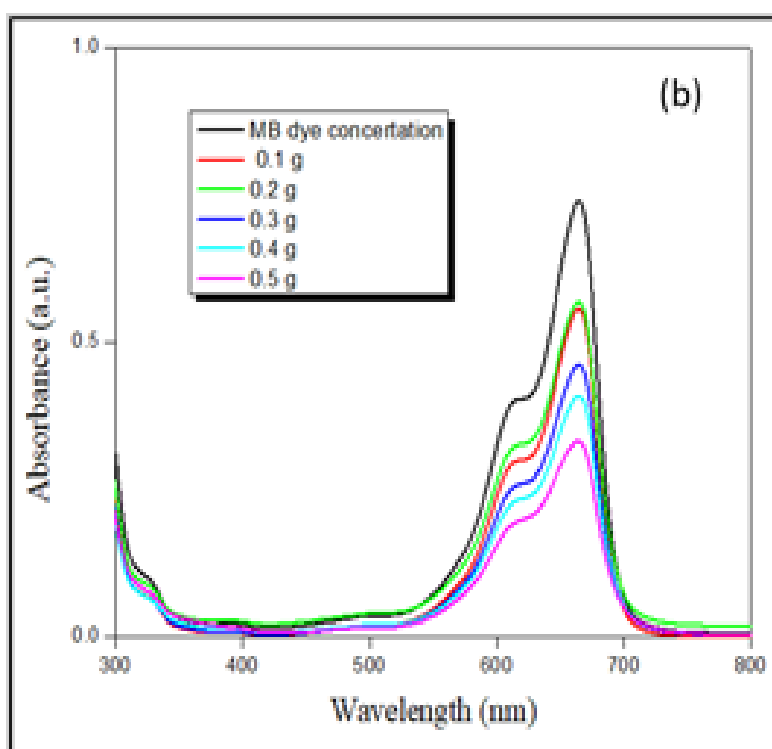
Figure 3.11 UV-Vis spectra of zinc sulfide nanoparticles with MB dye as a function of the amount of ZnS particles. The absorption band of MB dye is 666 nm**.**

Table 3.2 Displays the percentage of removal versus change in amount ZnS NPs.

DR%	C_e	Abs.	ZnS	No.
49.72	2.514	0.545	0.1 g	1
47.79	2.611	0.566	0.2 g	2
57.47	2.126	0.461	0.3 g	3
62.45	1.877	0.407	0.4 g	4
69.46	1.527	0.331	0.5 g	5

3.3.3 Effect of temperature on the adsorption process

To study the effect of temperature on degradation efficiency of MB on the surface of ZnS nanoparticles, the ZnS:MB solutions were heated to 25, 30, 40, and 50 ^{o}C. According to the Figure 3.12, the peaks intensity decreases as the temperature increases and the optimal temperature for dye degradation was found to be 50 ^{o}C. take 0.3 g from zinc sulfide.
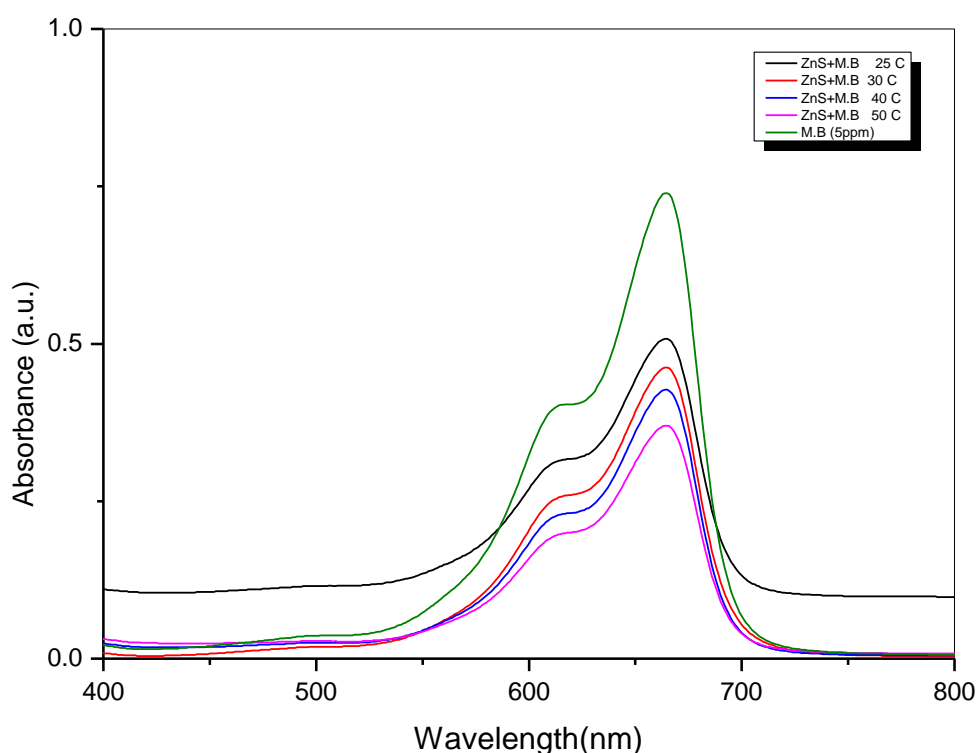
Figure 3.12 The effect of temperature on the adsorption behavior of zinc sulfide nanoparticles for MB dye.

Table 3.3 Displays the percentage of removal versus change in temperature.

DR%	C_e	Abs.	TMP.	No.
57. 47	2.126	0.461	25 °C	1
53.14	2.343	0.508	30 °C	2
60.61	1.970	0.427	40 °C	3
65. 87	1. 707	0.37	50 °C	4

3.3.4 **Effect of pH on the adsorption process**

Due to the high surface area of as-synthesized ZnS nanoparticles, they consider as an excellent candidate to remove the wastewater from aqueous solutions. Thereby, pH solution is expected to influence the adsorption of MB dye. It seems from Figure 3.13 that the intensity of the MB dye peaks increase at pH 7.
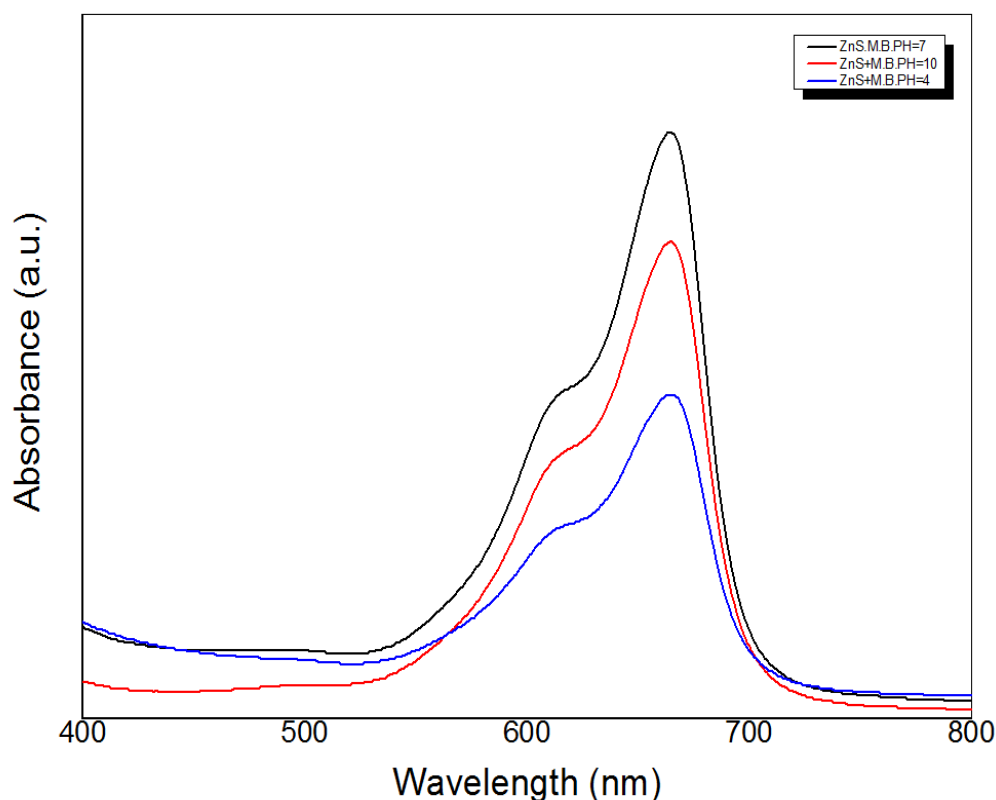
Figure 3.13 The effect of pH on the adsorption.

Table 3.4 Displays the percentage of removal versus change in (PH) for ZnS.

DR%	C_e	Abs.	pH	No.
79.98	1.001	0.217	4	1
79.61	1.019	0.221	7	2
69.28	1.536	0.333	10	3

3.4 ZnS nanoparticles properties formed from green synthesis approach

3.4.1 The optical properties of B:ZnS

3.4.1.1 The influence of extract amount on the optical absorption of B:ZnS

The appearance of white color after mixing starting materials with broccoli flowers extract is an indicator for the formation of biosynthesis ZnS particles (B:ZnS). Another evidence for the formation of ZnS particles has been provided by studying their optical properties.

Different amounts of broccoli extract (6 mL, 10 mL, 20 mL, and 40 mL) were chosen to identify the optimal conditions for producing small nanoparticles with a high surface-to-area ratio, while the amount of the other two precursors were kept the same (100 mL). Figure 3.14 shows that the absorption peaks depend strongly on the extract concentration. At a lower concentration (6 mL) no obvious peak was observed. When 10 mL of the broccoli extract was added to the solution, a significant absorption peak was seen at 275 nm which is in blue shift with respect to the bulk ZnS (340 nm), which could be probably due to the quantum confinement phenomena.[147] At high concentrations (i.e. 20 mL and 40 mL) significant shifts towards the low energies were noted.
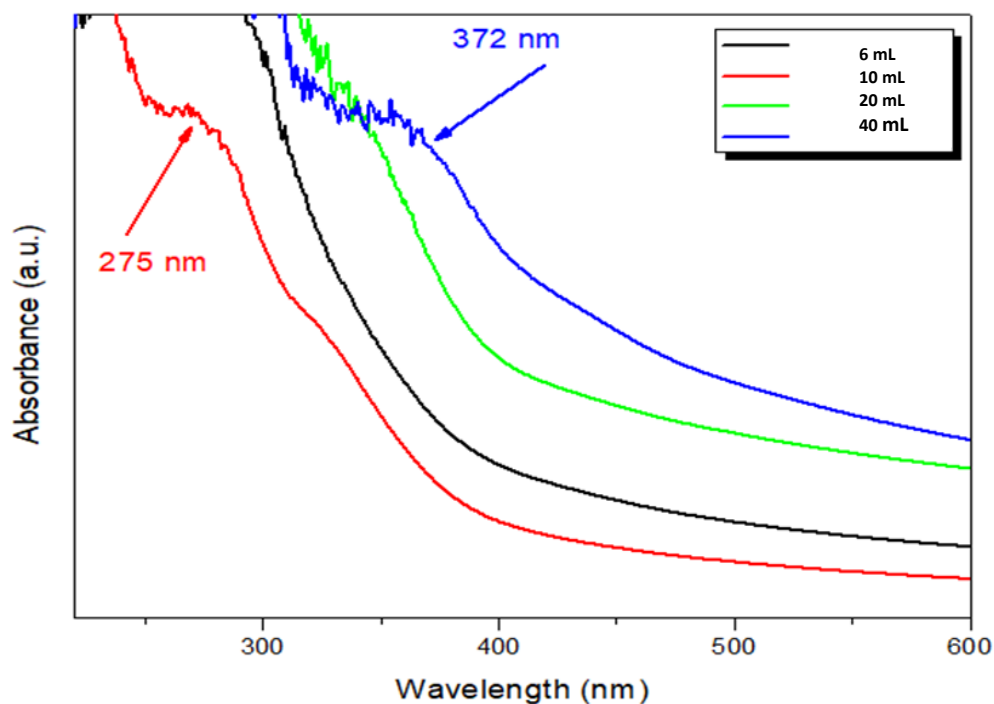
Figure 3.14 UV-Vis spectra of zinc sulfide nanoparticles formed in the presence of broccoli extract as a function of the extract concentrations after one hour of starring.

3.4.1.2 The effect of pH on the B:ZnS nanoparticles formation

After establishing the best extract concentration that should be used in the formation process of ZnS nanoparticles, the influence of pH on the production of ZnS particles was investigated. By adding 0.1 M of HCl and 0.1 M of NaOH, several pH values (3, 5, 7, 9, 11, and 12) were selected. As shown in Figure 3.15 a shift in the absorption edge ($\lambda = 275$ nm) towards the high-energy region was observed at pH 5. The peak positions shift towards the high wavelengths (377 nm) as the solution becomes basicity, which is higher than the absorption edge of bulk ZnS (340 nm). [147,148] Furthermore, at pH 12, the absorption peak declines and becomes less than at a pH 11. This might be attributed to the formation of zinc hydroxide in the solution, resulting in a decrease in Zn^{+2} ions, which consequently reduces the yield of ZnS particles. [135]
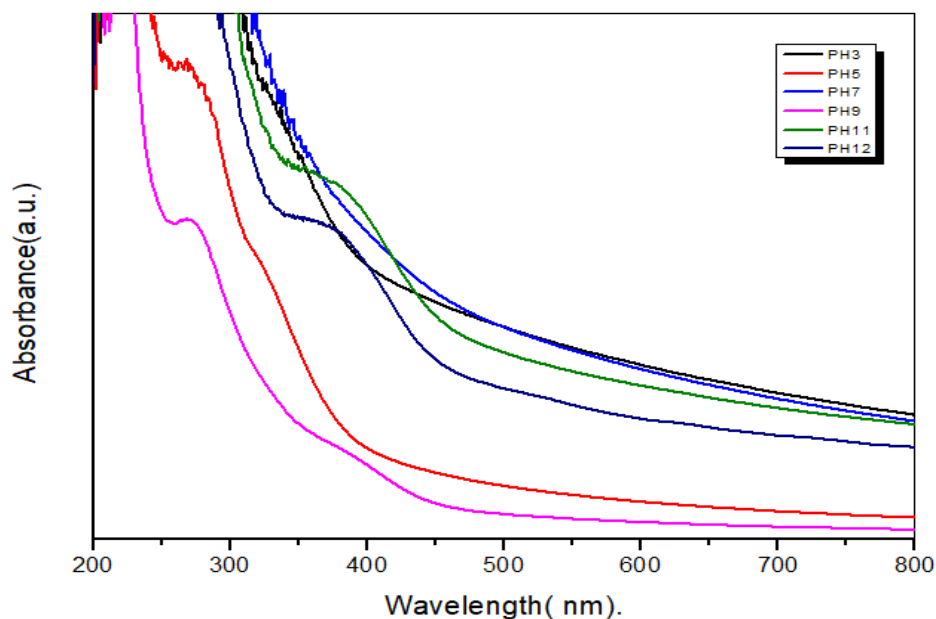
Figure 3.15 The optical absorption spectra of B:ZnS nanoparticles at different pH values.

3.4.1.3 Band gap energy for B:ZnS nanoparticles

Tauc plot was used to estimate the band gap energy from the UV-Vis spectrum that was recorded when 10 ml of the extract was added (absorption edge of 275 nm) to zinc sulfate solution. The band gap energy (see Figure 3.16), which was calculated from the extrapolation of the linear curve with the x-axis, shifts towards the lower energy (3.9 eV) compared to that one of bulk ZnS (3.6 eV) due to the confinement of elections at nanoscale.
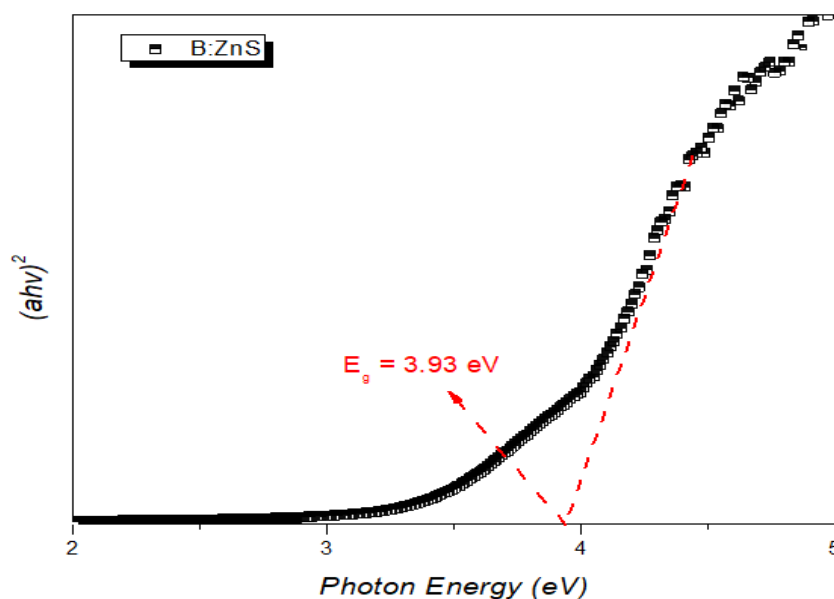
Figure 3.16 The band gap energy was estimated from the UV-Vis spectrum that was recorded when 10 mL of the extract was added (the absorption edge is ~ 275 nm).

The important thing here is that the prepared zinc sulfide particles formed with the presence of broccoli extract have band gap energy higher than that of ZnS particles formed in the absence of extract (E_g = 3.8 eV, λ = 295 nm). This wide band gap may offer a number of uses such as allowing devices to operate at much higher temperatures (~300 ^{o}C) and high voltages. The high-temperature tolerance also means that these devices can operate at higher power levels under normal conditions.

3.4.2 Structural properties of (B:ZnS) nanoparticles

3.4.2.1 X-rays Diffraction of B:ZnS

Figure 3.17 shows the XRD pattern for B:ZnS nanocrystal. A clear evidence for the formation of crystalline zinc sulfide nanoparticles was reported. Three diffraction peaks appear at theta 28.76^o, 47.97^o and 56.6^o are corresponding

to the planes (111), (220), and (311), respectively. According to previous works, B:ZnS nanoparticles have zinc blende structure (cubic structure). [127,149]

According to the Scherrer formula (see equation 3.2),[142] the average crystallite size was calculated, and is found to be around 2.4 nm. It is worth to note that the crystallite size is a part of the particles, therefore, Sherrer equation doesn't give the real size for ZnS nanoparticles instead give small values[150]. XRD diffraction gives an average interplaner distance of 0.22 nm.
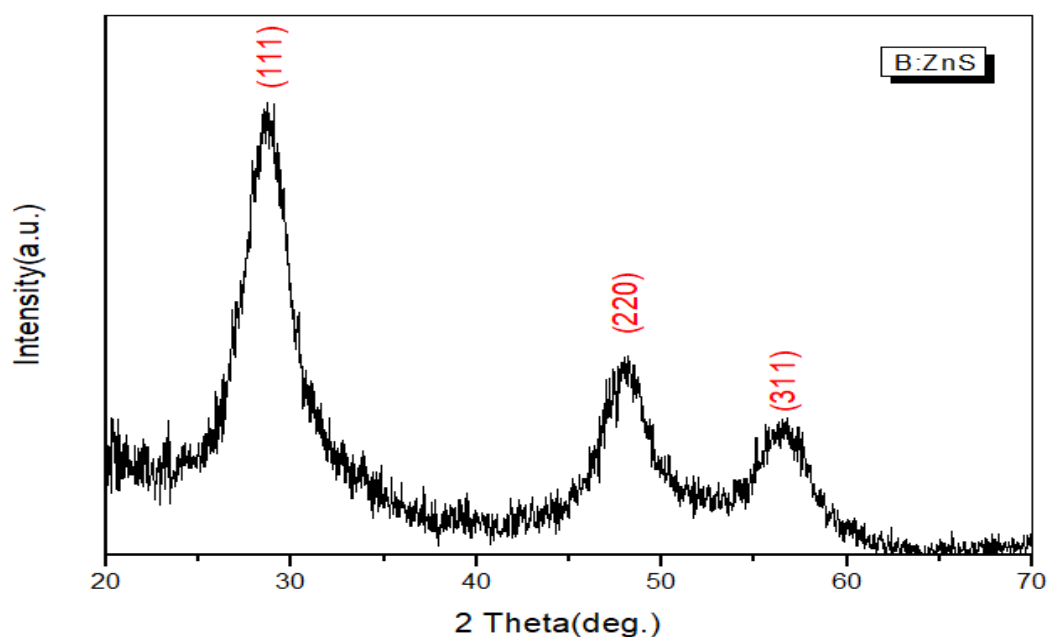
Figure 3.17 X-rays diffraction patterns of ZnS nanocrystals which is formed in the presence of 10 mL broccoli extract.

3.4.2.2 FE-SEM analysis

FE-SEM images in Figure 3.18 show the surface morphology of biosynthesized ZnS particles. A number of spherical particles with an average size of nearly 5-7 nm were observed during FE-SEM analysis. This size is greater than that one obtained from the Scherrer equation because the latter measure only the crystallite size.

An interesting point here is by introducing broccoli extract to the formation process of zinc sulfide nanoparticles, the size of the particles is reduced compared

to that without the extract. The reason could be because the presence of intermolecular forces that are formed between the extract bio-components such as phenols and polyphenolic with the zinc sulfide particles, leading them to act as a protecting agent which can control the size of ZnS particles.
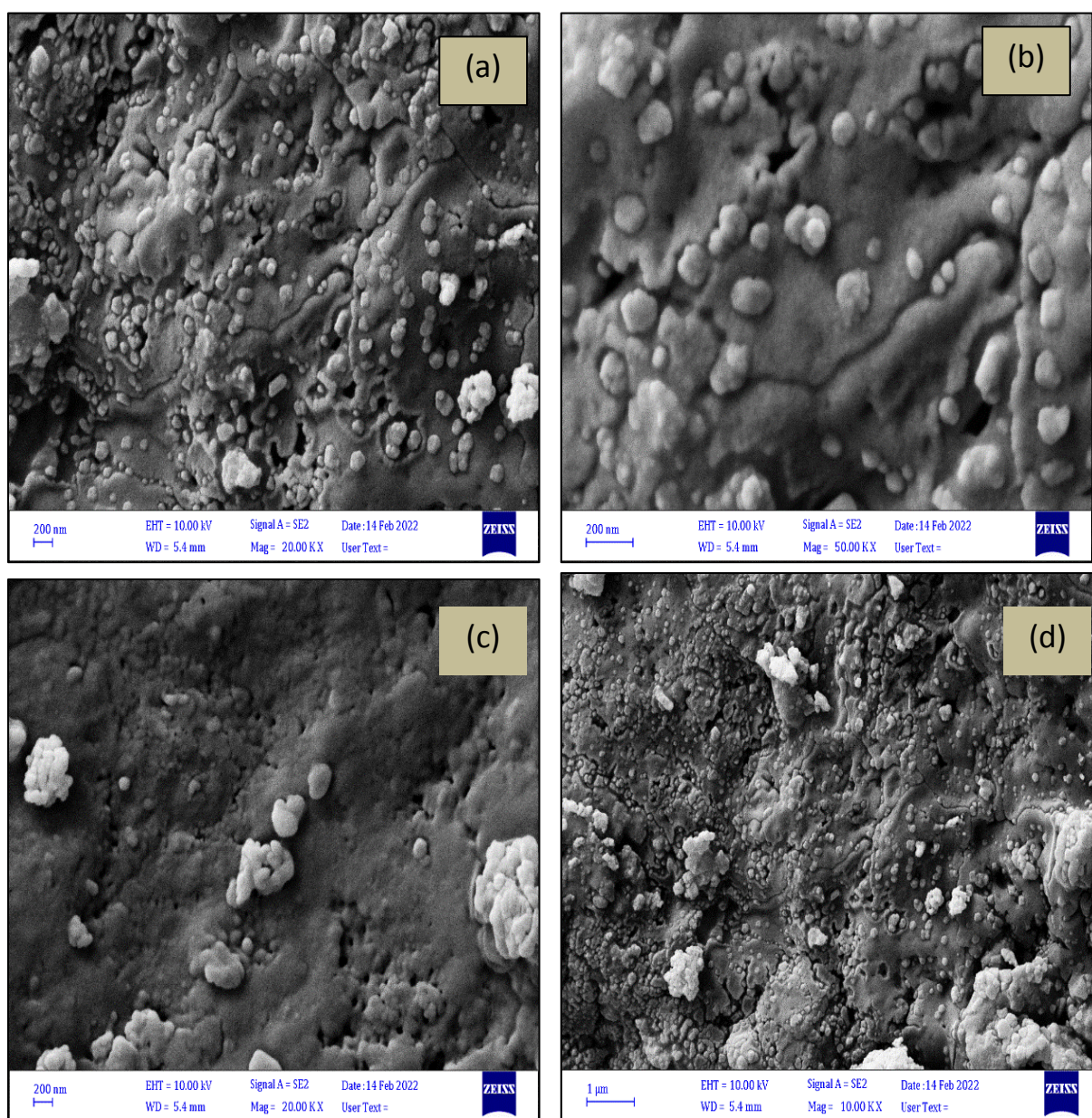
Figure 3.18 FE-SEM images of ZnS nanoparticles formed in the presence of broccoli extract as a capping agent.

3.4.2.3 TEM analysis

Although broccoli extract was used as a capping agent, some agglomeration of ZnS particles was seen in the TEM image (see Figure 3.19). A possible interpretation is the association of ZnS particles through drying the sample before introducing it to the TEM. In addition, many small spherical particles are seen as shown in the expanded view.
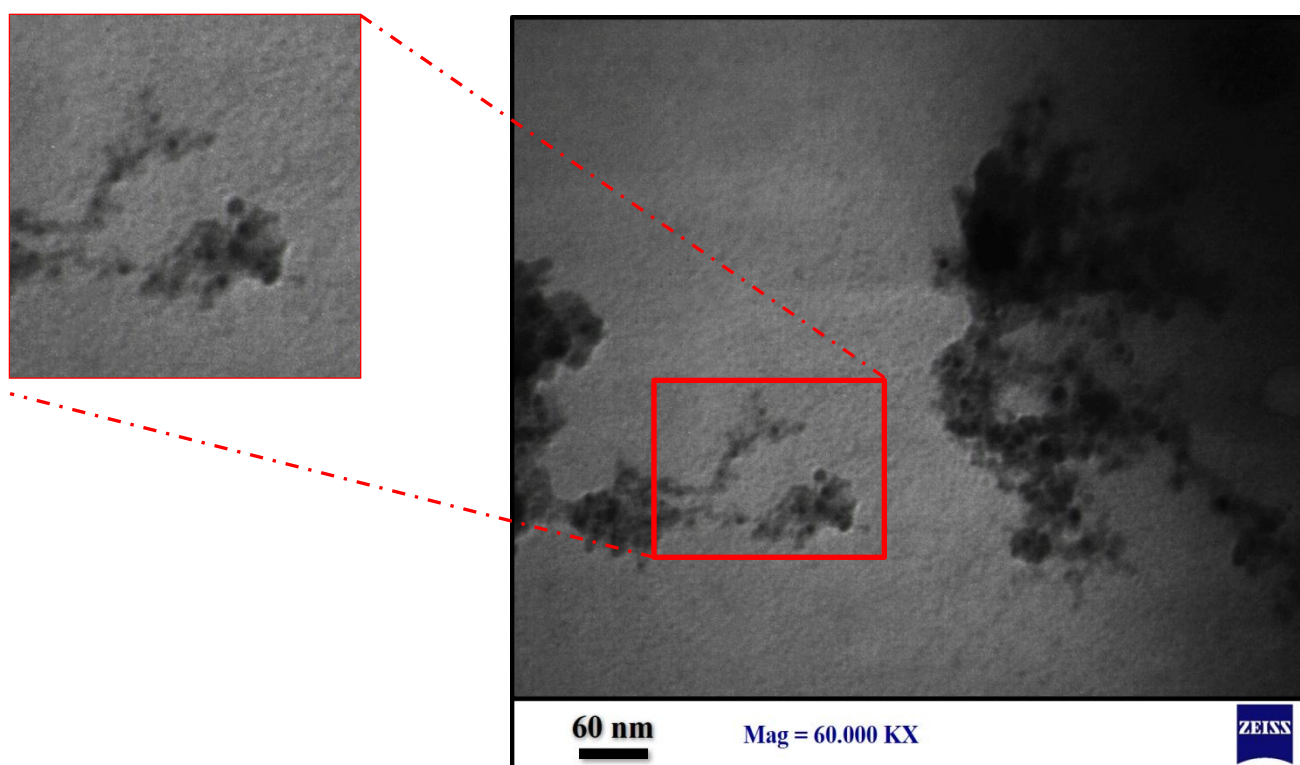
Figure 3.19 TEM image of ZnS nanoparticles formed in the presence of broccoli extract (the extended view shows the formation of small spherical particles). The scale bar of images is 60 nm.

3.4.2.4 FTIR measurement

In order to investigate the functional groups that are attached to the surface of ZnS particles, FTIR spectroscopy was used and the spectrum was recorded in the range of 400 - 4000 cm^{-1}. Figure 3.20 shows the peaks centered at 612 and 657 cm^{-1} representing the Zn-S bond. .[71,151] The peak at 1411 cm^{-1} is assigned to the presence

of C=C group from the aromatic conjugates from broccoli extract. [152] The peak appears at 1629.55 cm^{-1} suggesting the presence of vibration of OH group. [127] At 1005 cm^{-1}, a strong peak was observed and it is possibly assigned to the organic components which may come from the extract.[153]

The broad peak around 3200 to 3500 cm^{-1} is attributed to the OH group of phenol in the extract. Sharp peaks in the range of 2330 to 2380 cm^{-1} could be assigned to the S-H bond.
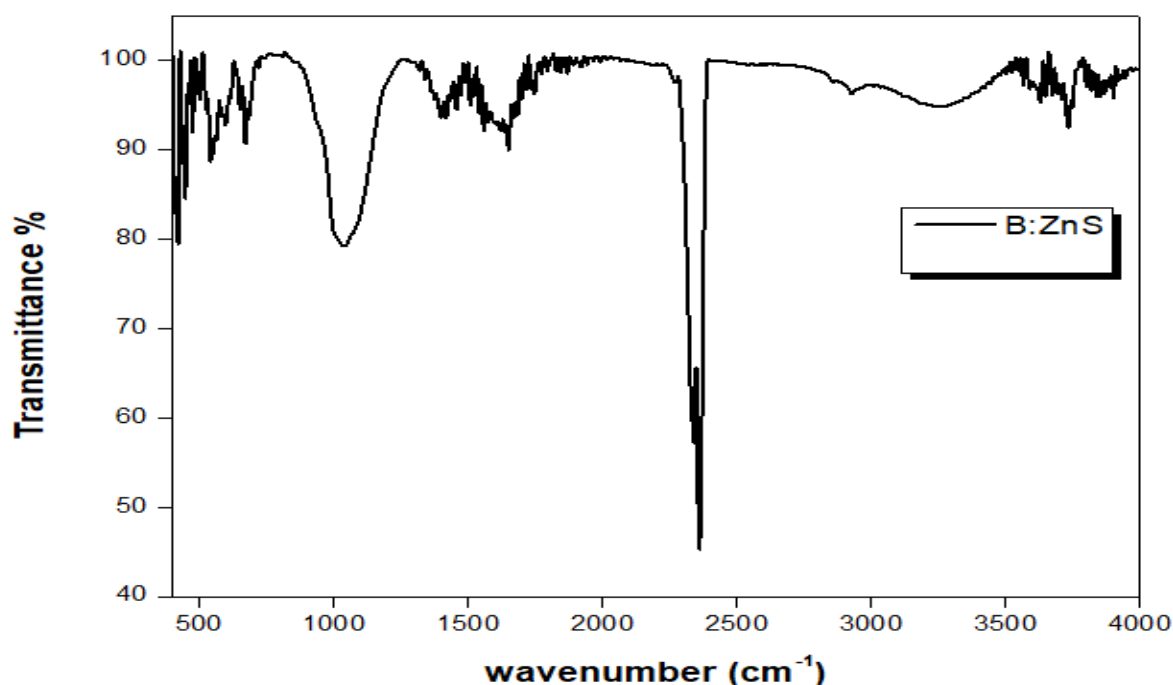
Figure 3.20 FTIR spectrum of (B:ZnS) nanoparticles formed in the presence of broccoli extract

3.5 The ability of B:ZnS nanoparticles for removal MB dye

3.5.1 The influence of contact time on the adsorption ability

The time required for the B:ZnS nanoparticles to adsorb and remove MB dye from wastewater was studied using UV-Visible spectroscopy. Figure 3.21 shows that MB dye has an absorption peak at 666 nm and the intensity of this peak decreased as the contact time increased from 5, 15, 30 to 60 min.
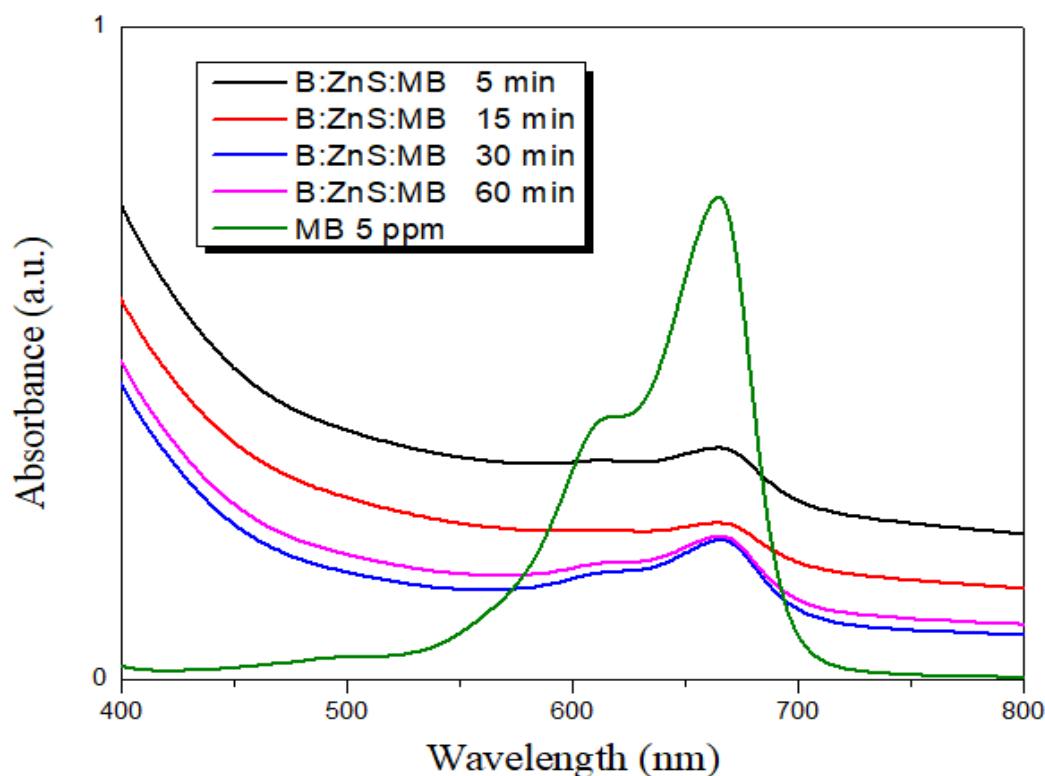
Figure 3.21 UV-Vis spectra of MB dye after the addition of ZnS particles formed with the presence of broccoli (B:ZnS) as a function of the contact time. The absorption band of MB dye is 666 nm.

3.5.2 Effect of B:ZnS nanoparticles on the adsorption process

The addition of different amount of B:ZnS nanoparticles (0. 1, 0.2, 0.3, 0.4, and 0. 5 g) to the MB dye solution leading to decreasing the peak intensities of MB dye as shown in Figure 3.22, indicating the adsorption ability of our prepared nanoparticles for adsorbing MB dye. However, a decrease in adsorption efficiency occurs as the B:ZnS nanoparticles dosage increases, this could be attributed due to overlapping or aggregation of adsorption sites leads to decrease in available adsorbent surface area for methylene blue.[154] The percentage of dye removal (*%DR*) was calculated and it is found to be 90 %.
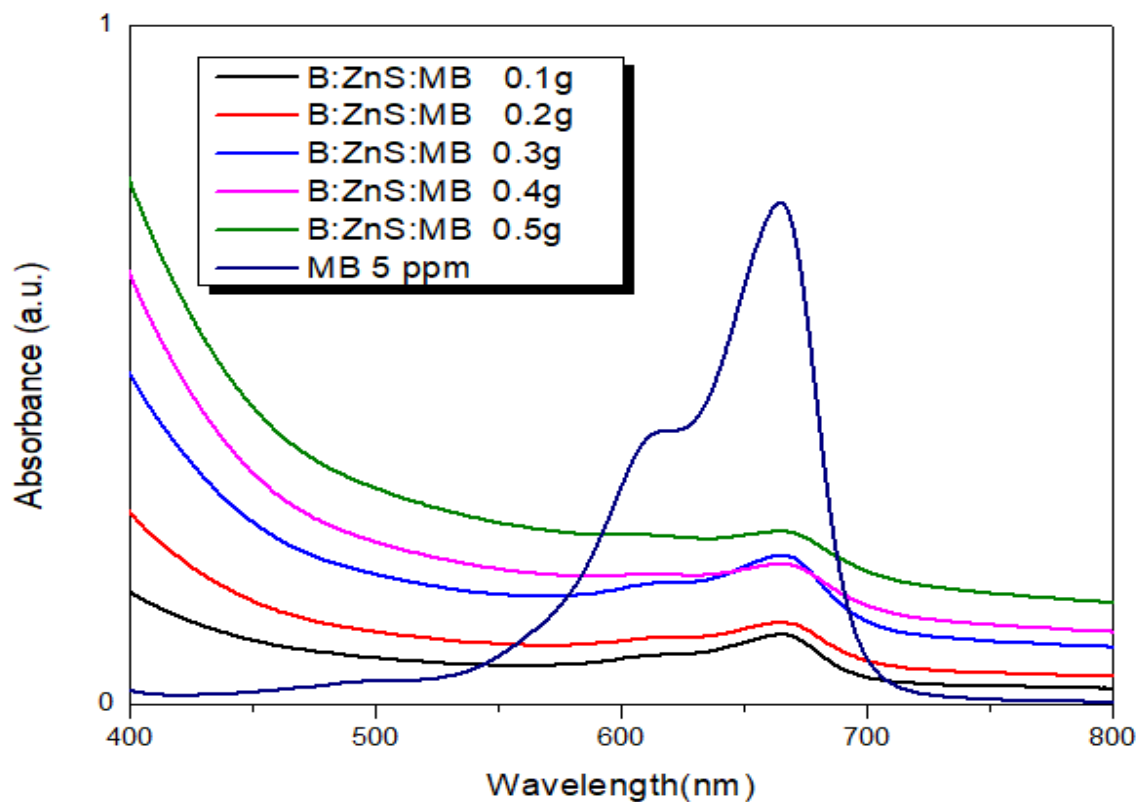
Figure 3.22 UV-Vis spectra of the dye removal after addition different amounts of ZnS particles formed with the presence of broccoli (B:ZnS). The absorption band of MB dye is 666 nm.

Table 3.5 shows the percentage of removal versus change in amount B: ZnS.

DR%	C_e	Abs.	B: ZnS	No.
90.41	0.480	0.104	0.1 g	1
88.75	0.563	0.122	0.2 g	2
79.61	1.019	0.221	0.3 g	3
80.81	0.959	0.208	0.4 g	4
76.38	1.181	0.256	0.5 g	5

3.5.3 The effect of temperature on adsorption of MB dye

To determine the best temperature required for removal MB dye, different samples were prepared and heated to different temperature (25, 30, 40, and 50 ^{o}C). It is clear from Figure 3.23 that the peaks intensity of MB decreases as the temperature decrease. Because the adsorption is chemical on the surface, as well as the lower the temperature, the slower the diffusion speed of the dye molecules, and the lower the kinetic energy of the dye molecules
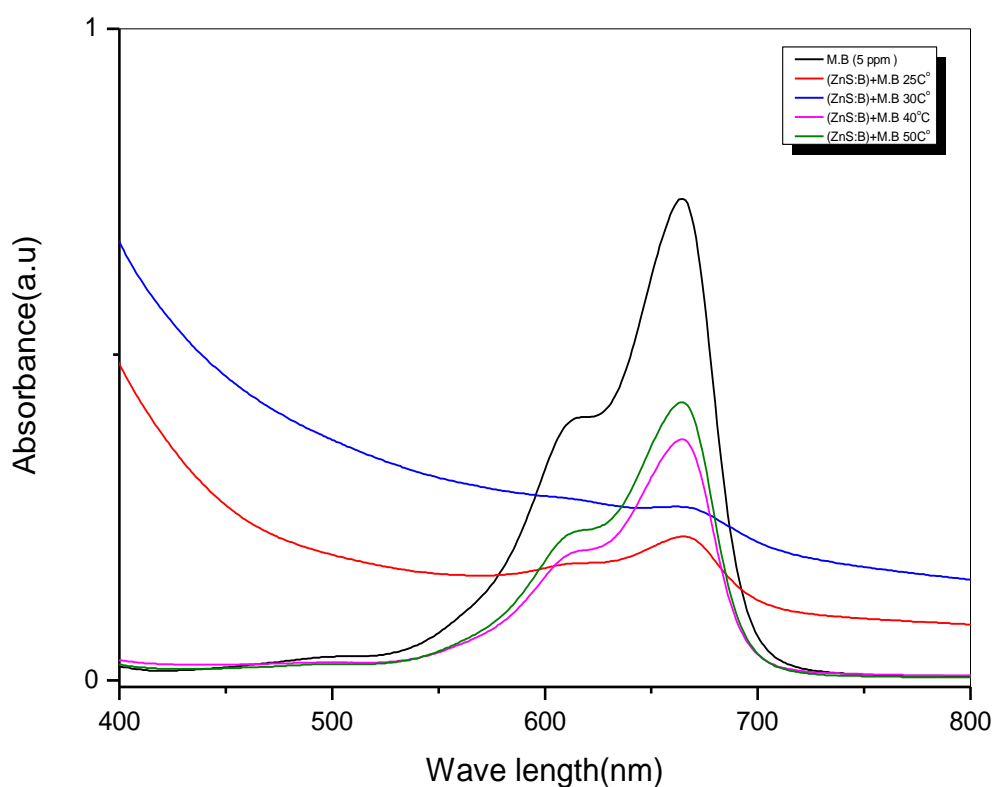
Figure 3.23 UV-Vis spectra of B:ZnS nanoparticles with MB dye as a function of temperature.

3.5.4 Effect of pH on the adsorption process

The effect of pH on the adsorption process of MB dye was investigated. From Figure 3.24, it was observed that the optimum pH of the process was 7. This is due to the fact that the degradation of MB dye was increased, in other words, more active sites will be available at the surface of zinc sulfide nanoparticles formed in the presence of broccoli extract. The removal ratio was found to be 84.13%.
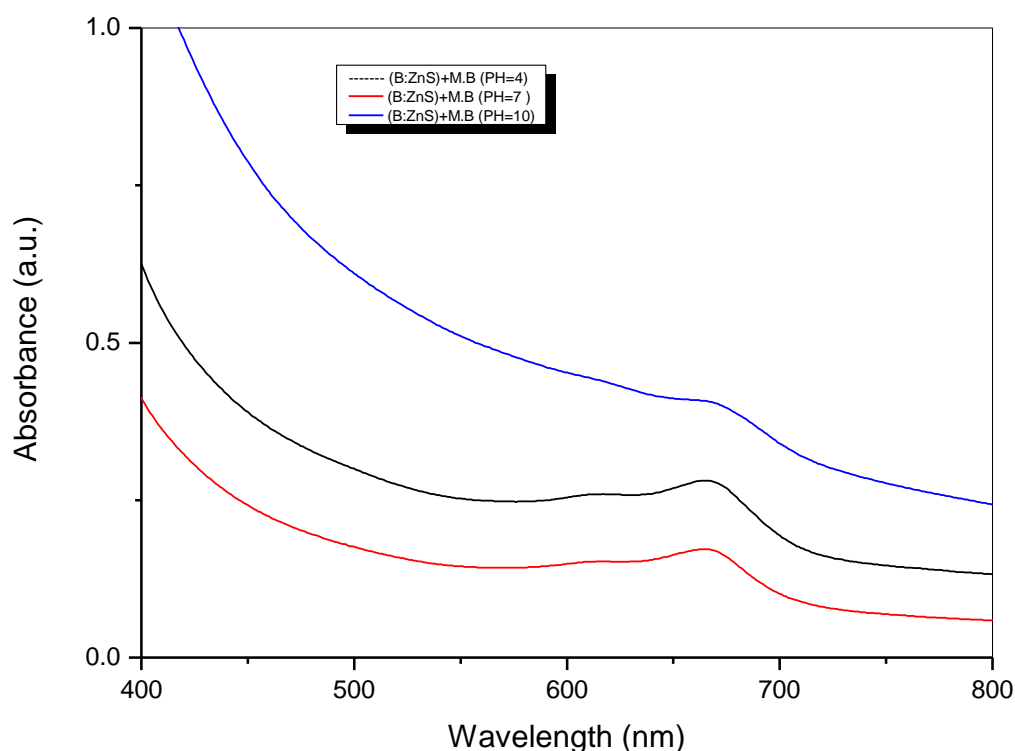
Figure 3.24 Effect of pH on the methylene blue dye adsorption the biosynthesized B:ZnS nanoparticles.

Table 3.6 Displays the percentage of removal versus change in (PH)for B:ZnS.

DR%	C_e	Abs.	pH	No.
74.08	1.296	0.281	4	1
84.13	0.793	0.172	7	2
62. 36	1.882	0.408	10	3

3.6 Conclusions

The main conclusions in this work can be summarized to:

1. ZnS nanoparticles were prepared successfully using chemical precipitation method.

2. The particles size and morphology were determined using microscopic techniques (FE-SEM and TEM).

3. The optical spectrum shows an absorption peak at 296 nm at the optimal conditions (pH 5, 25 ^{o}C and 1 hours of shaking). This blue shift of the absorption band of ZnS nanoparticles compared to the bulk is attributed to the effects of quantum confinement.

4. The band gap energy was estimated from the UV-Vis spectrum using tauc relationship to be 3.8 eV. Our prepared nanoparticles have a cubic phase with (111), (220) and (311) lattice planes.

5. The size of zinc sulfide nanoparticles was measured using Scherre formula and it was 1.5 nm.

6. FR-IR analysis shows evidence for the formation of ZnS particles in the presence of broccoli extract through the peaks that appears at 612 and 657 cm^{-1}.

7. These ZnS nanoparticles were employed for removal of methylene blue dye. The maximum dye removal was found to be 80% with initial concentration of dye 5 ppm at pH = 4 for 30 min, with 0.5 g ZnS nanoparticles.

8. Conclusive evidence for the formation of zinc sulfide nanoparticles using broccoli extract has been recorded for the first time. This extract acts as a bio-reducing agent. XRD analysis shows that B:ZnS particles are cubic (zinc blend) structure with a size of 2.4 nm and the interplanar distance is 0.22 nm.

9. A small amount of B:ZnS particles (0.1 g) are able to adsorb methylene blue dye (MB) from wastewater. The percentage of dye removal (*%DR*) was calculated and it is found to be 90 %.

10. Introducing broccoli extract in the formation process of ZnS nanoparticles leads to the form of small nanoparticles with a wide band gap 3.93 eV compared to ZnS particles formed through the chemical precipitation method 3.8 eV. These small particles have large surface-to-area and consequently can be used in removing process of industrial dyes with high efficiency

.

3.7 Recommendations:

1. Study the linear and non-linear optical properties of ZnS nanoparticles.

2. Doping the ZnS nanoparticles with some metal or semiconductor materials to improve their optical properties and consequently increase their ability to absorb different dyes.

3. Study the photocatalytic activity of ZnS nanoparticles.

4. Study the bioactivity of ZnS nanoparticles.

References

1-   Albrecht, P. J.; Davar, G.; Eisenberg, E.; Pare, M.; Rice, F. L. Response to Editorial on Albrecht et al.(2006). *Pain* **2006**, *123*, 217.

2-   Haruta, M. When gold is not noble: catalysis by nanoparticles. *The chemical record* **2003**, *3*, 75-87.

3-   Hidalgo-Manrique, P.; Lei, X.; Xu, R.; Zhou, M.; Kinloch, I. A.; Young, R. J. Copper/graphene composites: a review. *Journal of materials science* **2019**, *54*, 12236-12289.

4-   Awwad, A. M.; Salem, N. M. Green synthesis of silver nanoparticles byMulberry LeavesExtract. *Nanoscience and Nanotechnology* **2012**, *2*, 125-128.

5-   Ansari, A. A.; Nazeeruddin, M.; Tavakoli, M. M. Organic-inorganic upconversion nanoparticles hybrid in dye-sensitized solar cells. *Coordination Chemistry Reviews* **2021**, *436*, 213805.

6-   Barzinjy, A. A.; Azeez, H. H. Green synthesis and characterization of zinc oxide nanoparticles using Eucalyptus globulus Labill. leaf extract and zinc nitrate hexahydrate salt. *SN Applied Sciences* **2020**, *2*, 1-14.

7-   Akbar, S.; Tauseef, I.; Subhan, F.; Sultana, N.; Khan, I.; Ahmed, U.; Haleem, K. S. An overview of the plant-mediated synthesis of zinc oxide nanoparticles and their antimicrobial potential. *Inorganic and Nano-Metal Chemistry* **2020**, *50*, 257-271.

8-   Yousefi, M.; Dadashpour, M.; Hejazi, M.; Hasanzadeh, M.; Behnam, B.; de la Guardia, M.; Shadjou, N.; Mokhtarzadeh, A. Anti-bacterial activity of graphene oxide as a new weapon nanomaterial to combat multidrug-resistance bacteria. *Materials Science and Engineering: C* **2017**, *74*, 568-581.

9-   Doroudian, M.; O'Neill, A.; Mac Loughlin, R.; Prina-Mello, A.; Volkov, Y.; Donnelly, S. C. Nanotechnology in pulmonary medicine. *Current opinion in pharmacology* **2021**, *56*, 85-92.

10-   Mohammed, L.; Gomaa, H. G.; Ragab, D.; Zhu, J. Magnetic nanoparticles for environmental and biomedical applications: A review. *Particuology* **2017**, *30*, 1-14.

11-   Khan, F. H. Chemical hazards of nanoparticles to human and environment (a review). *Oriental Journal of Chemistry* **2013**, *29*, 1399.

12-   Klinkova, A.; Therien-Aubin, H.; Klabunde, K. J.; Sergeev, G. B.: *Nanochemistry*; Newnes, 2013.

13-   Yadav, T. P.; Yadav, R. M.; Singh, D. P. Mechanical milling: a top down approach for the synthesis of nanomaterials and nanocomposites. *Nanoscience and Nanotechnology* **2012**, *2*, 22-48.

14- Brock, S. L.: Nanostructures and Nanomaterials: Synthesis, Properties and Applications By Guozhang Cao (University of Washington). Imperial College Press (distributed by World Scientific): London. 2004. xiv+ 434 pp. $78.00. ISBN 1-86094-415-9. ACS Publications, 2004.

15- Arole, V.; Munde, S. Fabrication of nanomaterials by top-down and bottom-up approaches-an overview. *J. Mater. Sci* **2014**, *1*, 89-93.

16- Poinern, G. E. J.: *A laboratory course in nanoscience and nanotechnology*; CRC Press, 2014.

17- Chen, X.; Mao, S. S. Titanium dioxide nanomaterials: synthesis, properties, modifications, and applications. *Chemical reviews* **2007**, *107*, 2891-2959.

18- Kadhim, M. A.; Salman, H. E.; Hana'a, A. Adsorption of Albumin and Creatinine on Zinc Oxide (ZnO) Nanoparticles.

19- Aghaei, A.; Shaterian, M.; Monfared, H. H.; Farokhi, A. Designing a strategy for fabrication of single-walled carbon nanotube via CH4/N2 gas by the chemical vapor deposition method. *Advanced Powder Technology* **2022**, *33*, 103500.

20- Veksha, A.; Chen, W.; Liang, L.; Lisak, G. Converting polyolefin plastics into few-walled carbon nanotubes via a tandem catalytic process: Importance of gas composition and system configuration. *Journal of Hazardous Materials* **2022**, *435*, 128949.

21- Sulistyaningsih, T.; Santosa, S. J.; Siswanta, D.; Rusdiarso, B. Synthesis and characterization of magnetites obtained from mechanically and sonochemically assissted co-precipitation and reverse co-precipitation methods. *Int. J. Mater. Mech. Manuf* **2017**, *5*, 16-19.

22- Kumar, H.; Manisha, S. P.; Sangwan, P. Synthesis and characterization of MnO2 nanoparticles using co-precipitation technique. *Int J Chem Chem Eng* **2013**, *3*, 155-160.

23- Basiuk, V. A.; Basiuk, E. V. Green processes for nanotechnology. *Springer* **2015**, 446.

24- Kuunal, S.; Rauwel, P.; Rauwel, E.: Plant extract mediated synthesis of nanoparticles. In *Emerging applications of nanoparticles and architecture nanostructures*; Elsevier, 2018; pp 411-446.

25- Fariq, A.; Khan, T.; Yasmin, A. Microbial synthesis of nanoparticles and their potential applications in biomedicine. *Journal of Applied Biomedicine* **2017**, *15*, 241-248.

26- Barabadi, H.; Mojab, F.; Vahidi, H.; Marashi, B.; Talank, N.; Hosseini, O.; Saravanan, M. Green synthesis, characterization, antibacterial and biofilm inhibitory activity of silver nanoparticles compared to commercial silver nanoparticles. *Inorganic Chemistry Communications* **2021**, *129*, 108647.

27-   Ghosh, S.; Ahmad, R.; Banerjee, K.; AlAjmi, M. F.; Rahman, S. Mechanistic aspects of microbe-mediated nanoparticle synthesis. *Frontiers in Microbiology* **2021**, *12*, 638068.

28-   Suriyaraj, S. P.; Ramadoss, G.; Chandraraj, K.; Selvakumar, R. One pot facile green synthesis of crystalline bio-ZrO2 nanoparticles using Acinetobacter sp. KCSI1 under room temperature. *Materials Science and Engineering: C* **2019**, *105*, 110021.

29-   Gong, J.; Song, X.; Gao, Y.; Gong, S.; Wang, Y.; Han, J. Microbiological synthesis of zinc sulfide nanoparticles using Desulfovibrio desulfuricans. *Inorganic and Nano-Metal Chemistry* **2018**, *48*, 96-102.

30-   Jain, A.; Patel, N. B.; Tailor, V.; Sathvara, S.; Kalasariya, H. S. An Appraisal on Antimicrobial applicability of Marine Macroalgae. *Int. Res. J. Eng. Technol* **2020**, *7*, 735-739.

31-   Mukherjee, P.; Ahmad, A.; Mandal, D.; Senapati, S.; Sainkar, S. R.; Khan, M. I.; Parishcha, R.; Ajaykumar, P.; Alam, M.; Kumar, R. Fungus-mediated synthesis of silver nanoparticles and their immobilization in the mycelial matrix: a novel biological approach to nanoparticle synthesis. *Nano letters* **2001**, *1*, 515-519.

32-   Tran, T. V.; Nguyen, D. T. C.; Kumar, P. S.; Din, A. T. M.; Jalil, A. A.; Vo, D.-V. N. Green synthesis of ZrO2 nanoparticles and nanocomposites for biomedical and environmental applications: a review. *Environmental Chemistry Letters* **2022**, 1-23.

33-   Roy, A.; Bulut, O.; Some, S.; Mandal, A. K.; Yilmaz, M. D. Green synthesis of silver nanoparticles: biomolecule-nanoparticle organizations targeting antimicrobial activity. *RSC advances* **2019**, *9*, 2673-2702.

34-   Negi, S.; Singh, V. Algae: A potential source for nanoparticle synthesis. *Journal of Applied and Natural Science* **2018**, *10*, 1134-1140.

35-   Rao, M. D.; Pennathur, G. Facile bio-inspired synthesis of zinc sulfide nanoparticles using Chlamydomonas reinhardtii cell free extract: optimization, characterization and optical properties. *Green Processing and Synthesis* **2016**, *5*, 379-388.

36-   Ustyuzhanina, N. E.; Bilan, M. I.; Dmitrenok, A. S.; Shashkov, A. S.; Ponce, N. M.; Stortz, C. A.; Nifantiev, N. E.; Usov, A. I. Fucosylated chondroitin sulfate from the sea cucumber Hemioedema spectabilis: Structure and influence on cell adhesion and tubulogenesis. *Carbohydrate polymers* **2020**, *234*, 115895.

37-   Vijayaraghavan, K.; Ashokkumar, T. Plant-mediated biosynthesis of metallic nanoparticles: a review of literature, factors affecting synthesis, characterization techniques and applications. *Journal of environmental chemical engineering* **2017**, *5*, 4866-4883.

38-   Xu, C.; Huang, S.; Huang, Y.; Effiong, K.; Yu, S.; Hu, J.; Xiao, X. New insights into the harmful algae inhibition by Spartina alterniflora:

cellular physiology and metabolism of extracellular secretion. *Science of the Total Environment* **2020**, *714*, 136737.

39- Chokriwal, A.; Sharma, M. M.; Singh, A. Biological synthesis of nanoparticles using bacteria and their applications. *American Journal of PharmTech Research* **2014**, *4*, 38-61.

40- Xaba, T.; Moloto, M. J.; Malik, M. A.; Moloto, N. The Influence of Temperature on the Formation of Cubic Structured CdO Nanoparticles and Their Thin Films from Bis (2-hydroxy-1-naphthaldehydato) cadmium (II) Complex via Thermal Decomposition Technique. *Journal of Nanotechnology* **2017**, *2017*.

41- Ahmed, S.; Ahmad, M.; Swami, B. L.; Ikram, S. A review on plants extract mediated synthesis of silver nanoparticles for antimicrobial applications: a green expertise. *Journal of advanced research* **2016**, *7*, 17-28.

42- Haller, E. Germanium: From its discovery to SiGe devices. *Materials science in semiconductor processing* **2006**, *9*, 408-422.

43- Găiceanu, M.: Introductory Chapter: Electric Power Conversion. In *Electric Power Conversion*; IntechOpen, 2019.

44- Kour, J.; Chopra, K. Solar Cells–A Review.

45- Shimizu, H. General Purpose Technology, Spin-Out, and Innovation. *Advances in Japanese Business and Economics* **2019**.

46- Arrigoni, M.; Morioka, B.; Lepert, A. Optically pumped semiconductor lasers: Green OPSLs poised to enter scientific pump-laser market. *Laser Focus World* **2009**, *45*.

47- Soclof, S.; Watson, J.; Brews, J. R.; Stiegler, H. J.; Morris, J. E. 3.1 Junction Field-Effect Transistors. *Electronics, Power Electronics, Optoelectronics, Microwaves, Electromagnetics, and Radar* **2018**.

48- Yang, Z.; Wang, M.; Qiu, H.; Yao, X.; Lao, X.; Xu, S.; Lin, Z.; Sun, L.; Shao, J. Engineering the exciton dissociation in quantum-confined 2D CsPbBr3 nanosheet films. *Advanced Functional Materials* **2018**, *28*, 1705908.

49- Tong, H.; Ouyang, S.; Bi, Y.; Umezawa, N.; Oshikiri, M.; Ye, J. Nano-photocatalytic materials: possibilities and challenges. *Advanced materials* **2012**, *24*, 229-251.

50- Bredas, J.-L. Mind the gap! *Materials Horizons* **2014**, *1*, 17-19.

51- Smith, A. M.; Nie, S. Semiconductor nanocrystals: structure, properties, and band gap engineering. *Accounts of chemical research* **2010**, *43*, 190-200.

52- Wilson, N. P.; Yao, W.; Shan, J.; Xu, X. Excitons and emergent quantum phenomena in stacked 2D semiconductors. *Nature* **2021**, *599*, 383-392.

53-   Shanmugam, N.; Cholan, S.; Viruthagiri, G.; Gobi, R.; Kannadasan, N. Synthesis and characterization of Ce3+-doped flowerlike ZnS nanorods. *Applied Nanoscience* **2014**, *4*, 359-365.

54-   Kaur, N.; Kaur, S.; Singh, J.; Rawat, M. A review on zinc sulphide nanoparticles: from synthesis, properties to applications. *J Bioelectron Nanotechnol* **2016**, *1*, 1-5.

55-   Priya, K.; Ashith, V.; Rao, G. K.; Sanjeev, G. A comparative study of structural, optical and electrical properties of ZnS thin films obtained by thermal evaporation and SILAR techniques. *Ceramics International* **2017**, *43*, 10487-10493.

56-   Bodo, B.; Prakash, D.; Kalita, P. Synthesis and Characterization of ZnS: Mn Nanopartilces. *International Journal of Applied Physics and Mathematics* **2012**, *2*, 181.

57-   Le Donne, A.; Cavalcoli, D.; Mereu, R.; Perani, M.; Pagani, L.; Acciarri, M.; Binetti, S. Study of the physical properties of ZnS thin films deposited by RF sputtering. *Materials Science in Semiconductor Processing* **2017**, *71*, 7-11.

58-   Ummartyotin, S.; Infahsaeng, Y. A comprehensive review on ZnS: From synthesis to an approach on solar cell. *Renewable and Sustainable Energy Reviews* **2016**, *55*, 17-24.

59-   Fang, X.; Zhai, T.; Gautam, U. K.; Li, L.; Wu, L.; Bando, Y.; Golberg, D. ZnS nanostructures: from synthesis to applications. *Progress in Materials Science* **2011**, *56*, 175-287.

60-   Rogach, A. L. Semiconductor nanocrystal quantum dots. *Verlag: Wien* **2008**.

61-   Ramalingam, G.; Kathirgamanathan, P.; Ravi, G.; Elangovan, T.; Manivannan, N.; Kasinathan, K.: Quantum confinement effect of 2D nanomaterials. In *Quantum Dots-Fundamental and Applications*; IntechOpen, 2020.

62-   Binns, C.: *Introduction to nanoscience and nanotechnology*; John Wiley & Sons, 2021.

63-   Burda, C.; Chen, X.; Narayanan, R.; El-Sayed, M. A. Chemistry and properties of nanocrystals of different shapes. *Chemical reviews* **2005**, *105*, 1025-1102.

64-   Khalil, M. H.; Mohammed, R. Y.; Ibrahem, M. A. The influence of CBD parameters on the energy gap of ZnS Narcissus-like nanostructured thin films. *Coatings* **2021**, *11*, 1131.

65-   Jiang, C.; Zhang, W.; Zou, G.; Yu, W.; Qian, Y. Hydrothermal synthesis and characterization of ZnS microspheres and hollow nanospheres. *Materials Chemistry and Physics* **2007**, *103*, 24-27.

66-   Chen, W.; Wang, Z.; Lin, Z.; Lin, L. Absorption and luminescence of the surface states in ZnS nanoparticles. *Journal of applied physics* **1997**, *82*, 3111-3115.

67-   Shakil, M. A.; Das, S.; Rahman, M. A.; Akther, U. S.; Majumdar, M. K. H.; Rahman, M. K. A Review on zinc sulphide thin film fabrication for various applications based on doping elements. *Materials Sciences and Applications* **2018**, *9*, 751-778.

68-   Tsuji, I.; Kato, H.; Kudo, A. Visible-light-induced H2 evolution from an aqueous solution containing sulfide and sulfite over a ZnS–CuInS2–AgInS2 solid-solution photocatalyst. *Angewandte Chemie* **2005**, *117*, 3631-3634.

69-   Synnott, D. W. Microwave Synthesis and Characterisation of Zinc Sulfide Nanomaterials for Photocatalytic and Anti-Bacterial Applications. **2019**.

70-   Han, B.; Fang, W. H.; Zhao, S.; Yang, Z.; Hoang, B. X. Zinc sulfide nanoparticles improve skin regeneration. *Nanomedicine: Nanotechnology, Biology and Medicine* **2020**, *29*, 102263.

71-   Labiadh, H.; Lahbib, K.; Hidouri, S.; Touil, S.; Chaabane, T. B. Insight of ZnS nanoparticles contribution in different biological uses. *Asian Pacific journal of tropical medicine* **2016**, *9*, 757-762.

72-   Zang, X.; Song, J.; Li, Y.; Han, Y. Targeting necroptosis as an alternative strategy in tumor treatment: From drugs to nanoparticles. *Journal of Controlled Release* **2022**, *349*, 213-226.

73-   Ganesh, S.; Venkatakrishnan, K.; Tan, B. Quantum scale organic semiconductors for SERS detection of DNA methylation and gene expression. *Nature communications* **2020**, *11*, 1-15.

74-   Al Hindawi, A. M.; Joudah, I.; Hamzah, S.; Tarek, Z. In *Tilte*2019; IOP Publishing.

75-   A. Al Hindawi, N. H. O., I. Joudah, N. Shiltagh and K. Taher. **,** *International Journal of Pharmaceutical Research,* **2020,** 12, 985–988.

76-   Shiltagh, N. M.; Ridha, N. J.; Hindawi, A. M. A.; Tahir, K. J.; Madlol, R. A.; Alesary, H. F.; Luna, L. G. M.; Watkins, M. J. In *Tilte*2020; AIP Publishing LLC.

77-   Sabaghi, V.; Davar, F.; Fereshteh, Z. ZnS nanoparticles prepared via simple reflux and hydrothermal method: Optical and photocatalytic properties. *Ceramics International* **2018**, *44*, 7545-7556.

78-   Al-Zahra, A.; Al-Sammarraie, A. K. Synthesis and Characterization of Zinc Sulfide Nanostructure by Sol Gel Method. *Chemical Methodologies* **2022**, *6*, 67-73.

79-   Sousa, D. M.; Alves, L. C.; Marques, A.; Gaspar, G.; Lima, J. C.; Ferreira, I. Facile microwave-assisted synthesis manganese doped zinc sulfide nanoparticles. *Scientific reports* **2018**, *8*, 1-7.

80-   Choudapur, V.; Kapatkar, S.; Raju, A. Structural and optoelectronic properties of zinc sulfide thin films synthesized by Co-precipitation method. *Acta Chem. Iasi* **2019**, *27*, 287-302.

81- Karimi, F.; Rajabi, H. R.; Kavoshi, L. Rapid sonochemical water-based synthesis of functionalized zinc sulfide quantum dots: study of capping agent effect on photocatalytic activity. *Ultrasonics Sonochemistry* **2019**, *57*, 139-146.

82- Mani, S. K.; Saroja, M.; Venkatachalam, M.; Rajamanickam, T. Antimicrobial activity and photocatalytic degradation properties of zinc sulfide nanoparticles synthesized by using plant extracts. *Journal of Nanostructures* **2018**, *8*, 107-118.

83- Chandran, A.; Francis, N.; Jose, T.; George, K. Synthesis, structural characterization and optical bandgap determination of ZnS nanoparticles. *Acad Rev* **2010**, *17*, 17-21.

84- Pathak, C.; Mandal, M. K.; Agarwala, V. Synthesis and characterization of zinc sulphide nanoparticles prepared by mechanochemical route. *Superlattices and Microstructures* **2013**, *58*, 135-143.

85- Goharshadi, E. K.; Hadadian, M.; Karimi, M.; Azizi-Toupkanloo, H. Photocatalytic degradation of reactive black 5 azo dye by zinc sulfide quantum dots prepared by a sonochemical method. *Materials Science in Semiconductor Processing* **2013**, *16*, 1109-1116.

86- Abbas, N. K.; Al-Rasoul, K. T.; Shanan, Z. J. New method of preparation ZnS nano size at low pH. *Int. J. Electrochem. Sci* **2013**, *8*, 3049-3056.

87- Iranmanesh, P.; Saeednia, S.; Nourzpoor, M. Characterization of ZnS nanoparticles synthesized by co-precipitation method. *Chinese Physics B* **2015**, *24*, 046104.

88- Kanude, K.; Jain, P. Biosynthesis of CdS nanoparticles using Murraya Koenigii leaf extract and their biological studies. *Int. J. Sci. Res. Multidiscip. Stud.* **2017**, *3*, 5-10.

89- Zhuravliova, O.; Voeikova, T.; Khaddazh, M. K.; Bulushova, N.; Ismagulova, T.; Bakhtina, A.; Gusev, S.; Gritskova, I.; Lupanova, T.; Shaitan, K. Bacterial synthesis of cadmium and zinc sulfide nanoparticles: characteristics and prospects of application. *Molecular Genetics, Microbiology and Virology* **2018**, *33*, 233-240.

90- Bera, K.; Saha, S.; Jana, P. C. Investigation of Structural and Electrical properties of ZnS and Mn doped ZnS nanoparticle. *Materials Today: Proceedings* **2018**, *5*, 6321-6328.

91- Alijani, H. Q.; Pourseyedi, S.; Mahani, M. T.; Khatami, M. Green synthesis of zinc sulfide (ZnS) nanoparticles using Stevia rebaudiana Bertoni and evaluation of its cytotoxic properties. *Journal of Molecular Structure* **2019**, *1175*, 214-218.

92- Kannan, S.; Subiramaniyam, N.; Sathishkumar, M. A novel green synthesis approach for improved photocatalytic activity and antibacterial properties of zinc sulfide nanoparticles using plant extract of Acalypha

indica and Tridax procumbens. *Journal of Materials Science: Materials in Electronics* **2020**, *31*, 9846-9859.

93- Zhang, X.; Shan, C.; Ma, S.; Zhao, S.; Yang, J. Synthesis of nano-ZnS by lyotropic liquid crystal template method for enhanced photodegradation of methylene blue. *Inorganic Chemistry Communications* **2022**, *135*, 109089.

94- Xu, L.; Cao, J.; Chen, W. Structural characterization of a broccoli polysaccharide and evaluation of anti-cancer cell proliferation effects. *Carbohydrate polymers* **2015**, *126*, 179-184.

95- Hassaan, M. A.; El Nemr, A.; Madkour, F. F. Environmental assessment of heavy metal pollution and human health risk. *American Journal of Water Science and Engineering* **2016**, *2*, 14-19.

96- Shah, M. P.: *Removal of emerging contaminants through microbial processes*; Springer, 2021.

97- Agamuthu, P.; Mehran, S.; Norkhairah, A.; Norkhairiyah, A. Marine debris: A review of impacts and global initiatives. *Waste Management & Research* **2019**, *37*, 987-1002.

98- Sillanpää, M.; Metsämuuronen, S.; Matilainen, A.; Mänttäri, M.: Integrated methods. In *Nat. Org. Matter Water Charact. Treat. Methods*, 2014; pp 275-301.

99- Kansal, S.; Singh, M.; Sud, D. Studies on photodegradation of two commercial dyes in aqueous phase using different photocatalysts. *Journal of hazardous materials* **2007**, *141*, 581-590.

100- Benjamin, S.; Vaya, D.; Punjabi, P.; Ameta, S. C. Enhancing photocatalytic activity of zinc oxide by coating with some natural pigments. *Arabian Journal of Chemistry* **2011**, *4*, 205-209.

101- Apostolescu, G. A.; Cernatescu, C.; Cobzaru, C.; Tataru-Farmus, R. E.; Apostolescu, N. Studies on the photocatalytic degradation of organic dyes using CeO2-ZnO mixed oxides. *Environ. Eng. Manag. J* **2015**, *14*, 415-420.

102- Khezrianjoo, S.; Revanasiddappa, H. D. Photocatalytic degradation of acid yellow 36 using zinc oxide photocatalyst in aqueous media. *Journal of Catalysts* **2013**, *2013*.

103- Sakthivel, S.; Neppolian, B.; Shankar, M.; Arabindoo, B.; Palanichamy, M.; Murugesan, V. Solar photocatalytic degradation of azo dye: comparison of photocatalytic efficiency of ZnO and TiO2. *Solar energy materials and solar cells* **2003**, *77*, 65-82.

104- Crepy, M. Dermatoses professionnelles aux colorants. *Documents pour le médecin du travail* **2004**, 565-576.

105- Balkrishna, A.; Kumar, A.; Arya, V.; Rohela, A.; Verma, R.; Nepovimova, E.; Krejcar, O.; Kumar, D.; Thakur, N.; Kuca, K. Phytoantioxidant Functionalized Nanoparticles: A Green Approach to

Combat Nanoparticle-Induced Oxidative Stress. *Oxidative medicine and cellular longevity* **2021**, *2021*.

106- Tafer, R. Photodégradation directe et induite de micro-polluants organiques (cas d'un colorant azoique). **2007**.

107- Adegoke, K. A.; Oyewole, R. O.; Lasisi, B. M.; Bello, O. S. Abatement of organic pollutants using fly ash based adsorbents. *Water Science and Technology* **2017**, *76*, 2580-2592.

108- Amar, I.; Sharif, A.; Alkhayali, M.; Jabji, M.; Altohami, F.; Qadir, A.; Ahwidi, M. Adsorptive removal of methylene blue dye from aqueous solutions using CoFe1. 9Mo0. 1O4 magnetic nanoparticles. *Iranian (Iranica) Journal of Energy & Environment* **2018**, *9*, 247-254.

109- Li, X.; Wu, S.; Kan, C.; Zhang, Y.; Liang, Y.; Cui, G.; Li, J.; Yang, S. In *Tilte*2021; EDP Sciences.

110- Demirbas, E.; Kobya, M. Operating cost and treatment of metalworking fluid wastewater by chemical coagulation and electrocoagulation processes. *Process Safety and Environmental Protection* **2017**, *105*, 79-90.

111- MERZOUG, N. N. Application des tiges de dattes dans l'adsorption de polluants organiques. University of Souk Ahras, 2014.

112- Heinfling, A.; Martinez, M.; Martinez, A.; Bergbauer, M.; Szewzyk, U. Transformation of industrial dyes by manganese peroxidases from Bjerkandera adusta and Pleurotus eryngii in a manganese-independent reaction. *Applied and Environmental Microbiology* **1998**, *64*, 2788-2793.

113- Wu, T.; Cai, X.; Tan, S.; Li, H.; Liu, J.; Yang, W. Adsorption characteristics of acrylonitrile, p-toluenesulfonic acid, 1-naphthalenesulfonic acid and methyl blue on graphene in aqueous solutions. *Chemical Engineering Journal* **2011**, *173*, 144-149.

114- Zhu, C.; Feng, Q.; Ma, H.; Wu, M.; Wang, D.; Wang, Z. Effect of methylene blue on the properties and microbial community of anaerobic granular sludge. *BioResources* **2018**, *13*, 6033-6046.

115- Albanis, T.; Hela, D.; Sakellarides, T.; Danis, T. Removal of dyes from aqueous solutions by adsorption on mixtures of fly ash and soil in batch and column techniques. *Global Nest: Int. J* **2000**, *2*, 237-244.

116- Lima, M. X. V. F. Avaliação de resinas de troca iônica para o tratamento de hidrolisado hemicelulósico de bagaço de cana-de-açúcar. **2001**.

117- Siriwardane, R. V.; Shen, M.-S.; Fisher, E. P.; Poston, J. A. Adsorption of CO2 on molecular sieves and activated carbon. *Energy & Fuels* **2001**, *15*, 279-284.

118- Shah, J.; Jan, M. R.; Jamil, S.; Haq, A. U. Magnetic particles precipitated onto wheat husk for removal of methyl blue from aqueous solution. *Toxicological & Environmental Chemistry* **2014**, *96*, 218-226.

119- Babick, F.; Schießl, K.; Stintz, M. van-der-Waals interaction between two fractal aggregates. *Advanced Powder Technology* **2011**, *22*, 220-225.

120- Dias, B. P. Study of obtaining thin films of CeO2 doped with 2 and 4 mol% of europium, terbium and thulium obtained by spin-coating: Photocatalytic properties. Universidade Federal do Rio Grande do Norte, 2019.

121- McKay, G.; Otterburn, M.; Sweeney, A. The removal of colour from effluent using various adsorbents—III. Silica: Rate processes. *Water Research* **1980**, *14*, 15-20.

122- Velintine, V. A.; Wee, B. S.; Droepenu, E. K.; Chin, S. F.; Kok, K. Y. Effects of humic acid and natural sunlight irradiation on the behaviour of zinc oxide nanoparticles in the aqueous environment. **2020**.

123- Shirzadeh, M.; Sepehr, E.; Rasouli Sadaghiani, M.; Ahmadi, F. Effect of pH, initial concentration, background electrolyte, and ionic strength on cadmium adsorption by TiO2 and γ-Al2O3 nanoparticles. *Pollution* **2020**, *6*, 223-235.

124- Ayawei, N.; Ebelegi, A. N.; Wankasi, D. Modelling and interpretation of adsorption isotherms. *Journal of chemistry* **2017**, *2017*.

125- Clark, R. M.; Adams, J. Q. Evaluation of BAT for VOCs in drinking water. *Journal of environmental engineering* **1991**, *117*, 247-268.

126- Schobert, H.: *Chemistry of fossil fuels and biofuels*; Cambridge University Press, 2013.

127- Hamed, Z. H.; Ahmed, K. E. A.; Elsheikh, H. A. Synthesis and characterization of ZnS nanoparticles by chemical precipitation method. *Aswan University Journal of Environmental Studies* **2021**, *2*, 147-154.

128- Rasband, W.; ImageJ, U.; Health, N. I. o. Bethesda, Maryland, USA, 1997–2016. *ImageJ.[Google Scholar]* **2018**.

129- Ahmed, T.; Shahid, M.; Noman, M.; Niazi, M. B. K.; Mahmood, F.; Manzoor, I.; Zhang, Y.; Li, B.; Yang, Y.; Yan, C. Silver nanoparticles synthesized by using Bacillus cereus SZT1 ameliorated the damage of bacterial leaf blight pathogen in rice. *Pathogens* **2020**, *9*, 160.

130- Arularasu, M.; Harb, M.; Sundaram, R. Synthesis and characterization of cellulose/TiO2 nanocomposite: Evaluation of in vitro antibacterial and in silico molecular docking studies. *Carbohydrate polymers* **2020**, *249*, 116868.

131- Kennedy, N. W.; Hershewe, J. M.; Nichols, T. M.; Roth, E. W.; Wilke, C. D.; Mills, C. E.; Jewett, M. C.; Tullman-Ercek, D. Apparent size and morphology of bacterial microcompartments varies with technique. *PloS one* **2020**, *15*, e0226395.

132- Miller, B. D.; Gan, J.; Madden, J.; Jue, J.-F.; Robinson, A.; Keiser Jr, D. D. Advantages and disadvantages of using a focused ion beam to

prepare TEM samples from irradiated U–10Mo monolithic nuclear fuel. *Journal of nuclear materials* **2012**, *424*, 38-42.

133- Hirvonen Grytzelius, J.: Atomic Force and Scanning Tunneling Microscopy Studies of Single Walled Carbon Nanotubes. 2006.

134- Hasan, F. A.; Hussein, M. T. Study of some electronic and spectroscopic properties of ZnO nanostructers by density functional theory. *Materials Today: Proceedings* **2021**, *42*, 2638-2644.

135- Uchil, J.; Pattabi, M. Effect of pH on the size of CdS nanoparticles synthesized by chemical diffusion across a biological membrane. *Journal of New Materials for Electrochemical Systems* **2005**, *8*, 155-161.

136- Tomar, S.; Gupta, S.; Mukherjee, S.; Singh, A.; Kumar, S.; Choubey, R. K. Manganese-doped ZnS QDs: an Investigation into the optimal amount of doping. *Semiconductors* **2020**, *54*, 1450-1458.

137- Tauc, J.: Optical properties of amorphous semiconductors. In *Amorphous and liquid semiconductors*; Springer, 1974; pp 159-220.

138- Khiew, P.; Radiman, S.; Huang, N.; Ahmad, M. S.; Nadarajah, K. Preparation and characterization of ZnS nanoparticles synthesized from chitosan laurate micellar solution. *Materials Letters* **2005**, *59*, 989-993.

139- Parker, A.; Ollier, C. Discussion of A modelling study of coastal inundation induced by storm surge, sea-level rise, and subsidence in the Gulf of Mexico: the US average tide gauge is not accelerating consistently with the worldwide average. *Physical Science International Journal* **2015**, *7*, 49-64.

140- Ji, J.; Ge, Y.; Balsam, W.; Damuth, J. E.; Chen, J. Rapid identification of dolomite using a Fourier Transform Infrared Spectrophotometer (FTIR): A fast method for identifying Heinrich events in IODP Site U1308. *Marine Geology* **2009**, *258*, 60-68.

141- Ju, L.; Chen, Z.; Fang, L.; Dong, W.; Zheng, F.; Shen, M. Sol–gel synthesis and photo-Fenton-like catalytic activity of EuFeO3 nanoparticles. *Journal of the American Ceramic Society* **2011**, *94*, 3418-3424.

142- Patterson, A. The Scherrer formula for X-ray particle size determination. *Physical review* **1939**, *56*, 978.

143- Saravanan, L.; Diwakar, S.; Mohankumar, R.; Pandurangan, A.; Jayavel, R. Synthesis, structural and optical properties of PVP encapsulated CdS nanoparticles. *Nanomaterials and Nanotechnology* **2011**, *1*, 17.

144- Farooqi, M. M. H.; Srivastava, R. K. Structural, optical and photoconductivity study of ZnS nanoparticles synthesized by a low temperature solid state reaction method. *Materials science in semiconductor processing* **2014**, *20*, 61-67.

145- Rasband, W. US National Institutes of Health. *http://imagej. nih. gov/ij/* **2011**.

146- Ismail, H. K.; Ali, L. I. A.; Alesary, H. F.; Nile, B. K.; Barton, S. Synthesis of a poly (p-aminophenol)/starch/graphene oxide ternary nanocomposite for removal of methylene blue dye from aqueous solution. *Journal of Polymer Research* **2022**, *29*, 1-22.

147- Yang, H.; Zhao, J.; Song, L.; Shen, L.; Wang, Z.; Wang, L.; Zhang, D. Photoluminescent properties of ZnS: Mn nanocrystals prepared in inhomogeneous system. *Materials letters* **2003**, *57*, 2287-2291.

148- John, R.; Florence, S. Optical, Structural and morphological Studies of Bean-Like ZnS Nanostructures by Aqueous Chemical method. *Chalcogenide letters* **2010**, *7*.

149- Kole, A. K.; Kumbhakar, P. Cubic-to-hexagonal phase transition and optical properties of chemically synthesized ZnS nanocrystals. *Results in physics* **2012**, *2*, 150-155.

150- Ermrich, M.; Opper, D. XRD for the analyst. *Getting acquainted with the principles. Second. Panalytical* **2013**.

151- Othman, R. S.; Omar, R. A.; Omar, K. A.; Gheni, A. I.; Ahmad, R. Q.; Salih, S. M.; Hassan, A. N. Synthesis of Zinc Sulfide Nanoparticles by Chemical Coprecipitation Method and its Bactericidal Activity Application. *Polytechnic Journal* **2019**, *9*, 156-160.

152- Osuntokun, J.; Onwudiwe, D. C.; Ebenso, E. E. Green synthesis of ZnO nanoparticles using aqueous Brassica oleracea L. var. italica and the photocatalytic activity. *Green chemistry letters and reviews* **2019**, *12*, 444-457.

153- Wu, M.; Wei, Z.; Zhao, W.; Wang, X.; Jiang, J. Optical and magnetic properties of Ni doped ZnS diluted magnetic semiconductors synthesized by hydrothermal method. *Journal of Nanomaterials* **2017**, *2017*.

154- Thakur, P.; Kumar, V. Kinetics and thermodynamic studies for removal of methylene blue dye by biosynthesize copper oxide nanoparticles and its antibacterial activity. *Journal of Environmental Health Science and Engineering* **2019**, *17*, 367-376.

الخلاصة

ركز هذا العمل بشكل أساسي على تحضير وتشخيص بلورات كبريتيد الزنك النانوية باستخدام طريق الترسيب الكيميائي. تم تصنيع جسيمات كبريتيد الزنك النانوية ذات الشكل شبه الكروي من خلال التحكم في تركيز المواد الأولية ووقت التفاعل ودرجة الحموضة للمحلول. وكذلك تم التأكد من تكوين البلورات النانوية لكبريتيد الزنك من خلال تقنيات TEM و FE-SEM و XRD و EDX. وكذلك تم قياس فجوة الطاقة من طيف الأشعة المرئية وفوق البنفسجية ووجد أنها (3.8 الكترون-فولت) وتعزى هذه الازاحه الزرقاء مقارنة بفجوه الطاقة ل ZnS الكبيره إلى تأثير الحبس الكمومي- quantum confinement -وكذلك تم دراسة سلوك الامتزاز للجسيمات النانوية ZnS ووجد أن جزيئات ZnS لديها القدرة على امتزاز صبغة الميثيلين الزرقاء (MB) من المحلول المائي. وجد أنه مع زيادة كمية الزنك في محلول الصبغة ، تزداد إزالة صبغه الميثيلين الزرقاء.

في الجزء الثاني من هذا المشروع ، تم تحضير جزيئات كبريتيد الزنك النانوية باستخدام الطرق الخضراء. في هذه الطريقة، يتم استخدام أجزاء من النباتات كعوامل اختزال وعوامل عزل بدلاً من استخدام المواد الكيميائية. تم تعديل المتغيرات مثل تركيز المستخلص ودرجة الحموضة في المحلول للتحكم في عملية نمو الجسيمات النانوية ZnS. وكذلك تم تحديد فجوة الطاقة من طيف الامتصاص ووجدت أنها (3.93 الكترون-فولت) ، والتي تكون في انزياح أزرق مقارنة بفجوه الطاقة ل ZnS الكبيره. تم توضيح سلوك الامتزاز لجسيمات كبريتيد الزنك النانوية ، ووجد أن كمية صغيرة من جزيئات ZnS (0.1 جم) قادرة على امتزاز صبغة الميثيلين الزرقاء (MB) من مياه الصرف الصحي.

جامعة كربلاء

كلية التربية للعلوم الصرفة

قسم الكيمياء

تحضير و تشخيص دقائق كبريتيد الخارصين النانوية وتطبيقاتها في ازالة صبغة المثيلين الزرقاء من المحاليل المائية

الرسالة مقدمة الى مجلس كلية التربية للعلوم الصرفة ــ جامعة كـربلاء، كجزء من متطلبات نيل شهادة الماجستير في علوم الكيمياء

من قبل

امير قاسم عبد جواد

بإشـــــراف

الاستاذ المساعد الدكتور

علا مهدي عبد علي الهنداوي

1444 . هـ

الاستاذ المساعد الدكتور

حسن فيصل اليساري

2022 . م